DEFINING THE PATHWAY TO CELLULAR SENESCENCE: IMPLICATIONS FOR CANCER THERAPY AND PHYSIOLOGY

By

Caroline Gleason

A Dissertation

Presented to the Faculty of the Louis V. Gerstner, Jr.

Graduate School of Biomedical Sciences,

Memorial Sloan Kettering Cancer Center

in Partial Fulfillment of the Requirements for the Degree of

Doctor of Philosophy

New York, NY

June 2022

_____ _____

Andrew Koff, PhD — Date

Dissertation Mentor

© Caroline Gleason 2022

ALL RIGHTS RESERVED

DEDICATION

I would like to dedicate this thesis to my mother, Carol Gleason – my #1 cheerleader, role model, best friend, and all-around favorite person. Mom, without you, I would never have made it this far. Of course, without you, I wouldn't exist at all, but let's not go down that road. Thank you for your constant love, support, and unwavering belief in me, and most importantly, thank you for your round-the-clock services as my devoted in-house statistician. Sorry that the thing I'm dedicating to you is this rather dull dissertation and not something a bit more exciting, but don't worry, you only have to read this page.

ABSTRACT

Senescence is an irreversible, stress-induced, non-proliferative state in which cells mount a program of gene expression designed to modulate their interaction with the environment. A large swath of biology is affected by cellular senescence, including tumor suppression, embryonic development, wound repair, and stem cell reprogramming. Senescence can also account for the beneficial response of cancer cells to chemotherapy, and the accumulation of senescent cells in multiple tissues is associated with both normal and pathological aging.

Although much is known about the contexts in which senescent cells appear, critical questions remain as to how cells achieve this state. Very little is known about what is required for a cell to move from reversible to irreversible growth arrest, a process called geroconversion, and how that transition is linked to the elaboration of the senescence-associated secretory program (SASP), a gene expression and secretion program through which the senescent cell can modulate its local environment. There are many models in which to study cellular senescence and gain insight into its various hallmarks, but experimentally, it has been difficult to separate the decision to exit the cell cycle from the commitment to stable growth arrest.

Treatment with CDK4/6 inhibitors, such as palbociclib and abemaciclib, can induce cellular senescence in cancer cell lines. In these cells, changes in the recruitment of the chromatin- remodeling enzyme ATRX, and a decrease in the abundance of the tumor suppressor MDM2, are necessary to provoke irreversible arrest and elaboration of the inflammatory program. Stabilization of MDM2 permits cells treated with palbociclib

to exit the cell cycle but prevents progression into a full senescent state.

In my thesis work, I took advantage of this MDM2-dependency to generate a temporally-organized map of phenotype acquisition and gene expression in a liposarcoma cell line during the transition from reversible into irreversible arrest and beyond. Using this system, I determined that *ANGPTL4*, a common SASP factor that appeared coincident with geroconversion, was necessary for both the establishment of stable growth arrest and for the accumulation of later SASP transcripts, including those associated with a mature, robust, inflammatory program. After defining the role of *ANGPTL4* during senescence in cultured cells, I was able to use it as a marker to identify senescent cells in samples from a phase II clinical trial of abemaciclib in liposarcoma patients. This work demonstrated the importance of therapy-induced senescence and its subsequent inflammation for patient response to CDK4/6 inhibitors.

Though discovered in the context of cancer cells treated with CDK4/6 inhibitors, the role of *ANGPTL4* in senescence was conserved in other, more normal physiological contexts, including in primary cells undergoing replicative senescence. It also extended to excisional wound healing in mice, another process dependent on cellular senescence. Thus, by defining the relationships between markers of cellular senescence in the CDK4/6 inhibitor therapy-induced senescence model, I was able to demonstrate that *ANGPTL4* is regulator of late senescent events in multiple contexts, and that it can be used to identify mature, inflammation-provoking senescent cells. My work also examined, for the first time in human patients, the effects of therapy-induced senescence on patient outcome to CDK4/6 inhibition, and how this differs from the acute phase to the chronic phase of cellular senescence.

ACKNOWLEDGEMENTS

"Still, there are times I am bewildered by each mile I have traveled, each meal I have eaten, each person I have known, each room in which I have slept. As ordinary as it all appears, there are times when it is beyond my imagination."

- Jhumpa Lahiri*, Interpreter of Maladies*

First and foremost, I must give the biggest thank you to Andrew Koff, thesis mentor extraordinaire. Andy – I never thought I'd have a boss who could teach me as much about sipping tequilas as experimental design, but you have managed to do both, with equal enthusiasm. Thank you for letting me follow my scientific curiosity down (almost) any path I wanted (although I still maintain that *PLAT* is the key to senescence, and someday, I'm going to read this to you and say, "I TOLD YOU SO!"). I can honestly say that my years in the Koff lab have flown by. I will always look back fondly on the countless hours spent in your office debating science and politics, spilling the tea (you get that reference now, right?), trying to decipher your incomprehensible handwriting as you scribbled ideas on the whiteboard, and taking the odd shot from a pipette. You have been better than the best mentor I could have hoped for. You have truly changed how I think about science, and life, and I think I'm finally ready, in these waning days of my PhD, to concede that you *might* have *occasionally* been right about *a limited number* of things (not the *PLAT* thing, though).

I am deeply indebted to all the scientists who helped guide me throughout my PhD, and to our many collaborators, both at MSK and around the world, who made this work possible. Thank you to my committee members, Charlie Rudin and Ping Chi, for

many years of great discussions and advice, and to Sarat Chandarlapaty and Jesús Gil for volunteering their time to serve as my chair and external advisor. Thank you to Bill Tap, Cristina Antonescu, Mark Dickson, and the entire Sarcoma service at MSK for lots of thoughtful conversations about how best to integrate clinical and basic work. I also owe many thanks to our bioinformaticians/sequencing geniuses, Martina Bradic and Rodrigo Gularte-Merida, and to the talented (and handsome!) data scientist Daniel Firester for working his Bayesian magic (more about him later). Thank you to the Tan lab in Singapore for sharing samples from their mouse model, and to Raghu Kataru for his expertise in staining and imaging those samples. Finally, I am endlessly grateful to the Molecular Cytology Core Facility for their constant help over the years, and especially Katia Manova-Todorova, Afsar Barlas, Mesruh Turkekul, Ning Fan, and Eric Chan, for guiding me on every aspect of tissue preparation, staining, imaging, and analysis.

I feel very lucky to have picked a thesis lab full of coworkers whom I also consider lifelong friends. Everything I have accomplished in the last six years has only been possible because of my talented predecessors, Marta Kovatcheva and Mary Klein. I'm grateful to have been able to stand on the shoulders of their incredible work and to have had the chance to learn from them both. Marta – I joined the Koff lab in no small part because I watched you in action and thought, "wow, that's exactly who I want to be when I grow up." Thank you for teaching me so much about science, for always knowing the best restaurants in every single city in the entire world, and for still being willing to answer questions about where to find things in the lab 5+ years after you left. Perhaps you thought you'd escape my constant gossiping and complaining by moving to Barcelona, and if so, you were sorely mistaken, so thanks for the past few years of

continuing to listen to me gossip and complain via Whatsapp, instead. I'm still holding out hope that I'll turn out to be you when I grow up.

Mari and Julie – Next Gen Koff Lab is looking pretty incredible. You two came into the lab at just the right time, bringing some much-needed sunshine into the jaded last few years of my PhD. It has been a joy to build Koff Lab snowmen out of defrosted freezer ice with you, throw themed dinner parties with you, and host afternoon tea sessions in lab with you. I can't wait to see what you both will do next, and to find out whether Julie is going to have those twins. Whatever you do, I know it will be amazing.

I would like to thank all my friends, within GSK, in NYC, and beyond, for sticking by me over the years, and for reminding me that there is life outside the lab, even when your paper has been rejected yet again. Rachel – I still remember sitting in Simon Lab meetings and feeling completely in awe of your ability to ask the most insightful questions no matter the research topic. All these years later, I continue to be in awe of your brilliance, your passion for science, and your perfect, beautiful face. I love you so much. Jane – your eternal optimism is just the right antidote to my natural cynicism. Thank you for your support, your constant willingness to be my cheerleader, and for directly fueling my writing process with an entire box full of candy, Cheez-its, and uplifting notes. You make my life so much brighter and I'm extremely fortunate to have you on my side.

I am forever grateful for my incredible family. Mom and Dad – it's kind of your fault that I had to write this gigantic dissertation, since you're the ones who always encouraged me to go to graduate school. I guess now that I'm on the other side of this whole PhD thing, I can just say thank you. I'm a lucky girl to have two such loving and

brilliant parents who support me in every crazy idea I've ever had and who can also patiently(ish) explain to me for the 100th time when to use a two-tailed test (I've already forgotten, by the way). Elizabeth – thank you for being the best big sissy. I've been trying to copy you since the era of "six-o-clock!" and to this day, I'm still inspired by your persistence and determination in the face of great adversity. Suzie and Jason – you guys have been redefining the meaning of Cool Aunt/Uncle for the last 30+ years, and Grace, you are the baby sister I never had. Thank you for all the delicious dinners, many (many many) bottles of wine, dance parties, and sleepovers, and for always being there when I need you, aperol spritz in hand. To the Firester clan – thank you for welcoming me into your family with open arms. I can't wait for us to become official family in a few months' time!

Finally, Daniel – probably the best thing that happened during grad school was stumbling upon you, dressed in a flowery apron, making sourdough pizza from scratch in my friend's apartment. That night really set the tone for the next six years of wacky shirts and homemade carbs. You have helped and supported me in more ways than you know, throughout grad school in general and through the writing of this dissertation specifically. I'm grateful for all the ways you take care of me, make me laugh, and, of course, for the way you text me every Friday to ask what kind of pasta I want for dinner. That right there is the definition of true love. I wouldn't have wanted to weather the storm of two simultaneous PhD journeys with anyone else. Looking forward to a lifetime of adventures and Pasta Fridays with you and the little Lum.

It truly does take a village, so thank you to everyone who has been a part of mine.

TABLE OF CONTENTS

LIST OF TABLES

LIST OF FIGURES

LIST OF ABBREVIATIONS

53BP1	p-53 binding protein 1
α-SMA	Alpha smooth muscle actin
γH2AX	Gamma H2A histone family member X
ANGPTL4	Angiopoietin-like four
ANOVA	Analysis of variance
ATRX	Alpha-Thalassemia/Mental Retardation Syndrome X-Linked
BrdU	5-bromo-2'-deoxyuridine
cANGPTL4	C-terminal Angiopoietin-like four
CCL20	C-C Motif Chemokine Ligand 20
CCD	Coiled-coil domain
CCNE2	Cyclin E2
CD3/4/8/11b/68	Cluster of differentiation 3/4/8/11b/68
CDH18	Cadherin 18
cDNA	Complementary deoxyribonucleic acid
CDK	Cyclin-dependent kinase
CDK4/6i	Cyclin-dependent kinase 4/6 inhibitor
CDKN2A	Cyclin-dependent kinase inhibitor 2A
CXCL1/9/10/11	C-X-C Motif Chemokine Ligand 1/9/10/11
DAPI	4′,6-diamidino-2-phenylindole
DDIS	DNA damage-induced senescence
DNA	Deoxyribonucleic acid
Dox	Doxycycline
Doxo	Doxorubicin
EGFP	Enhanced green fluorescent protein
EGFR	Epidermal growth factor receptor
EMT	Epithelial-mesenchymal transition
ER	Estrogen receptor
FBS	Fetal bovine serum
FFPE	Formalin-fixed, paraffin-embedded
flANGPTL4	Full-length Angiopoietin-like four
FLD	Fibrinogen-like domain
F-MDM2	FLAG-tagged mouse double minute 2 homolog
GCV	Ganciclovir
GO	Gene ontology
GSEA	Gene set enrichment analysis

H&E	Hematoxylin and eosin
HP1y	Heterochromatin protein 1 gamma
HPDF	Human primary dermal fibroblast
IGFBP3	Insulin Like Growth Factor Binding Protein 3
IGFBP7	Insulin Like Growth Factor Binding Protein 7
IHC	Immunohistochemistry
IL-1A	Interleukin 1 alpha
IL-1A	Interleukin 1 beta
IL6	Interleukin 6
INK4	Inhibitors of CDK4
KO	Knockout
LPL	Lipoprotein lipase
MDM2	Mouse double minute 2 homolog
MEF	Mouse embryonic fibroblast
MEK	Mitogen-activated protein/extracellular signal-regulated kinase
MMP1/3	Matrix metalloproteinase 1/3
mRNA	Messenger ribonucleic acid
mTOR	Mammalian target of rapamycin
nANGPTL4	N-terminal Angiopoietin-like four
NSCLC	Non-small cell lung cancer
OIS	Oncogene-induced senescence
PCR	Polymerase chain reaction
PD	Palbociclib (PD0332991)
PDLIM7	PDZ and LIM domain protein 7
PFS	Progression-free survival
PLAT	Plasminogen Activator, Tissue Type
qPCR	Quantitative polymerase chain reaction
rANGPTL4	Recombinant Angiopoietin-like four
RB	Retinoblastoma
RECIST	Response evaluation criteria in solid tumors
RNA	Ribonucleic acid
ROS	Reactive oxygen species
SAHF	Senescence-associated heterochromatic foci
SASP	Senescence-associated secretory phenotype
SA-β-gal	Senescence-associated beta-galactosidase
SD	Standard deviation
SEM	Standard error of the mean
Seq	Sequencing

SWI/SNF	SWItch/Sucrose Non-Fermentable
Tet-ON	Tetracycline inducible
shRNA	Short hairpin ribonucleic acid
TF	Transcription factor
TIS	Therapy-induced senescence
WD/DDLS	Well differentiated/dedifferentiated liposarcoma
WT	Wild-type

Chapter 1: Introduction

Overview: the discovery of cellular senescence

In the early 1960s, two scientists, Leonard Hayflick and Paul Moorhead, made a controversial claim. After conducting many experiments culturing normal human fibroblasts, they proposed that the cells could only undergo a finite number of population doublings, and that those doublings occurred in three distinct phases: phase I, exponential growth; phase II, diminished growth; and phase III, cessation of proliferation [1, 2]. This challenged the prevailing view in the field at the time, which, based largely on observation of cell lines like HeLa, was that cultured cells were immortal and could grow indefinitely, if given the right culture conditions [3]. The loss of proliferative potential, now known as the Hayflick limit, was not merely an effect of culturing, as cells taken from older donors had shorter lifespans in culture than those taken from younger donors, suggesting that these cells contained a kind of endogenous clock that allowed them to "remember" their age. Hayflick and Moorhead thus postulated that this process must be an underlying cause of aging and named it cellular senescence.

Decades later, the *ras* oncogene was discovered and shown to transform immortalized cells, but only in the presence of another cooperating oncogene. [4]. When expressed alone, oncogenic *ras* resulted in a phenotype that was indistinguishable from the one observed by Hayflick in his primary cells [5]. This gave rise to the idea that senescence functions as a natural barrier to tumor formation, arresting any aberrantly proliferating cells before additional oncogenic events can occur. This theory was later

supported by the finding that benign melanocytic nevi, more than 90% of which have activating mutations in *BRAF,* show signs of senescence *in vivo* [6].

Today, we have evidence to suggest that both theories are correct – senescence does relate to aging, and it does have anti-tumorigenic properties. It also contributes to wound healing, development, tissue regeneration, stem cell exhaustion, tumor regression, and, paradoxically, tumor promotion [7]. Senescence, a state in which cells are alive and metabolically active, but growth arrested and impervious to pro-proliferative signals from their environment, can be triggered by many inducers. Though the field has come far in the 60 years since Hayflick's discovery, many questions remain about how cells become and remain senescent, and how they interact with their environments.

Many pathways converge into senescence

A cell that has undergone division and arrived at the G_1 phase of the cell cycle faces a choice. It can re-enter the proliferative cycle and divide again, or it can "choose" to exit into one of several cell fates: apoptosis, differentiation into a more terminal cell type, quiescence, or senescence. Quiescence is a temporary break from the cell cycle, although it can last for months or even years, while senescence is generally viewed as a permanently arrested state [8]. It is, fundamentally, a stress response, and it can be induced by many different stress triggers.

The phenomenon observed by Hayflick and Moorhead is now known as replicative senescence, and in normal, untransformed human cells, it is the outcome of telomeric stress. In somatic cells lacking active telomerase, the end replication problem results in the shortening of telomeres with each successive passage. Once a critically

short length has been reached, the ends of the telomeres are recognized as double strand breaks, triggering a DNA damage response that results in senescence [9]. Replicative senescence is not, therefore, tied to cellular age *per se*, as Hayflick had thought, but rather to replication events. Primary mouse cells, despite having much longer telomeres than human cells, exhibit a much shorter lifespan in culture [10]. In mouse cells, replicative senescence appears to be connected to oxidative stress, rather than telomere crisis, as culturing mouse primary embryonic fibroblasts (MEFs) at physiological oxygen concentrations extends their replicative lifespan [11].

DNA damage that occurs separately from telomere shortening is another common trigger for senescence. DNA damage-induced senescence (DDIS) can result from sub-lethal doses of any treatment that generates irreparable DNA lesions, such as radiation or genotoxic chemicals. Detection of the lesions activates the DNA damage response, and ATM or ATR kinases block re-entry into the cell cycle by stabilizing the tumor suppressor protein p53 and activating the cell cycle inhibitory protein p21 [12]. In oncogene-induced senescence (OIS), excessive growth signaling from overexpression of an oncogene, such as *ras*, typically results in a wave of hyperproliferation, followed by entry into senescence. Although the specific factors driving OIS seem to vary from model to model, they all converge on one of two major tumor suppressor pathways: p53 and retinoblastoma (RB) [13]. Both DDIS and OIS are thought to act as barriers against the continued proliferation of damaged or oncogenic cells.

Disruption of cellular metabolism and oxidative stress are both known inducers of senescence [14]. Mitochondrial dysfunction, associated with loss of mitochondrial enzymes SIRT3 and SIRT5, can induce senescence through an NADH/AMPK/p53

signaling pathway [15]. Loss of superoxide dismutase 2 (SOD2), the main reactive oxygen species (ROS) scavenging antioxidant, results in DNA damage and mitochondrial dysfunction that triggers senescence in mouse skin, demonstrating that ROS can drive induction of senescence [16]. OIS is associated with activation of pyruvate dehydrogenase (PDH), the mitochondrial enzyme that links glycolysis with oxidative metabolism. This activation results in increased tricarboxylic acid cycle activity, increased respiration, and redox stress [17].

Many other cellular stressors, both intrinsic and extrinsic, have also been associated with senescence, including dysfunction of proteostasis, epigenetic changes, developmental signals, and, importantly, chemotherapy [18]. With so many different triggers driving entry into senescence, a key question in the field is how broadly the molecular events that lead into senescence are conserved. Most senescence pathways seem to converge upon the RB and/or the p53 signaling axes, and many cell cycle regulators have been implicated in senescence, including p16, p21, and p27, in addition to RB and p53 [19]. However, it remains unclear whether those factors are truly involved in the regulation of the senescence phenotype, or merely the exit from the cell cycle that necessarily occurs as the first step towards senescence. Another crucial question is the extent to which the terminal state of senescence is the same in these different contexts. In order to facilitate the study of senescence and address these important issues, it is first essential to be able to identify senescent cells inside both *in vitro* and *in vivo* systems.

Hallmarks of senescence: a complex and variable phenotype

Senescence is fundamentally a state of withdrawal from the proliferative cell cycle, but it is not the only such state. Quiescent cells, like senescent cells, have also left the cell cycle, and it is therefore necessary to distinguish between these two types of growth arrest. Quiescence can be measured by accumulation of cells in G_0/G_1 phase, as determined by flow cytometry, by a loss of phosphorylated RB, and by decreased incorporation of BrdU [20]. By definition, quiescent cells are reversibly arrested and return to the cell cycle upon removal of the inducing stimulus, even after weeks or years of cytostasis. Sequencing analysis of different populations of quiescent cells has revealed that in terms of gene expression, quiescence is more complicated than simple exit from the cell cycle [21]. In order to maintain reversibility, and avoid becoming senescent or undergoing differentiation, cells need to activate a gene expression program that blocks entry into terminal cell fates. In both quiescent fibroblasts and neurons, regulation of this program is dependent on expression of the transcription factor *HES1* [21-23].

Senescent cells exhibit all the same phenotypic markers of cell cycle exit as quiescent cells, but they also display a diverse range of cytological phenotypes, including enlarged and flattened cell morphology, increased expression of the cell cycle inhibitor *CDKN2A/*p16, and accumulation of a lysosomal marker known as senescence-associated beta-galactosidase (SA-β-gal) [24]. Senescent cells often undergo rearrangements in chromatin that lead to the formation of senescence-associated heterochromatic foci (SAHF), dense regions of heterochromatin that accumulate near and repress expression of pro-proliferative genes, including E2F target genes [25]. As senescent cells are not proliferating, they have different energy needs, and therefore display altered cellular

metabolism, including decreased production of all four dNTPs and increased lipid metabolism [26-28]. Senescent cells can also exhibit cytoplasmic chromatin fragments, markers of DNA damage like 53BP1 and γH2AX foci, alterations in the plasma membrane, signs of endoplasmic reticulum stress, and accumulation of lysosomes and mitochondria [29, 30]. Additionally, the Koff lab has identified a novel marker of senescence: increased numbers of the chromatin remodeler ATRX foci in the nucleus [31].

Some markers of senescence are also regulators of the process and serve an important function, while others are simply bystander phenotypes that are not essential for progression into the senescent state. For example, ATRX foci play a critical role in the onset of senescence, and at least in some contexts, knockdown of ATRX prevents cells from becoming senescent [31]. In contrast, SA-β-gal, although commonly observed in many types of senescent cells, is not thought to play an active role, and knockdown of *GLB1,* the gene that encodes β-galactosidase, does not affect the ability of cells to become senescent [32]

The difficulty of defining and identifying senescent cells

Though all these cellular phenotypes, and more, have been associated with senescence, none is universally found in all senescent cells, and none is completely unique to senescent cells. For example, SA-β-gal expression, which is simply lysosomal beta-galactosidase that is active at the sub-optimal pH of 6.0, has also been linked to autophagy, a process that involves high levels of lysosome content and activity [33]. SA-

β-gal activity can be detected in cells that have been serum starved for extended periods of time, and in cells grown to high confluency, suggesting that it is more accurately a marker of general cellular stress than cellular senescence specifically [34, 35]. Senescence is often, but not necessarily, regulated by increased expression and/or activation of p16 and/or p53, as well as DNA damage response pathways [20, 36]. Even metabolic requirements of senescent cells seem to be inconsistent; utilization of glucose, for example, has been shown to increase [37], decrease [38], and remain unchanged [17], all in similar models of OIS.

The characterization, isolation, and study of senescent cells is thus confounded by the struggle in definitively identifying them. To say with confidence that senescence occurs, it is necessary to probe for a suite of different markers in the same sample. This makes it challenging to study senescence in tissue, as many of the techniques developed for the *in vitro* study of senescence are difficult to perform on tissue samples, and it especially complicates the ability to identify senescent cells in tissue from human subjects, which is often extremely limited. SA-β-gal, which, despite its shortcomings, is arguably the most used marker of senescent cells, can often not be assessed in tissue samples. Because SA-β-gal staining requires lysosomal activity, it can only be performed on fresh or frozen tissue, making it incompatible with many clinical samples, which are typically formalin-fixed and paraffin-embedded [39]. In the context of cancer, identifying senescent cells is further convoluted by the fact that many factors involved in regulating senescence pathways are also oncogenes or tumor suppressors, whose expression might be altered as a result of the tumorigenic process [40]. There is clearly an urgent need for

markers that can reliably identify senescent cells and that can be used both *in vitro* and *in vivo*.

A conserved, tripartite phenotype of senescent cells

The heterogeneity observed among phenotypes associated with senescent cells has prompted the idea of defining the minimum requirements of a senescent cell – in other words, what phenotypes must a cell absolutely possess to be considered senescent? Consensus in the field is that there is a conserved, tripartite senescence phenotype consisting of three indispensable, functional hallmarks that are foundational to the state [41]. Perhaps the most fundamental phenotype associated with senescence is the stability of growth arrest. Theoretically, senescence is an irreversible state to which a cell commits, such that even if the inducing trigger is removed, the cell cannot or will not return to the cell cycle [29, 42]. The definition of senescence as irreversible has recently been the subject of debate, largely due to experimentally induced modifications, such as loss/inactivation of p53, p16, or RB, that allow cells to "escape" senescence [43, 44]. This debate might well be simplified to a matter of semantics – if genetic manipulation of protein X results in senescent cells regaining their proliferative potential, is it true that senescence is reversible, or is it true that protein X is an essential part of the machinery that makes senescence irreversible? Throughout this dissertation, senescence is referred to interchangeably as a stable, permanent, and irreversible state of growth arrest, but the caveat that it is impossible to prove that a cell will *never* divide again is duly acknowledged.

Another functional, widely observed phenotype of senescent cells is that they are resistant to apoptosis, which appears to be mediated through up-regulation of the pro-survival gene *BCL2* [45-47]. The mechanism by which senescent cells develop a pro-survival, anti-apoptotic phenotype is incompletely understood, but there is evidence to show that in senescent fibroblasts, p53 is preferentially recruited to the promoters of cell cycle inhibitory genes like p21, rather than the promoters of apoptotic regulatory genes like *PUMA* [48].

The final conserved, functional hallmark of a true senescent cell is the development of a program of secreted proteins called the senescence-associated secretory phenotype (SASP). The SASP is one of the most intriguing and confounding aspects of senescent cells. At its core, it represents a dynamic, bioactive secretome elaborated by cells that have undergone senescence, and typically consists of a mixture of cytokines, chemokines, secreted extracellular matrix components, proteases and protease inhibitors, growth factors, and exosomes, which, together, facilitate the interaction of the senescent cell with its environment. The proposed functions of the SASP are manyfold, and include immune cell recruitment, modulation of the extracellular environment, degradation of signaling molecules, and stimulation of angiogenesis, among others [49].

The SASP was originally described as a group of approximately 50 cytokines, growth factors, and extracellular matrix remodeling proteins that were commonly secreted by senescent cells. However, these early experiments used biased approaches, like antibody arrays, to characterize the SASP, and more recent studies using unbiased approaches have shown that it is much more complex than previously thought, and that it might consist of many hundreds of different secreted proteins (Basisty 2020). SASP gene

expression is thought to be highly context-specific, depending both on the trigger inducing the senescent growth arrest and on the cell type in which senescence occurs.

Regulation of SASP gene expression also appears to be a multifaceted process. Induction of p16 expression alone, or activation of p53 or RB alone, is enough to cause growth arrest, but not senescence, indicating the need for a cell to undergo some kind of transition after cell cycle exit before it becomes a SASP-producing cell [13, 50]. Activation of SASP expression has been linked to the DNA damage response [51], and a number of transcription factors have been shown to induce expression of various arms of the SASP, including NF-κB, C/EBPβ, and GATA4 [52-54]. The SASP is temporally dynamic and evolves over time, a feature that has been linked to *NOTCH1* activity. In the early stages of senescence, *NOTCH1* expression suppresses the pro-inflammatory arm of the SASP and promotes activity of TGF-β and its downstream effectors to enforce growth arrest. In the later stages of senescence, *NOTCH1* expression wanes, allowing induction of the pro-inflammatory SASP components [55].

The many faces of the senescence-associated secretory phenotype

Senescence has been linked to many biological processes, from tumor suppression to aging, and seems to act beneficially in some contexts and antagonistically in others. In many cases, this pleiotropic effect can be connected to the SASP, which has been shown to have a multitude of functions that can help or harm the organism, depending on the context (Fig. 1.1). For instance, the SASP appears to be essential for the kinetics of healthy wound repair in mice, where it also helps prevent scarring and fibrosis [56]. In

the wake of an injury, the SASP can act in an *IL6*-dependent manner to drive local proliferation and differentiation of stem cell pools and/or reprogramming and plasticity of neighboring cells to promote tissue regeneration [57].

The SASP also plays a role in reinforcing the stability of the senescence-associated growth arrest. This can occur in a cell-autonomous manner [58], but the SASP also mediates paracrine senescence, during which senescent cells in a population can stimulate nearby cells to enter senescence [59, 60]. This process is thought to be important for suppression of tumor growth. By inducing and propagating an anti-proliferative state, the SASP can serve as a barrier to tumor formation.

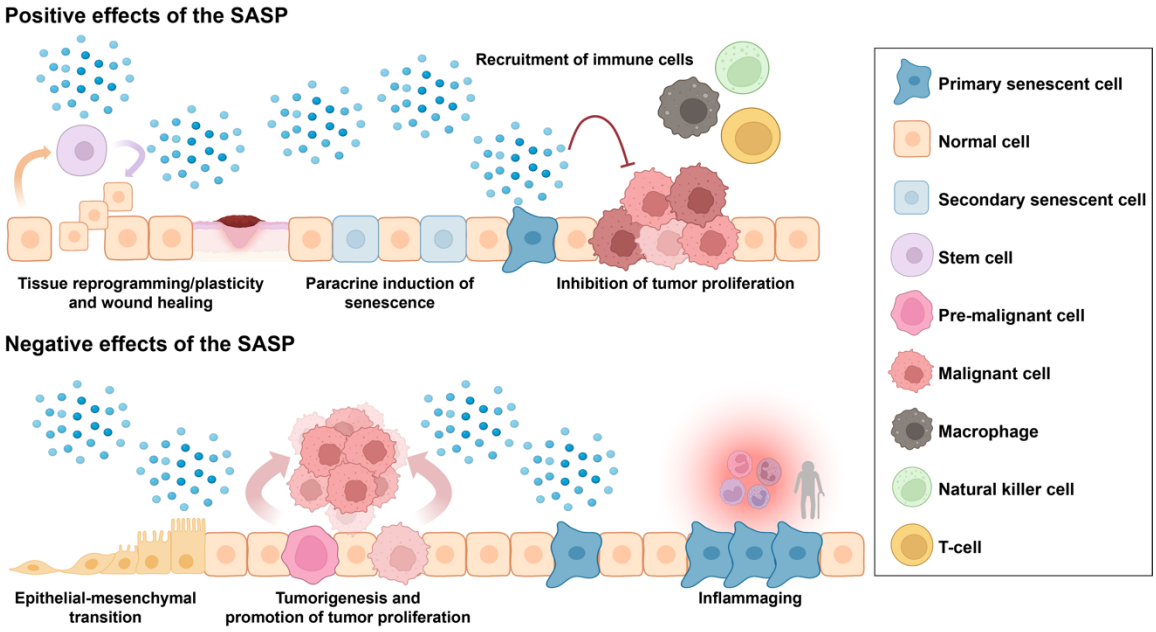

Figure 1.1 The positive and negative effects of the SASP.

Some of the known beneficial (top panel) and detrimental (bottom panel) effects associated with SASP expression are summarized.

In addition to its role in halting tumor growth, the SASP can also aid in tumor regression by interacting with the immune system to promote clearance of senescent cells, a process that has been linked to different immune cell types in different systems. In a mouse model of liver carcinoma, senescent tumor cells were eliminated by natural killer cells, which appeared to be recruited to the site of the tumor by senescence-related secretion of Ccl2 [61, 62]. A different model of murine liver cancer found a role for macrophages in clearance of senescent stromal cells. Incubation of macrophages with conditioned media from the senescent stromal cells induced a shift from the tumor-promoting M2 state to the tumor-suppressive M1 polarization, and these activated M1 macrophages showed a strong ability to eliminate senescent stromal cells *in vivo* [63]. A $CD4^+$ T-cell surveillance program has been linked to clearance of pre-malignant senescent hepatocytes in mice. Although the actual elimination of senescent cells was dependent on monocytes, $CD4^+$ T-cells, acting in a T-helper cell role, were required for the execution of this function. Disruption of the T-cell response prevented senescent cell clearance, which in turn allowed development of carcinomas [64]. Senescent cells, acting through the SASP, therefore have the ability to recruit a variety of immune cell types to promote their own clearance.

On the other side of the coin, the SASP has been shown to have pro-tumorigenic effects. In co-culture systems, senescent fibroblasts stimulated the growth of pre-malignant epithelial cells, but not normal epithelial cells. This growth was connected, at least in part, to the SASP secreted by the fibroblasts. When the preneoplastic cells were injected into mice, they failed to form tumors, but co-injection with senescent fibroblasts induced sizeable tumor formation [65]. A mouse model of hepatocellular carcinoma

(HCC) showed that tumor growth was stimulated by senescent stromal cells in the tumor microenvironment, which secreted SASP factors like *Il-1b, Il6*, *Cxcl1*, and *Cxcl9.* Knockout of *Il-1b* in the stromal cells abrogated expression of other SASP factors and significantly reduced tumor formation [66]. Similar results were seen in a model of HCC following liver injury: again, senescent stromal cells stimulated the transformation of adjacent epithelial cells into HCC tumors [63]. Thus, a preponderance of evidence exists to show that the SASP can stimulate progression of preneoplastic cells, as well as hyperproliferation of existing malignant cells.

SASP genes can also trigger epithelial-mesenchymal transition (EMT). When two relatively non-aggressive breast cancer cell lines, T47D and ZR-75-1, were cultured with conditioned media from senescent fibroblasts, they exhibited decreased expression of β-catenin, E-cadherin, and cytokeratins, and increased expression of vimentin. Incubation with senescent conditioned media also stimulated a panel of pre-malignant and malignant breast cancer cell lines to invade a basement membrane. These effects, which are consistent with EMT, were linked to the presence of IL6 and IL8 in the senescent conditioned media and were not recapitulated by treatment with conditioned media from pre-senescent fibroblasts [67]. Since EMT is an important mechanism by which tumor cells can gain invasive and metastatic properties, this represents another pathway through which the SASP can promote tumorigenesis.

Finally, senescent cells accumulate in various tissues and organs of aging mice and humans, where they contribute to many of the degenerative conditions associated with age [68]. The contribution of senescence to aging is largely mediated through the SASP, which drives a state of constant, low-grade inflammation. In fact, inflammation

and age-related dysfunction are so intricately connected that the term “inflammaging” has been coined to describe their relationship [69]. Inflammaging is characterized by high levels of circulating pro-inflammatory molecules, including common SASP factors like *IL6* and *IL1RA,* and it is a risk factor for cardiovascular dysfunction, cancer, and neurodegeneration, among other diseases [70]. Why senescent cells accumulate during aging, instead of being cleared by immune cells, remains a question of great interest. The answer likely lies at the intersection between an increased rate of formation of senescent cells with age, and age-associated decline in function of the immune system [71].

In summary, the SASP is a complex, dynamic, and often variable component of senescence. It is also one of the main ways in which senescent cells exert their myriad effects on the surrounding tissue. Manipulation of the SASP to promote its beneficial effects or repress its deleterious effects is an appealing approach, but to do so would require a much deeper understanding of the context-specific nuances of the SASP, and whether there is a conserved core set of SASP genes and/or component of the SASP regulatory mechanism that can be reliably targeted. Such an understanding would have sweeping implications for many different aspects of normal physiology and disease.

Senescence as an outcome of cancer therapy

Despite its discovery and frequent study in primary cells, senescence can also occur in cancer cells. More than 20 years ago, it was observed that classical methods of chemotherapy, like doxorubicin and ionizing radiation, are cytotoxic at high doses, but can be cytostatic at lower doses. Cancer cells in which these treatments induced cytostasis were then shown to have a phenotype similar to primary cells undergoing

replicative senescence: activation of p21 and p53, SA-β-gal expression, enlarged and flattened morphology, and reduced proliferative capacity following removal of the trigger, among other markers [72] This finding was then extended to an *in vivo* model: using SA-β-gal, p53, and p16 expression as markers, samples from breast cancer patients receiving neoadjuvant chemotherapy were shown to contain senescent cells [73]. Originally termed SLP for senescence-like phenotype, this phenomenon is now recognized as a legitimate form of senescence, known as therapy-induced senescence (TIS).

In addition to traditional chemotherapy, TIS can also be an outcome of treatment with a class of targeted cancer drugs called CDK4/6 inhibitors (CDK4/6i) [74]. An alternative strategy to typical, cytotoxic chemotherapies is to create drugs that induce cytostasis, which act by eliminating the proliferative potential of the tumor. Cancer is, fundamentally, a disease of inappropriate, uncontrolled cell proliferation, and thus components of the cell cycle machinery have long been targets of interest as cancer chemotherapeutics. Cyclin-dependent kinases (CDKs) are a family of serine/threonine kinases that regulate progression through the mitotic cell cycle. In order to commit to the cell cycle and replicate, a cell must first overcome the barrier of RB, which binds to the transcription factor E2F and represses transcription of the pro-proliferative E2F target genes. Phosphorylation of RB, which destabilizes this interaction, is performed sequentially, first by CDK4 or its structurally similar kinase CDK6, in complex with a D-type cyclin subunit, and then by cyclin E/CDK2 complexes. An additional layer of regulation for this transition is provided by CDK inhibitors, like p16, which inhibits CDK4 and CDK6, and p21 and p27, which inhibit CDK2 [75]. Dysregulation of the RB

pathway occurs in most human cancers, either through mutation or loss of p16 or RB, overexpression of Cyclin D, or genomic or transcriptional alterations that lead to activation of CDK4/6 [76].

As members of this key RB signaling axis and vital regulators of the G_1->S transition of the cell cycle, CDK4 and CDK6 are particularly attractive druggable candidates, and since 2017, three CDK4/6i have been FDA approved for use in humans [77]. Since their introduction, lingering questions have persisted about their mechanism of action *in vivo.* First, it has been difficult to determine whether these drugs induce senescence in patients, as they do in cultured cells and in mouse models, due to the lack of clear senescent markers that are applicable to patient samples [74]. Secondly, therefore, it remains unknown whether senescence is a desirable outcome of chemotherapy. From a simple cell cycle perspective, permanent exit from the cell cycle is an ideal response to treatment. However, it is well-established that senescent cells are not merely growth arrested, and that the SASP can have many effects that are both pro- and anti-tumorigenic (Fig. 1.1). And finally, as discussed above, the extent to which the regulation of senescence is conserved in response to different stimuli has long been a subject of debate in the field, and the extent to which senescence in a cancer cell is the same as senescence in a primary cell is a particularly controversial topic. Further study of these drugs, including a deeper understanding of their mechanism of action and its connection to senescence, is essential for maximizing the clinical benefit of CDK4/6i.

Thesis Objectives

In the 60 years since the discovery of cellular senescence, a great deal has been learned about how specific types of cells achieve this state in response to specific stimuli, but many questions persist as to whether senescence is a single cellular state or a collection of similar states that share common properties. Whether phenotypes, mechanisms, and properties discovered in one context of senescence are applicable to other contexts remains unclear. This is complicated by the fact that the most essential task, the identification of senescent cells in culture and particularly in tissues, is convoluted. In my thesis work, I attempt to address some of these outstanding issues in the field.

In chapter three, I identify *ANGPTL4,* a secreted protein and member of the SASP, as an important regulator of the later stages of senescence in the context of cancer cells undergoing TIS in response to CDK4/6i. I demonstrate that the loss of *ANGPTL4* prevents liposarcoma cells from committing to stable growth arrest and dampens their ability to express the pro-inflammatory arm of the SASP. I also determine that this role of *ANGPTL4* is not unique to liposarcoma cells but is applicable in lung cancer cell lines as well.

In chapter four, I investigate the similarities and differences between two distinct CDK4/6i, palbociclib and abemaciclib, as inducers of senescence in liposarcoma cancer cell lines. I then translate my *in vitro* findings to the clinic by using *ANGPTL4* as a marker of senescence to study the response of liposarcoma patients enrolled in a Phase II clinical trial of abemaciclib. I show that abemaciclib induces both cellular senescence and

inflammation in liposarcoma patients, and that the combination of these two phenotypes results in increased risk of progression.

Finally, in chapter 5, I examine the role of *ANGPTL4* in senescence in more naturally occurring, physiologically relevant contexts. I demonstrate that it can also be used a marker of senescence in both human and mouse primary cells undergoing senescence in response to different triggers. I also make use of an *in vivo* model of excisional wound healing, a process that is dependent upon senescent cells, to show that *ANGPTL4* is essential for the recruitment of the immune system and other processes that are involved in normal wound healing. Collectively, my work nominates *ANGPTL4* as both a regulator and a hallmark of senescence in multiple different contexts and cell types and provides a new tool for studying senescent cells *in vitro* and *in vivo*.

Chapter 2: Materials and Methods

Cell culture: The well-differentiated and dedifferentiated liposarcoma (WD/DDLS) cell lines used in this thesis were provided by Samuel Singer's lab and have been extensively characterized [20, 78]. The non-small cell lung cancer cell lines A549, H358, and H1975 were obtained from ATCC. Mouse embryonic fibroblasts (MEFs) were derived as previously described [79]. Human primary dermal fibroblasts were obtained from Cell Biologics. All cell lines were maintained in Dulbecco's Modified Eagle's medium with high glucose (4,500 mg/L) supplemented with 10% heat inactivated fetal bovine serum and 2 mM L-glutamine, except for the HPDFs, which were grown in media from the manufacturer according to their instructions. Palbociclib and trametinib were purchased from Selleck Chemicals and used at the concentrations indicated in the figure legends and text. Recombinant human ANGPTL4 was purchased from RD Biosystems (Full-length: 4487-AN-050; C-terminal: 3485-AN-050, N-terminal: 8249-AN) and reconstituted in sterile PBS. A549 cells treated with palbociclib for 2 days were then incubated with palbociclib + 100, 1000, or 2000 ng/mL rANGPTL4 for a total of 6 days, with one media change.

Lentiviral constructs: $DDLS^{TetON\text{-}FMDM2}$ cells were generated by transduction of FLAG-tagged MDM2 cloned into the LT3 lentiviral vector backbone and selected with puromycin. Three lines were isolated from the transduced cells and results were similar in all cases. Lentiviruses were generated as described previously [31] in 293T cells by triple

transfection with the vector of interest, psPAX2, and pMD2.G. $A549^{EGFP}$ and $A549^{ANGPTL4}$ cell lines were established by transduction of retrovirus produced using the vectors pBabeEGFP and pBabeANGPTL4, pUMVC, and pVSVG-CMV (all obtained from Addgene). Generation of retrovirus, transduction, and selection were performed similarly to the lentiviruses. Infected cells were selected using puromycin (1 μg/mL) for 2 days. shRNA hairpins were delivered in the pLKO.1 vector (Open Biosystems). shRNA sequences can be found in Table 2.1.

Gene	Gene ID	Clone ID	Hairpin targeting sequence
ANGPTL4	51129	TRCN0000155024	GAGAGGCAGAGTGGACTATTT
		TRCN0000150798	GCAGAGTGGACTATTTGAAAT
IGFBP3	3486	TRCN0000072509	CCTCCATTCAAAGATAATCAT
		TRCN0000072511	CCAGCGCTACAAAGTTGACTA
IGFBP7	3490	TRCN0000080109	CCTCATCTGGAACAAGGTAAA
		TRCN0000077944	GCTGGTATCTCCTCTAAGTAA
PLAT	5327	TRCN0000050913	CCGCTGCACATCACAACATTT
		TRCN0000050917	GCTGGGAAGTGCTGTGAAATA

Table 2.1 Sequences of the shRNA hairpins used in this work.

Immunoblots: The amount of FLAG-tagged MDM2 was measured by immunoblot after cells were lysed with a buffer containing 50 mM Tris-HCl, pH 7.4, 250 mM NaCl, 5 mM EDTA, 0.5% NP40, 2 mM PMSF, and protease inhibitors. Tubulin was detected with the Santa Cruz Biotechnology C-11 antibody at 1:2000, and FLAG-MDM2 with the Sigma M2 FLAG antibody at 1:1000.

Senescence Assays: Senescence-associated beta-galactosidase (SA-β-Gal) was assayed using the Senescence β-Galactosidase Staining Kit (Cell Signaling Technologies 9860) according to the manufacturer's instructions. Senescence-associated heterochromatic foci (SAHF), ATRX foci, 53BP1 foci, γH2AX foci, BrdU incorporation, and clonogenic growth arrest assays were performed as described previously [20]. Colony formation was quantitatively determined by calculating the percent area of the well that contained colonies using ImageJ.

Real-time quantitative PCR: RNA was extracted from cells using the QIAGEN RNeasy kit according to the manufacturer's instructions. Complementary DNA (cDNA) was synthesized and qPCR performed on the QuantStudio 6 system as described previously [31]. Data was analyzed using the ΔΔCt method and changes in gene expression were plotted relative to untreated cell controls. Primer sequences can be found in Table 2.2.

RNA sequencing and analysis of cell lines: RNA was isolated as described previously [31]. Quality was checked on a BioAnalyzer to ensure a minimum RNA Integrity Value of 7. Libraries were then generated using 500 ng of input RNA per sample, according to the manufacturer's instructions for TruSeq mRNA Library Prep Kit V2 (Illumina) with 8 cycles of PCR. Libraries were pooled and run on an Illumina HiSeq

Gene name	Forward primer sequence	Reverse primer sequence
ACTB	CATGTACGTTGCTATCCAGGC	CTCCTTAATGTCACGCACGAT
RNA18S2	GTAACCCGTTGAACCCCATT	CCATCCAATCGGTAGTAGCG
ANG	CTGGGCGTTTTGTTGTTGGTC	GGTTTGGCATCATAGTGCTGG
ANGPTL4	GGCTCAGTGGACTTCAACCG	CCGTGATGCTATGCACCTTCT
CCL20	TGCTGTACCAAGAGTTTGCTC	CGCACACAGACAACTTTTTCTTT
CCNE2	GGAACCACAGATGAGGTCCAT	CCATCAGTGACGTAAGCAAACT
CDKN2A	ATGGAGCCTTCGGCTGACT	GTAACTATTCGGTGCGTTGGG
CSF1	TGGCGAGCAGGAGTATCAC	AGGTCTCCATCTGACTGTCAAT
CSF2	TCCTGAACCTGAGTAGAGACAC	TGCTGCTTGTAGTGGCTGG
CXCL1	AGGGAATTCACCCCAAGAAC	TGTTCAGCATCTTTTCGATGA
CXCL9	CCAGTAGTGAGAAAGGGTCGC	AGGGCTTGGGGCAAATTGTT
CXCL10	GTGGCATTCAAGGAGTACCTC	TGATGGCCTTCGATTCTGGATT
CXCL11	GACGCTGTCTTTGCATAGGC	GGATTTAGGCATCGTTGTCCTTT
IGFBP3	AGAGCACAGATACCCAGAACT	GGTGATTCAGTGTGTCTTCCATT
IGFBP5	ACCTGAGATGAGACAGGAGTC	GTAGAATCCTTTGCGGTCACAA
IGFBP7	CGAGCAAGGTCCTTCCATAGT	GGTGTCGGGATTCCGATGAC
IL-1A	AGATGCCTGAGATACCCAAAACC	CCAAGCACACCCAGTAGTCT
IL-1B	TTCGACACATGGGATAACGAGG	TTTTTGCTGTGAGTCCCGGAG
IL6	ACTCACCTCTTCAGAACGAATTG	CCATCTTTGGAAGGTTCAGGTTG
GFP	ACCCTGAAGTTCATCTGCA	GGACTTGAAGAAGTCGTGC
MMP1	AAAATTACACGCCAGATTTGCC	GGTGTGACATTACTCCAGAGTTG
MMP3	CGGTTCCGCCTGTCTCAAG	CGCCAAAAGTGCCTGTCTT
PLAT	AGCGAGCCAAGGTGTTTCAA	CTTCCCAGCAAATCCTTCGGG
SERPINE1	AGTGGACTTTTCAGAGGTGGA	GCCGTTGAAGTAGAGGGCATT
TIMP1	ACCACCTTATACCAGCGTTATGA	GGTGTAGACGAACCGGATGTC
TNFRSF11B	CACAAATTGCAGTGTCTTTGGTC	TCTGCGTTTACTTTGGTGCCA
Mouse Actb	GTGACGTTGACATCCGTAAAGA	GCCGGACTCATCGTACTCC
Mouse RNA18S2	GCAATTATTCCCCATGAACG	GGCCTCACTAAACCATCCAA
Mouse Angptl4	GCATCCTGGGACGAGATGAAC	CCCTGACAAGCGTTACCACA
Mouse Cdkn2a	CCCAACGCCCCGAACT	GCAGAAGAGCTGCTACGTGAA

Table 2.2 Primer sequences for qPCR analysis

2500 high output to obtain 40 million paired-end 125 nucleotide-length reads. The reads were aligned to the human reference sequence hg19 using the STAR software version_2.4.0c package [80]. Raw counts were inputted into R studio version 3.2.0 (cran.r-project.org) and differential gene expression determined using the Bioconductor package DESeq2 [81] comparing expression in growth arrested DDLS$^{\text{Tet-ON FMDM2}}$ cells (DoxCDK4i) to each of the time points. Significant changes in gene expression were set at a fold change cutoff of ±1.5 and a false discovery rate of 0.5% (padj<0.005). Heatmaps were generated using gplots software. Hierarchical cluster analysis was performed with the hclust function in R. Software from the Broad Institute [82, 83] was used to perform gene set enrichment analysis on the significantly altered transcripts identified by DESeq2 compared against the C5 Gene Ontology (GO) gene sets. Pathways with a false discovery rate of padj<0.05 were considered significant. A conserved SASP signature of 151 transcripts (Table 3.1) was compiled from the overlap of gene expression or cytokine production in nine different RNA-seq, microarray, and secretome studies [53, 60, 67, 84-89].

Single cell analysis of cell lines: Palbociclib-treated and control single cell suspensions were prepared following 10X Genomics guidelines for cultured cells. Suspensions were adjusted to concentration of 1000 cells / µL and loaded to one capture well to obtain 10,000 cells. 10X genomics libraries were prepared using v3 chemistry and sequenced to an average of 23,000 reads per cell quantifying expression for a median of 1509, and 2733 genes per cell for palbociclib-treated and control, respectively.

Sequence reads were aligned to the GRCh37/hg19 human genome reference using STAR [80] as implemented by the Cellranger v3.0.2 pipeline. Subsequently, we analyzed the resulting BAM file with velocyto to obtain gene read counts [90]. Merged treatment and control spliced read counts were used for clustering with Seurat [91] implementing the SCTransform pipeline, with 20 dimensions [92]. Differential expression analyses between palbociclib treated vs control, and within treated cells, comparing *ANGPTL4* high vs low were carried out in Monocle3 [93, 94]. Finally, a SASP score was computed based on joint expression of SASP upregulated genes at 28 days (*ANGPTL4, CDKN2A, CCL20, CSF1, CXCL1, CXCL5, CXCL9, CXCL16, CXCL11, IGFBP3, IL1A, IL1B, IL1RN, IL6, IL7R, IL12A, MMP3, PLAT, TNFRSF11B, FGF2, FGF7, CSF2, CSF3, SERPINE1, TIMP1, VEGFA*) using AddModuleScore [95]. For visualization, data was imputed using ALRA and kernel density estimates for cell expression were computed using Nebulosa [96]. Significance thresholds were set at an FDR corrected p-value ≤ 0.05. Gene set enrichment analysis (GSEA) was performed on the MSigDB v7.2 Hallmark, and Oncogenic gene sets using clusterProfiler [83, 97]

Clinical trial design: This was an investigator-initialed, single center non-randomized open-label phase 2 study. The trial was intended to evaluate the biological activity of abemaciclib. Eligible patients were adults with advanced Dedifferentiated Liposarcoma (DDLS), ECOG performance status of 0 or 1, and progression of disease by RECIST 1.1 in the 6 months prior to study entry. CDK4 amplification was not required at study entry (because it is nearly ubiquitous in this disease), but it was determined retrospectively using next-generation sequencing. Any number of prior systemic therapies were allowed,

including none. Patients were treated with 200 mg of abemaciclib by mouth twice daily in 4-week cycles. PFS at 12 weeks was the primary endpoint, defined as time from initiating abemaciclib treatment until disease progression according to RECIST 1.1. PFS at 12 weeks of > 60% was considered promising and a PFS of < 35% was considered not promising. With a one-stage design based on the exact binomial test, the study would be positive if 15 of 30 patients were progression-free at 12 weeks, with type I error 0.07 and type II 0.10 (Fleiss JL, Statistical Methods for Rates and Proportions (1981), pp 13-15.)

Samples were divided into two PFS groups based on PFS median (33 weeks). A univariate Cox proportional hazardous model was used to evaluate correlation between clinical variables (i.e., age at study entry, gender, number of prior lines of therapy) and PFS groups. Correlation was assessed with the Wald test, and adjusted p-values were calculated using false discovery rate. The protocol was approved by the Institutional Review Board of Memorial Sloan Kettering Cancer Center and all patients provided written informed consent

RNA sequencing and analysis of clinical samples: Total RNA from 21 samples was quantified and quality control was performed using Agilent BioAnalyzer. Samples then underwent polyA selection, and TruSeq library was prepared according to instructions provided by Illumina (TruSeq Stranded mRNA LT Kit, catalog # RS-122-2102), with 8 cycles of PCR. Samples were barcoded and run on a HiSeq 4000 in a PE100 run, using the HiSeq 3000/4000 SBS Kit (Illumina). An average of 43 million paired reads was generated per sample. Ribosomal reads represented 1.9–19% of the total

reads generated and the percent of mRNA bases averaged 69%.The fastqs were aligned using STAR v2.7.0f [80] and Ensembl v75 [98]. Quality control of the resulting bams was performed using Picard v. 2.22.0. Expression was quantified using Kallisto v0.46.2 [99] tool and gene level expression was summarized based on Enembl v75. Normalized transcripts per million (TPM) were calculated using Sleuth v0.30 (sleuth_to_martix). To identify differentially expressed genes between samples with high and low PFS, we used a linear model where gene expression represented the dependent variable, and PFS represented the independent variable (model: gene expression ~ PFS). No other clinical covariates were used in the model as they were not correlated with PFS. The Wald test was used to determine significantly expressed genes, and genes were considered differentially expressed if $p < 0.05$. Pathway enrichment analysis was performed on 50 Hallmark pathways downloaded from MSigDB (https://www.gsea-msigdb.org/gsea/msigdb/). R package clusterProfiler and gsea function in R [83, 97] were used in Gene set enrichment analysis. Genes were ranked by the effect size, which was calculated by multiplying P-value (P value based on comparison between two conditions high and low PFS) with the *sin* of log-fold change. These values were then used for the ranking of the genes, and weighted enrichment statistics and 100,000 gene set permutations were subsequently calculated and used for detection of significantly enriched pathways. We quantified immune cell populations using the immunedeconv R package v.2.0.2-1 [100]. Within this package, we used quanTIseq [101]from which Z-scores ($z = (x-\mu)/\sigma$) of each cell type, where x is the raw cell fraction, μ is the all samples mean, and σ is the standard deviation for all samples). These scores were used for hierarchical clustering of samples (i.e., maximum clustering distance).

Immunofluorescence and immunohistochemistry for patient biopsies:

RNAscope was performed on FFPE sections of patient biopsies following the manufacturer's instructions (ACD Inc). *ANGPTL4* mRNA was detected with ACD 455358 and *CDKN2A* mRNA (encoding both p16INK4A and p14ARF1) was detected with ACD 310188. Positive and negative control probes were provided by the manufacturer. 1:100 Tyramide Alexa Fluor 488 (Life Technologies, B40932) replaced the DAB step. Sections were counterstained with 10 mg/ml DAPI (Sigma-Aldrich, D9542) and mounted with Mowiol 18-88 mounting media (Sigma-Aldrich, 81365).

To quantify mRNA expression, slides were scanned on a Panoramic P250 Flash scanner (3DHistech, Hungary) using 20x/0.8NA objective lens. Tumor regions were identified in H&E-stained sections by pathology and exported as .tif files from those scans using Caseviewer (3DHistech, Hungary). Each image was divided into a grid and each tile was analyzed using ImageJ/FIJI (NIH, USA). Median filter, thresholding, and watershedding were used to segment the nuclei in the DAPI channel and obtain cell counts. Signal intensity was measured using a threshold, and maxima were found to determine foci counts per region. All tiles for a time point were then plotted and the median expression level defined. Changes in the distribution were assessed by both Mann-Whitney and Kolmogorov-Smirnov non-parametric tests ($p<0.05$). Quantifying the number of CD8, CD68, CD4, and FOXP3 cells, as well as Ki67-positive cells, was performed in the same way, except that the hemotoxylin and DAB signals were separated using color deconvolution in ImageJ/FIJI (NIH, USA) prior to counting.

Bayesian statistics: To conduct our analysis of the survival rates associated with triple positive versus other patients, we employed a Cox proportional hazards model with time-variable effects. The model is specified by first defining the survival function, $S(t) = \exp(-\gamma(t))$ as a measure of the survival probability after time *t*, where $\gamma(t)$is the cumulative hazard function. The cumulative hazard function defines the risk accumulated over the interval (0, t), and can be further specified as the time-integral over the instantaneous hazard rate $\gamma(t) = \int_0^t \lambda(s)ds$.

To make the model tractable and allow for variation between the triple positive and not-triple positive groups, we introduce the coefficient β which represents the effect of group on the instantaneous hazard rate. Further, we allow for β to be time varying, and model it as a Weiner process specified by $\beta(t+u) - \beta(t) \sim N(0,u)$ which allows the model to learn slowly varying changes in the effect size. The Cox proportional hazards model can thus be specified as:

1. $\lambda(t) = \lambda_0(t)\exp(\boldsymbol{x_i}\beta(t))$

where $\lambda_0(t)$is the baseline instantaneous hazard rate, and $\boldsymbol{x_i}$ is the group index. To define the full model, we discretize the continuous variable t into blocks of 3 days, and treat each patient as having been exposed to the hazard rate $\lambda(t)$up until either tumor growth or censorship. The model is fully specified by modeling the observations of tumor growth as a Poisson process with underlying rate parameter $\lambda(t)$:

2. $G_i^j \sim Pois\left(E_i^j \lambda^i(t_j)\right)$
3. $\lambda(t_j) = \lambda_0(t_j)\exp(\boldsymbol{x_i}\beta(t_{j+1}))$
4. $\lambda_0(t_j) \sim Gamma(\alpha, \beta)$

5. $\beta(t_{j+1}) - \beta(t_j) \sim N(0,1)$

where α and β were chosen to be 0.01, and where the subscripts *i* and *j* refer to the individual, and the discretized time interval, respectively.

We sampled the model using PYMC3's NUTS sampler with a burn-in trace of 1000, followed by 1000 samples from the posterior distribution. Our sampler showed strong convergence, with tight estimates of parameter $\beta(t_{j+1})$ up through the 1500 day mark. Our posterior estimates of exp(β) indicate an overall effect of senescence+inflammation being associated with a 58 percent increase in hazard rate, with significance of p=0.0373 (measured using a ROPE correlate, defined as any decrease in hazard associated with senescence+inflammation).

Wound healing: Wild-type (Angtpl4$^{+/+}$) and knockout (Angptl4$^{-/-}$) mice were obtained and subjected to full-thickness excisional wounding as previously described [102]. Wound biopsies were harvested at day 1, 5, or 10, fixed in 4% PFA-PBS overnight, and then embedded in paraffin. Sections of 5-μm thickness were used for subsequent RNAscope and immunofluorescence staining. Measuring the expression of RNA was essentially as described above for patient biopsies, with the following changes: *Angptl4* mRNA was detected with ACD 474618 and *Cdkn2a* was detected with ACD 411018, and sections were imaged using a confocal microscope at 63X magnification. For quantification of mRNA particles, ten images were taken at random within the

boundaries of each wound sample. The number of particles relative to the number of nuclei in each image was quantified using ImageJ.

Immunofluorescence for immune cell and myofibroblast markers, except for CD11b, was carried out as described previously [103]. The following primary anti-mouse antibodies were used: rabbit polyclonal CD3 (1:200: #A0452) from Dako (Agilent); rat monoclonal F4/80 (1:200; ab16911) from Abcam; monoclonal Cy3-conjugated anti-smooth muscle actin (anti-SMA; 1:1000; #C6198) from Sigma-Aldrich. Monoclonal keratin 6 antibody (# ab18586) from Abcam. Secondary antibodies used were fluorescent-labeled conjugates (Alexa Flour 488 or 647; Life technologies). All sections were scanned using a Mirax slide scanner (Zeiss). Analysis was completed using Panoromic viewer (3D Histech). CD11b cells were detected by staining sections with a rabbit monoclonal antibody (Abcam, ab133357) at 1 mg/ml on a Discovery XT processor (Ventana Medical Systems). The incubation with the primary antibody was done for 4 hours, followed by a 32-minute incubation with biotinylated goat anti-rabbit IgG (Vector Laboratories, PK6101) in 5.75 mg/ml blocker D, streptavidin-HRP and followed by 16 minute incubation with TSA Alexa 6347 (Life Technologies, B40958). Immunofluorescent signal was quantified as described previously [104].

Chapter 3: *ANGPTL4* regulates irreversible growth arrest and SASP gene expression during CDK4/6 inhibitor therapy-induced senescence

Introduction

Geroconversion: a new pathway into senescence

When cells exit the cell cycle from the G_1 phase, they can undergo a number of different cell fates: quiescence, senescence, apoptosis (programmed cell death), or differentiation (a process by which cells develop into more specialized, post-mitotic forms) [8]. Quiescence and senescence differ from apoptosis in that cells remain alive and metabolically active but are removed from the proliferative cell cycle, either temporarily or permanently. Classically, quiescence and senescence have been viewed as distinct, binary cell fates; a cell was thought to "choose" one or the other and then embark upon that path (Fig. 3.1A) [8, 105]. In recent years, however, evidence has shown that senescence can happen in two steps: first, cell cycle exit, followed by the gradual development of the other phenotypes associated with the senescent state. In other words, cells can first become quiescent, then convert into senescence, a process termed geroconversion (Fig. 3.1B) [106].

This transition was first described in the context of mTOR inhibition. In this model, the human fibrosarcoma cell line HT1080 was modified to allow for inducible expression of the cell cycle inhibitors p16 or p21. When expression was turned on, the cells would exit the cell cycle, but for the first two to three days, they retained the ability

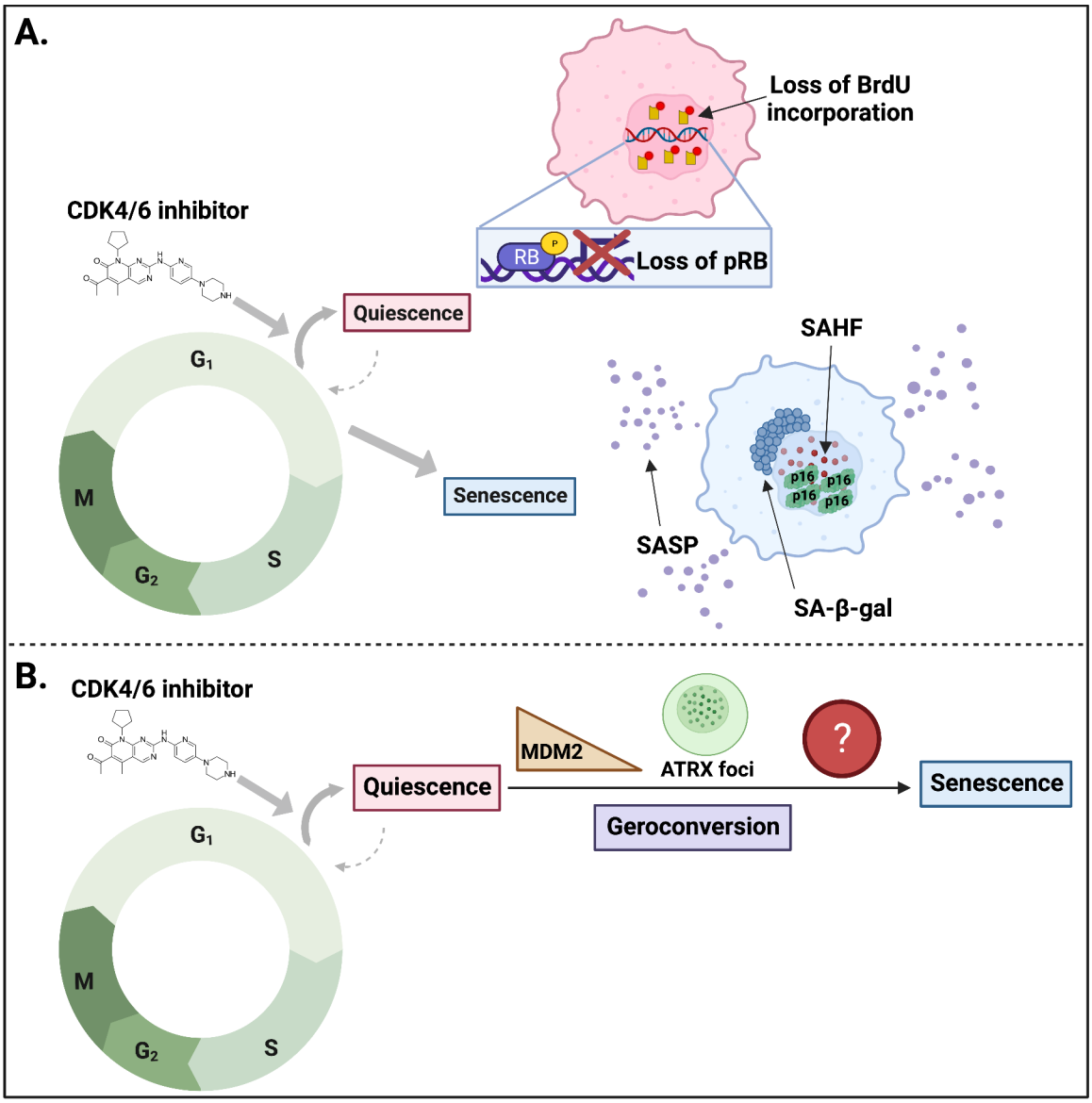

Figure 3.1 Two models of quiescence and senescence.

(A) The classical approach to cell cycle exit fates, in which a cell makes a binary choice in response to a trigger (here, treatment with CDK4/6 inhibitors) to enter quiescence (a reversible arrest characterized by loss of phospho-RB and BrdU incorporation) or senescence (an irreversible arrest characterized by expression of p16, senescence-associated heterochromatic foci (SAHF), senescence-associated β-galactosidase (SA-β-gal), and the expression of the senescence-associated secretory phenotype (SASP)). **(B)** A new model in which the trigger, in this case, CDK4/6 inhibitors, first causes cells to enter quiescence. From there, they can undergo geroconversion to become senescent. In the context of CDK4/6i, this process is dependent on MDM2 downregulation and ATRX foci formation, but little else is known about it.

to resume proliferation if expression of p16/p21 was turned off. After four days, the cells lost their proliferative capacity. Geroconversion in this model was linked to expression of mTOR, which remained active in the quiescent $p16^{+}/p21^{+}$ cells. Treatment with rapamycin, an mTOR inhibitor, blocked geroconversion and allowed quiescent cells to return to the cell cycle when expression of p16/p21 was turned off, even past the four day mark [107]. Geroconversion has also been observed as a naturally occurring phenomenon in the context of muscle satellite stem cells, which, in geriatric mice, lose their ability to reactivate in response to an injury and instead transition into a fully senescent state [108].

Work in the Koff lab over the last several years has identified a similar geroconversion pathway in a model of therapy-induced senescence (TIS) in cancer cell lines, induced by treatment with CDK4/6 inhibitors (CDK4/6i). The lab screened through 22 cell lines derived from human breast, lung, sarcoma, prostate, and glioma tumors, and found a conserved response to the drug: cells first exit the cell cycle into quiescence upon CDK4/6i, and from there, some undergo geroconversion to become senescent, while others remain reversibly arrested.

CDK4/6 inhibition can result in different cell fates in liposarcoma cell lines

To elucidate the molecular response of cancer cells to CDK4/6i, the Koff lab focused primarily on a set of patient-derived well-differentiated/de-differentiated (WD/DDLS) liposarcoma cell lines as a model. *CDK4* is amplified in more than 90% of WD/DDLS tumors, making this disease a prime candidate for treatment with CDK4/6i [109]. The clinical usage of CDK4/6i in patients with WD/DDLS will be discussed in more detail in **Chapter 4.**

Former members of the lab characterized the response of the WD/DDLS cell lines to treatment with palbociclib, a CDK4/6i. They determined that these cells first exit the cell cycle into quiescence, and from there, a subset of cell lines can undergo geroconversion to become senescent [20]. We term cell lines that undergo quiescence in response to CDK4/6i as non-responders, and cell lines that undergo senescence in response to CDK4/6i as responders. It was noted, in comparing responder and non-responder cell lines, that MDM2 protein levels decreased following CDK4/6i in responders but remained stable in non-responders. Further experiments showed that knocking down MDM2 in cycling cells was sufficient to induce senescence, and that forcing MDM2 expression and/or stabilizing MDM2 levels in CDK4/6i-treated cells was sufficient to prevent cells from moving along the geroconversion pathway, maintaining them instead in quiescence. These findings suggest that the decision of a quiescent cell to undergo geroconversion in response to CDK4/6i is dependent, at least in part, on the ability to reduce cellular levels of MDM2.

It is important to note that this finding is not unique to liposarcoma cell lines, in which *MDM*2, which is located near *CDK4* on chromosome 12, is also frequently amplified. The same link was established in many other cancer cell lines, including breast cancer, lung cancer, and prostate cancer [20, 31]. Additionally, the absolute levels of MDM2, either before or after treatment, are not linked to the quiescence/senescence decision. It is the delta, the change in level from pre-treatment to post-treatment, that is important for geroconversion.

In addition to MDM2, a second regulator of geroconversion in response to CDK4/6i has been identified: ATRX, a member of the SWI/SNF family of chromatin

remodelers. ATRX is recruited into nuclear foci that increase in number as cells become senescent. Cells in which ATRX has been knocked down cannot progress into senescence and remain trapped in quiescence in response to CDK4/6i. ATRX foci, therefore, are both a marker of senescence and a regulator of the geroconversion pathway in this context. Although the role of ATRX in senescence was discovered in CDK4/6i TIS, it is not limited to this model; ATRX foci increase in every type of senescence we have examined thus far [31] (**Chapter 5).**

The development of a synchronized system allows temporal separation of senescent phenotypes

Aside from MDM2 and ATRX, little is known about the regulation of the geroconversion pathway in response to CDK4/6i (Fig. 3.1B). A deeper understanding of how cells commit to transition into senescence would have important applications to cancer therapy, as well as to other fields of biology that are connected to senescence, like aging. To that end, Mary Klein, a former graduate student in the lab, created a system that would allow us to study geroconversion in enriched populations of synchronized cells. She took advantage of the fact that MDM2 can be used to control the decision between quiescence and senescence and developed a cell line with inducible MDM2 expression. One of our liposarcoma responder cell lines, LS8817 (hereafter referred to as simply as DDLS), was transduced with a tetracycline inducible (Tet-ON) MDM2 expression vector. These cells were selected with puromycin and single cell cloned to yield a new cell line, $DDLS^{Tet\text{-}ON\ FMDM2}$ (Fig 3.2A). In these cells, treatment with 10 μg/mL doxycycline induces expression of FLAG-tagged MDM2 (F-MDM2). Adding 0.1 μM palbociclib

along with doxycyline then arrests the cells in quiescence, where they can be stably maintained for at least 10 days by continued addition of both doxycycline and palbociclib. Progression into senescence is inhibited by the doxycycline, which continuously drives expression of F-MDM2. Once doxycycline is removed, however, F-MDM2 levels decrease over the course of 72 hours, and in the continued presence of 0.1 μM palbociclib, the cells begin to move along the geroconversion pathway (Fig 3.2A-B). This system is the first that induces and distinguishes between quiescence and senescence using the same trigger, with F-MDM2 expression acting as a molecular switch to control between the two states.

The advantage of using this system over adding CDK4/6i to a population of asynchronously cycling cells is that accumulating the cells in quiescence first allows them to progress into senescence in synchrony, which adds resolution to the temporal mapping of senescence markers. Using this system, Mary was able to show that ATRX foci are an early phenotype, reaching their peak around 3 days after release into palbociclib (Fig. 3.2C). Senescence-associated beta-galactosidase (SA-β-gal) and senescence-associated heterochromatic foci (SAHF, measured using HPγ foci) are mid-markers, peaking around day 5 (Fig. 3.2D-E). Notably, stable growth arrest doesn't occur until day 14 (Fig. 3.2F). Thus, using this system, Mary was able to show that many of the phenotypes commonly used to define senescent cells are temporally separated from, and occur earlier than, irreversible exit from the cell cycle. This is a particularly important

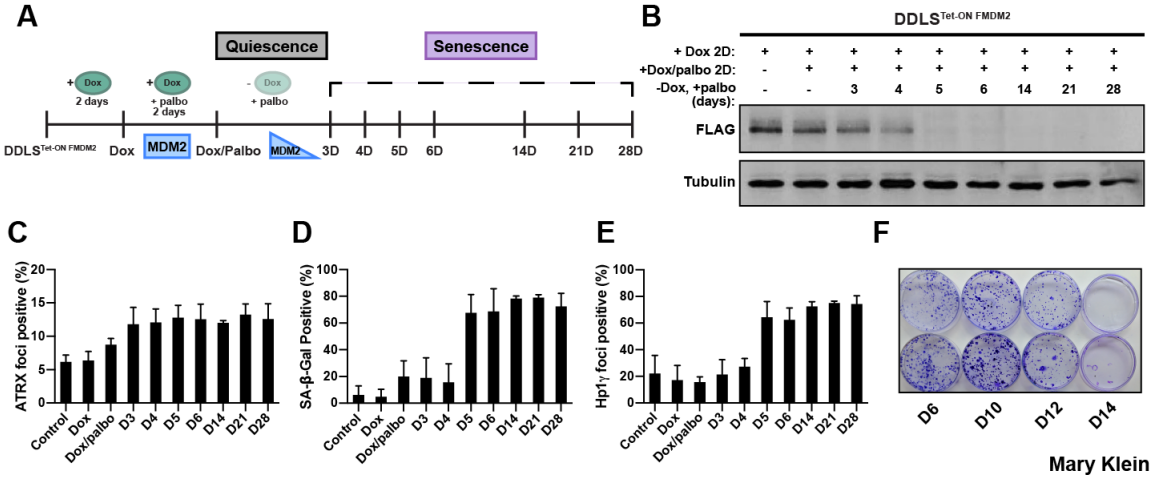

Figure 3.2 The synchronized DDLS$^{Tet\text{-}ON\ FMDM2}$ system allows for the temporal mapping of senescence phenotypes.

(**A**) Schematic of the DDLS$^{Tet\text{-}ON\ FMDM2}$ system. Cells were pre-treated with 10 μg/mL doxycycline (dox) for two days, followed by dox/0.1 μM palbociclib (palbo) for two days to induce cell cycle exit, then incubated in palbo alone. Cells were harvested at the indicated times. **(B)** Whole cell lysate was prepared and proteins detected by immunoblot with the antibodies indicated. The blot is representative of at least six independent biologic replicates. (**C-F**) Senescence status was assessed at each time point by quantifying the number of ATRX foci per cell (C), the percentage of cells expressing SA-β-gal (D), and the percentage of cells with HP1γ^{+} SAHF (E). The data shown are mean ± SD from at least three and as many as nine independent experiments. Irreversible growth arrest was assessed by re-plating cells at single cell density in drug-free media, culturing for 2-3 weeks, and staining with crystal violet (F). A representative plate with duplicate wells is shown.

finding, given that cells are often labeled as "senescent" because they express SA-β-gal. While this marker does occur in senescent cells and is generally easy to assay, the DDLS$^{\text{Tet-ON FMDM2}}$ system demonstrates that cells can express SA-β-gal and other "senescent" phenotypes without having progressed far enough into the state to commit to stable growth arrest.

Three replicates of this DDLS$^{\text{Tet-ON FMDM2}}$ time course were performed, and samples from cycling, quiescent (D0), and 3, 4, 5, 6, 14, 21, and 28 days of palbociclib treatment were sent for bulk RNA sequencing. DESeq2 analysis was performed to identify transcripts whose expression changed significantly during geroconversion, with significance defined as ±1.5 fold-change cutoff and $p_{adj}<0.005$. 819 transcripts were found to be significantly up-regulated (Fig. 3.3A) or down-regulated (Fig. 3.3B) as cells moved along the pathway from quiescence into senescence. When I first joined the lab, my goal was to sift through this sequencing data and use it to identify relevant genes that contribute to the regulation of geroconversion in response to CDK4/6 inhibitors.

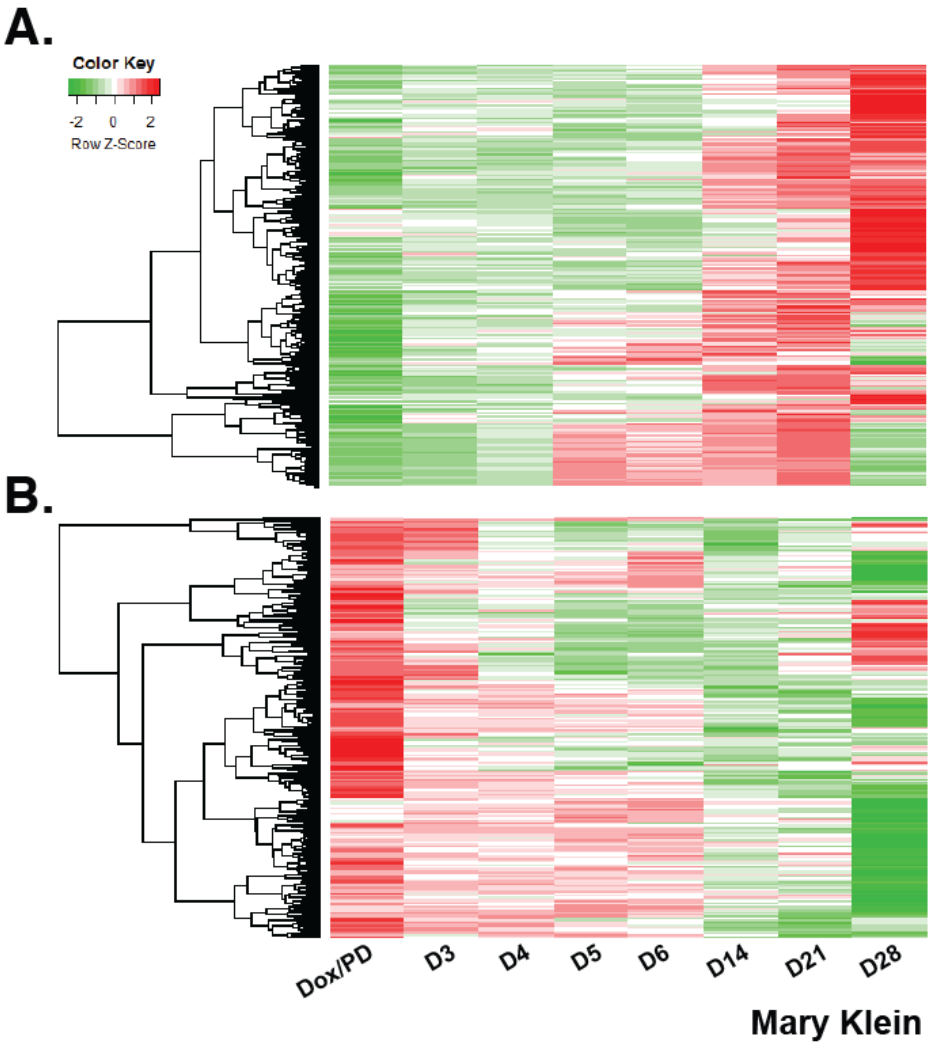

Figure 3.3 Heatmap of transcriptional changes that occur during CDK4/6i TIS in DDLS$^{Tet\text{-}ON\ FMDM2}$ cells.

(A-B) DEseq2 analysis was performed comparing quiescent cells treated with doxycycline + palbociclib and those released from doxycycline into palbociclib alone. The heatmap represents the average Z-score of changes in mRNA levels. A ±1.5 fold-change cutoff and p_{adj}<0.005 were used to assess significance. Transcripts whose expression mostly increased with time are shown in (A), and transcripts whose expression mostly decreased with time are shown in (B).

Results

The onset of stable growth arrest correlates with SASP gene expression in DDLS$^{Tet\text{-}ON\ FMDM2}$ cells

DESeq2 analysis identified 819 transcripts whose expression significantly changed in DDLS$^{Tet\text{-}ON\ FMDM2}$ cells undergoing geroconversion, when compared to quiescent cells. To begin to narrow down this list to a more manageable number of targets, we compared it with the C5 gene ontology (GO) gene sets (Fig 3.4A). In the early timepoints (D5 and D6), the top GO terms were associated with cell cycle exit, including processes related to mitosis, organelle fission, chromosome segregation, etc. In the later time points (D14 and D28), the top GO terms were mostly related to extracellular processes, including the immune response, cellular response to stress, response to external stimulus, etc. The common theme among these transcripts suggested that the foremost process occurring in senescent cells at these later times points is the SASP.

To delve further into the role of the SASP in DDLS$^{Tet\text{-}ON\ FMDM2}$ cells, Mary and I performed a literature review and compiled a list of 147 genes that have previously been implicated as members of the SASP in different senescent contexts (Table 3.1) [53, 59, 67, 84-89]. We then compared that list with the 819 transcripts that were significantly changed during our palbociclib time course and found 37 transcripts in common (Fig. 3.4B). Thus, we were able to define a SASP profile specific to DDLS$^{Tet\text{-}ON\ FMDM2}$ cells undergoing geroconversion (Fig. 3.4C). The individual SASP factors are listed in Table 3.2, categorized based on the day on which their expression was first significantly changed, and color coded based on whether their expression increased or decreased at

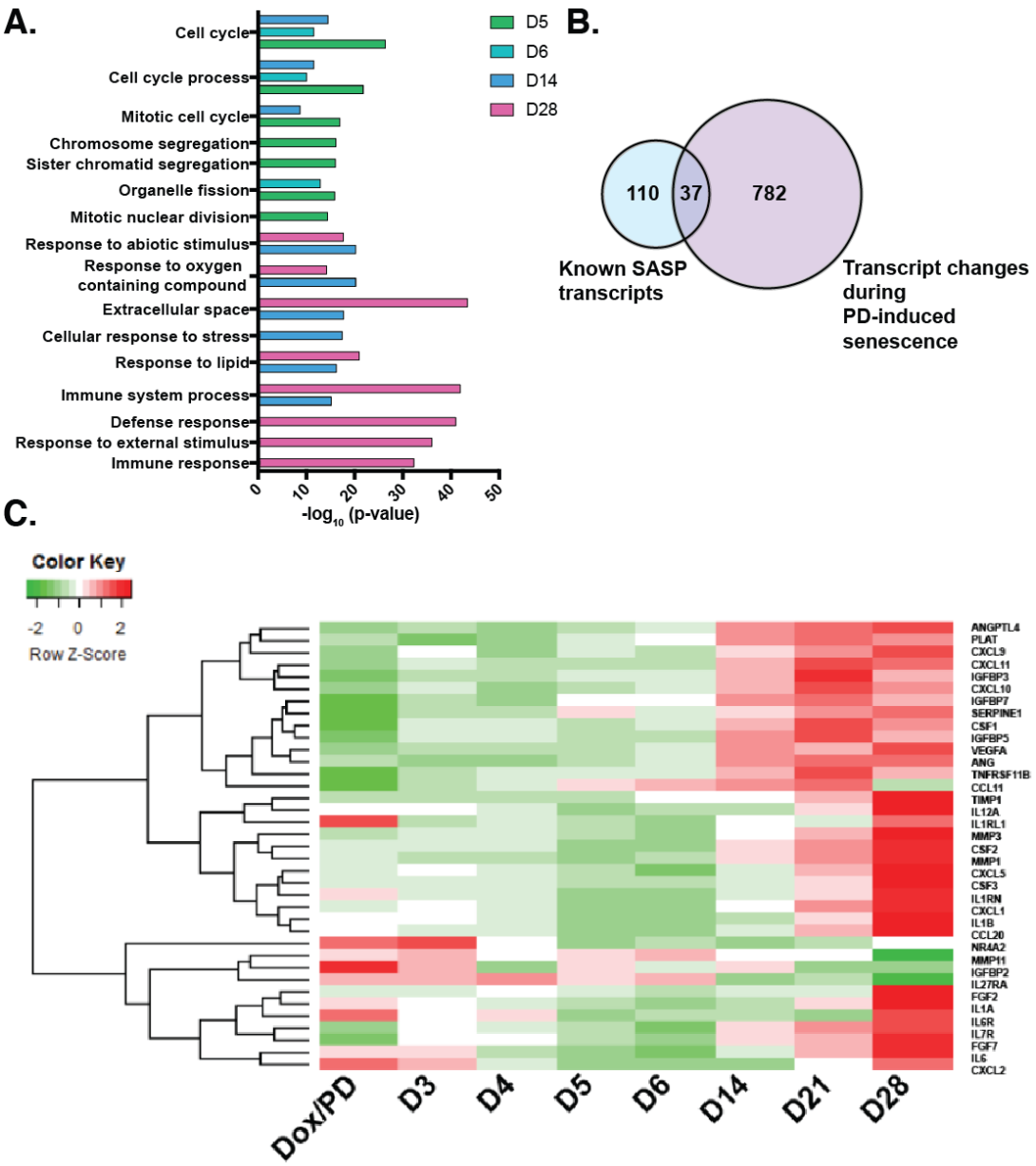

Figure 3.4 Gene ontology highlights the increase in SASP gene expression during late stage TIS in DDLS$^{\text{Tet-ON FMDM2}}$ cells.

(**A**) Transcripts from Fig. 3.3 were analyzed using the C5 gene ontology (GO) gene sets. The top GO terms are shown on the y-axis. The false discovery rate is indicated on the x-axis. (**B**) 819 protein-coding transcripts were compared to a 147-transcript SASP profile derived from literature review and shown in Table 3.1. **(C)** The 37 transcripts identified in the overlap in (B) were used to create a DDLS$^{\text{Tet-ON FMDM2}}$ SASP-specific heatmap.

ADIPOQ	CD9	FGF9	IL1RN	ITGA2	TGFB1
AGRP	CD55	FLT3LG	IL2	ITPKA	TGFB3
ANG	CNTF	GABRA2	IL2RA	KITLG	THPO
ANGPT2	CPE	GDNF	IL3	LEP	TIMP1
ANGPTL4	CSF1	GEM	IL4	LTA	TIMP2
AREG	CSF2	GMFG	IL4R	MIF	TIMP3
AXL	CSF3	HGF	IL5	MMP1	TIMP4
BDNF	CX3CL1	ICAM1	IL6	MMP2	TNF
BMP4	CXCL1	ICAM3	IL6R	MMP3	TNFRSF1A
BMP6	CXCL2	IFNG	IL6ST	MMP11	TNFRSF1B
BTC	CXCL5	IGF1	IL7	MST1	TNFRSF10C
CCL1	CXCL6	IGF1R	IL7R	NFKB1	TNFRSF10D
CCL2	CXCL8	IGF2	IL10	NFKB1E	TNFRSF11B
CCL7	CXCL9	IGF2R	IL11	NR4A2	TNFRSF18
CCL8	CXCL10	IGFBP1	IL12A	NTF3	TNFSF14
CCL11	CXCL11	IGFBP2	IL12B	OSM	TNFSF18
CCL13	CXCL13	IGFBP3	IL13	PCNX1	TUBGCP2
CCL17	CXCL16	IGFBP4	IL13RA2	PDGFA	TYRO3
CCL19	CXCR2	IGFBP5	IL15	PDGFB	VEGFA
CCL20	EGF	IGFBP6	IL16	PIGF	VGF
CCL22	EGFR	IGFBP7	IL17D	PLAT	WNT2
CCL24	FAM131A	IL1A	IL17RB	PLAU	XCL1
CCL25	FAS	IL1B	IL18BP	PLAUR	
CCL26	FGF2	IL1R1	IL20RB	PTGES	
CCL28	FGF7	IL1RL1	IL27RA	SERPINE1	

Table 3.1 Transcript signature for a common SASP profile.

A literature review identified these genes as common components of the SASP during different types of senescence.

Day 5	Day 6	Day 14	Day 21	Day 28
CCL11	IL1RL1	ANGPTL4	CCL20	ANG
CXCL2		CSF1	CSF3	CSF2
IL6		CXCL10	CXCL5	CXCL1
IL6R		CXCL11	IGFBP5	CXCL9
NR4A2		IGFBP3	IL12A	FGF2
		IGFBP7	IL1A	FGF7
		MMP3	IL1B	IL6
		PLAT	IL1RN	IL7R
		TNFRSF11B	TIMP1	MMP1
				SERPINE1
				VEGFA
				IGFBP2
				IL27RA
				MMP11

Table 3.2 Established SASP genes whose expression changes significantly during CDK4/6i TIS in DDLS$^{\text{Tet-ON FMDM2}}$ cells.

The 37 previously-identified SASP genes whose expression changed in our RNA sequencing are listed on the day at which they were first significantly altered. Expression of transcripts listed in green was significantly reduced, while expression of transcripts listed in red was significantly increased. *IL6* is listed twice, as it appeared significantly reduced first at Day 5, and then became significantly increased at Day 28.

that time point. We noticed that the first major time point at which the SASP began to increase in expression was day 14, the same day at which stable growth arrest was initiated. This led me to wonder whether there might be a relationship between the SASP and irreversible growth arrest, two of the foundational phenotypes of senescent cells.

To investigate this hypothesis, I focused on the SASP transcripts that first arise coincidently with stable growth arrest, at day 14. Nine genes were first changed significantly at this point (adjusted *p*-value <0.001) (Table 3.2). To validate these changes and determine whether they were seen in other cell lines undergoing senescence, I performed qPCR on six asynchronous sarcoma cell lines treated with 1 μM palbociclib for seven days, a time at which many senescence hallmarks are already elaborated (Fig. 3.5). I reasoned that analyzing mRNA expression in CDK4/6 inhibitor-treated cells using a secondary method would ensure that we focus on changes that are not mere artefacts of the synchronization procedure or the sequencing approach. Three of the cell lines (LS8817, LS141, LS0082) become senescent in response to palbociclib treatment, and three (LS8107, LS7785-1, U2OS) become quiescent under the same conditions [20, 31]. I also generated quiescent, serum-starved LS8817 cells [110], and included an independent biologic replicate of mRNA obtained from quiescent cells and day 14 cells from the DDLS$^{\text{Tet-ON FMDM2}}$ time course. Of these transcripts, *ANGPTL4* was the most consistently induced in senescent, but not quiescent, cells (Fig. 3.5). This raised the possibility that *ANGPTL4* might be a trigger for irreversible arrest during geroconversion in response to CDK4/6 inhibition.

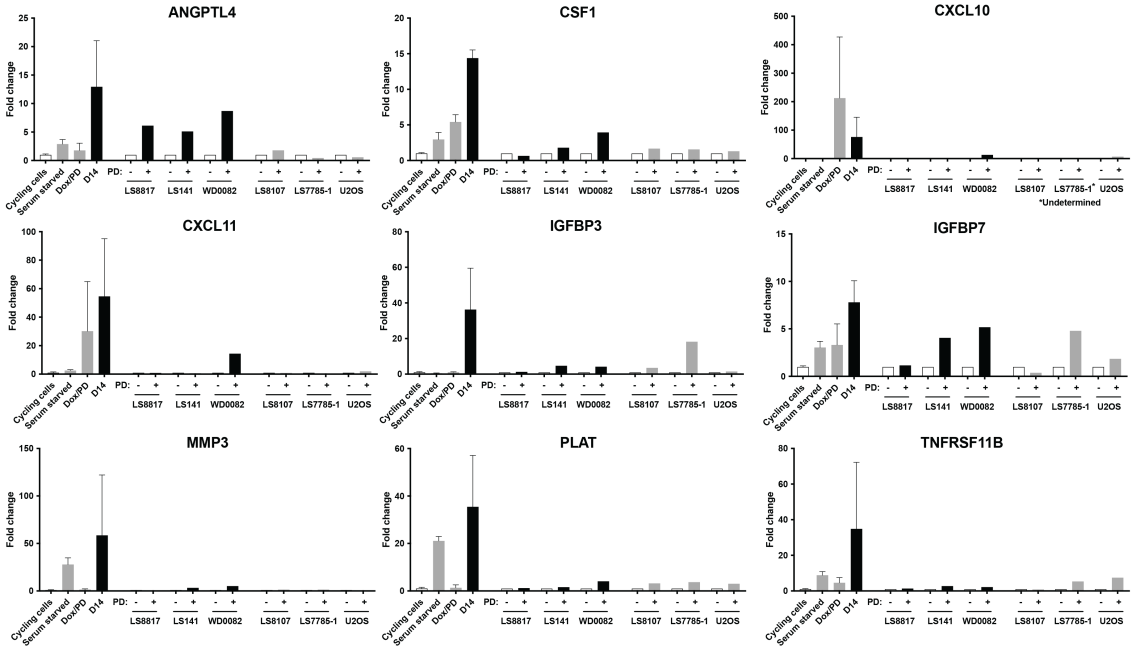

Figure 3.5 Analysis of SASP genes arising coincidently with irreversible growth arrest in DDLS$^{\text{Tet-ON FMDM2}}$ cells.

Transcript levels of nine SASP genes arising at day 14 were validated in synchronized cells during quiescence (dox/PD) and 14 days after doxycycline removal, when cells become senescent (D14). The data shown are mean ± SD of three independent experiments. Additionally, transcript levels were measured in quiescent, serum-starved LS8817 cells, and in six palbociclib-treated cell lines (1 μM for seven days) that have different responses to palbociclib. Bar color represents cell cycle state (white, cycling; grey, quiescent; black, senescent).

Knockdown of ANGPTL4 prevents the establishment of irreversible growth arrest in response to treatment with CDK4/6 inhibitors

To determine whether the relationship between the SASP and stable growth arrest was a functional one, rather than merely a temporal one, Mary and I performed an experiment in which we knocked down individual SASP factors using shRNA hairpins and examined the effect on various phenotypes relating to the senescent state. $DDLS^{Tet\text{-}ON\ FMDM2}$ cells were brought to quiescence by treating first with doxycycline for two days, and then with doxycycline/0.1 μM palbociclib for two days. At this point, two distinct shRNA hairpins against each SASP factor were individually introduced into cells using lentiviral transduction. Cells were maintained in the combination of doxycycline/palbociclib for a further two days while undergoing the process of selection with puromycin. After selection, the cells were placed in 0.1 μM palbociclib for a further 21 days, at which point senescent phenotypes were assessed. Three replicates of this experiment were performed. The benefit of doing this experiment in cells that had already been brought to the point of quiescence is that we were able to separate the effect that these genes had on geroconversion from any other role that they might play during the normal cell cycle, or during the initial process of cell cycle exit.

Although a number of different SASP gene knockdowns were tested, for simplicity, the data from just four of those genes are presented here: *ANGPTL4, IGFBP3, IGFBP7,* and *PLAT.* Validation of gene knockdown was done with qPCR, and only samples in which gene expression was reduced by at least 50%, compared to the scramble control treated with palbociclib for 21 days, were used for subsequent analysis

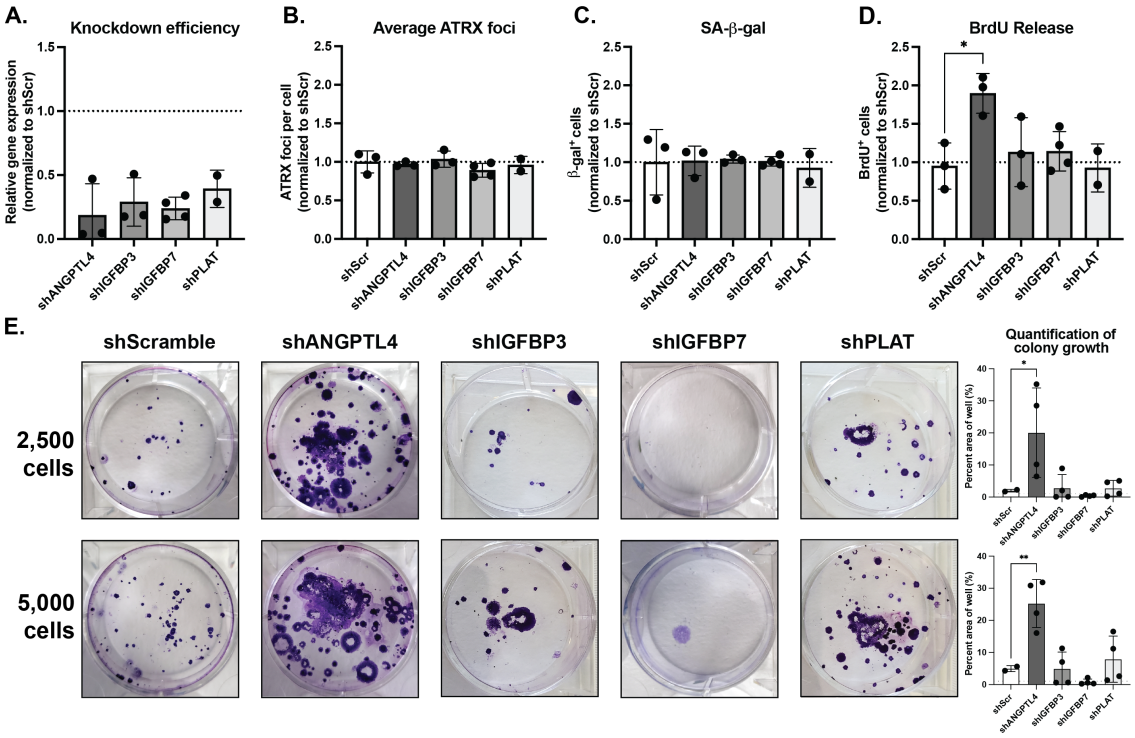

Figure 3.6 *ANGPTL4* is necessary for palbociclib-induced irreversible arrest.

Quiescent DDLS$^{\text{Tet-ON FMDM2}}$ cells were infected with one of two different lentiviruses, and, after selection in puromycin, were shifted to palbociclib alone. (**A**) After 21 days in palbociclib, the success of the knockdown was determined by measuring gene expression using qPCR. Only replicates with knockdown efficiency ≥ 50% are shown here and used for subsequent analysis. **(B-D)** Senescence status was assessed by quantifying the number of ATRX foci (B) and the percentage of cells expressing SA-β-gal (C). (**D-E**) Cells were removed from palbociclib and their ability to re-enter the cell cycle was assessed by incubation for 48 hours with 20 μM BrdU (D) and by a long-term clonogenic growth assay (E). *p < 0.05, **p<0.01 by one-way ANOVA.

(Fig. 3.6A). Knockdown of the various SASP factors did not change the accumulation of earlier senescence markers, such as ATRX foci (Fig. 3.6B) and SA-β-gal (Fig. 3.6C). Thus, disruption of SASP expression does not affect the appearance or maintenance of upstream phenotypes on the geroconversion pathway.

To determine if loss of any of these genes would affect the ability of cells to undergo irreversible growth arrest, we performed two assays. After the cells had been released into palbociclib for 21 days, we plated them in the absence of drug and the presence of BrdU for 48 hours, then quantified BrdU incorporation as a measurement of re-entry into S-phase. We also plated the cells at low density, again in the absence of drug, and let them form colonies for a subsequent three weeks to determine if the cells were able to continuously grow and divide over time. Knockdown of *ANGPTL4* with either hairpin significantly increased the proportion of cells that re-entered the cell cycle upon removal of palbociclib, compared to the scramble control (Fig. 3.6D). This effect was not reproducibly observed with knockdown of any of the other SASP genes. Additionally, when allowed to grow for several weeks, *ANGPTL4* knockdown cells formed colonies at a significantly higher rate than the scramble control (Fig. 3.6E). Again, this effect was not consistently seen with the other SASP gene knockdowns; although one hairpin against *PLAT* did result in colony formation, the second hairpin did not, whereas both hairpins against *ANGPTL4* resulted in significant colony formation.

Collectively, these data suggest that *ANGPTL4* is necessary for liposarcoma cells to undergo stable growth arrest in response to CDK4/6 inhibitors but is dispensable for the induction of senescence phenotypes that occur earlier on the geroconversion pathway.

Single cell seq confirms that ANGPTL4^{+} cells are also SASP^{+} cells

The previous experiment showed that *ANGPTL4* is essential for liposarcoma cells to commit to stable growth arrest in response to CDK4/6i. I next wanted to ask whether expression of *ANGPTL4* correlated with expression of other SASP genes and could thus be used as a marker of a cell that has committed to both stable growth arrest and to the elaboration of the SASP. In our time course RNA-seq experiment, expression of *ANGPTL4* occurred in the early phase of SASP development, at day 14, and continued to increase through day 28 (Fig. 3.4C). However, bulk RNA-seq cannot determine the percentage of the cell population that expresses a certain gene, nor can it show that expression of one gene correlates with expression of others within the same cell.

To answer this question, I performed another time course on the synchronized DDLS$^{\text{Tet-ON FMDM2}}$ cell line and compared the global transcriptional profiles of quiescent (day 0), and senescent cells (days 7, 14, 21, and 28) using single-cell RNA-seq. This experiment yielded 8,992 quiescent (D0) cells, 4,940 D7 cells, 4,076 D14 cells, 4,104 D21 cells, and 4,047 D28 cells. Cells were arranged into 25 unique clusters, of which #1, 5, 7, 9, 12, and 16 went extinct over the course of geroconversion, #0, 2, 6, 8, 10, 11, 13, 14, 15, and 17 expanded, and #19 and 20 were *de novo* from D7 (Fig. 3.7A). Given that palbociclib is a cytostatic agent, we predicted the cell cycle phase in our data and found that the vast majority of the cells were arrested in G1, although a few G2/M- and S-phase cells were also identified, particularly in clusters 10, 18, and 21 (Fig 3.7B). Senescent cells (D7-28) largely clustered separately from the quiescent (D0) cells, suggesting major changes in global transcription between the two states. D7 cells clustered close to, but

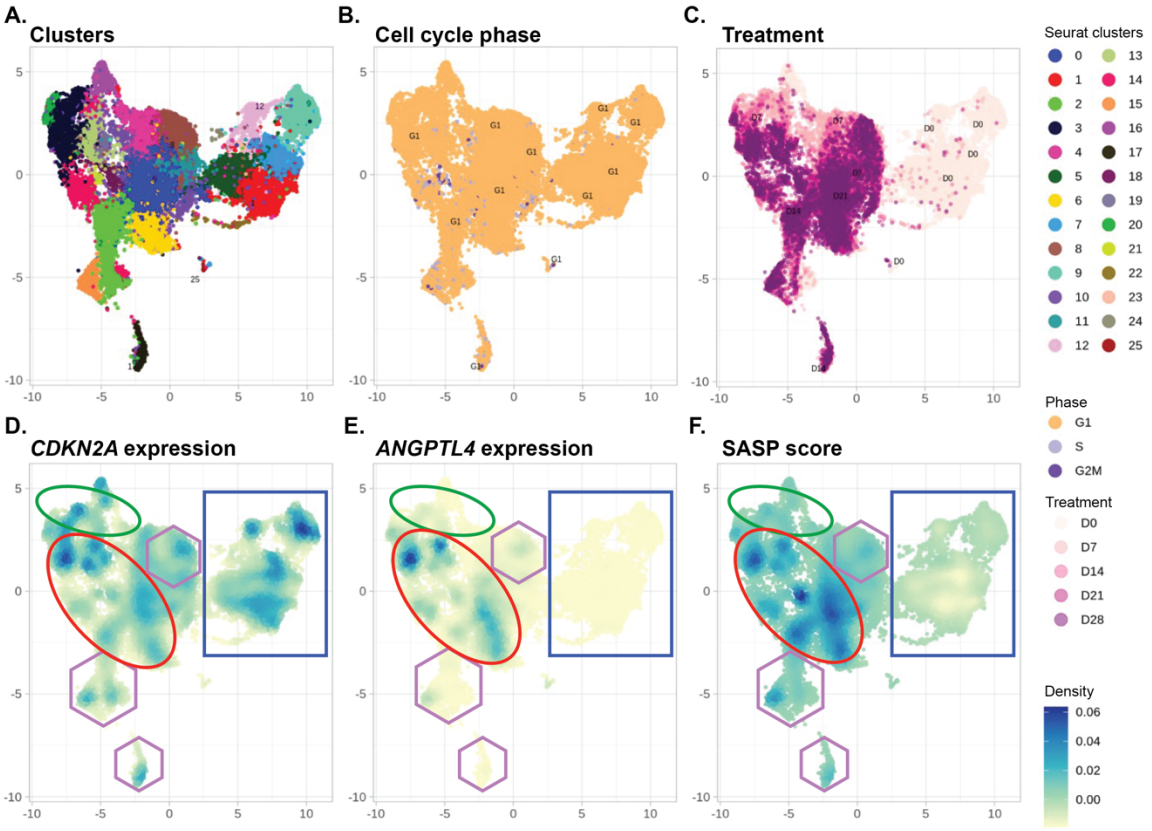

Figure 3.7 Single cell RNA-sequencing of DDLS$^{\text{Tet-ON FMDM2}}$ palbociclib time course.

(**A)** Depiction of the cluster heterogeneity of single cells based on overall gene expression. 25 unique clusters have been identified. (**B)** Depiction of cell cycle phase of individual cells (orange, G1; dark purple, G2/M; light purple, S). (**C**) UMAP showing that quiescent cells (light pink) cluster distinctly from the D7, D14, D21, and D28 senescent cells (increasingly darker shades of pink/purple). (**D-F**) Expression of senescence-associated genes was assessed by looking at each cell's levels of *CDKN2A*/p16 (D), *ANGPTL4* (E), and a SASP score (F), which was based on aggregate expression of previously identified SASP genes. Areas of differential expression are highlighted by shapes and are discussed in the text.

slightly separated from, the majority of the cells from later timepoints, but interestingly, there was little separation among D14, D21, and D28 cells (Fig 3.7C).

We then looked at expression of *CDKN2A, ANGPTL4,* and a SASP score that was calculated based on aggregate expression of the 37 SASP genes included in Table 3.2. *CDKN2A* expression was widely observed in cells from all timepoints, consistent with its early role in the decision to exit from the cell cycle (Fig. 3.7D). D0 quiescent cells largely expressed *CDKN2A* and had very low levels of SASP gene expression, although, importantly, no expression of *ANGPTL4* (Fig 3.7D-F, blue rectangle). This is in line with previous observations that quiescent cells, including those induced by serum starvation, can show expression of some SASP genes (Koff lab, unpublished data). Another cluster, largely made up of D7 cells, also expressed *CDKN2A* and low levels of SASP genes, but not *ANGPTL4* (Fig 3.7D-F, green oval). Peak expression of *ANGPTL4* was seen in clusters of D14+ cells and overlapped closely with both *CDKN2A* and high SASP-expressing cells (Fig 3.7D-F, red oval). Interestingly, while the strongest SASP gene expression mapped to *ANGPTL4*$^{+}$ cells, there were also several populations of D14+ cells that expressed *CDKN2A* and lower levels of SASP but lacked *ANGPTL4* (Fig. 3.7D-F, purple hexagons).

The data from this experiment confirm two important findings from our initial bulk RNA seq work: first, that expression of *ANGPTL4* is induced late in the senescent pathway, in D14+ cells, and is not seen in quiescent or early senescent cells (unlike *CDKN2A,* which is widely expressed in both senescent and quiescent cells); and second, that expression of *ANGPTL4* occurs in cells that also express other SASP genes. Thus,

ANGPTL4 can be used in this system to mark mature senescent cells that have already begun to elaborate a SASP.

Knockdown of ANGPTL4 affects the induction of SASP transcripts relating to inflammation

Given that induction of *ANGPTL4* mRNA correlated with other SASP genes, I next wanted to ask whether knockdown of *ANGPTL4* would affect the expression of other SASP factors. To that end, I used qPCR to examine the SASP of *ANGPTL4* knockdown cells. As a comparison, I also looked at cells in which *IGFBP7*, another SASP factor, had been knocked down. Unlike *ANGPTL4,* loss of *IGFBP7* had no significant effect on any phenotype of senescence that we examined (Fig. 3.6). The different genes that make up the SASP can be largely broken down into three categories: those that are related to inflammation, those that are related to extracellular matrix remodeling, and those relating to other cellular functions (growth factor signaling, angiogenesis, etc.). I found that loss of *ANGPTL4* abrogated expression of multiple other SASP factors, particularly those related to inflammation, including *CXCL11, CCL20, IL-1A, IL-1B,* and *IL6* (Fig. 3.8). Loss of *IGFBP7,* on the other hand, had a stronger effect on the SASP factors in the growth factor signaling/angiogenesis family of genes. These results suggest that *ANGPTL4* expression not only occurs in $SASP^{+}$ cells but is also necessary for the activation of the inflammatory arm of the SASP in liposarcoma cell lines treated with CDK4/6i.

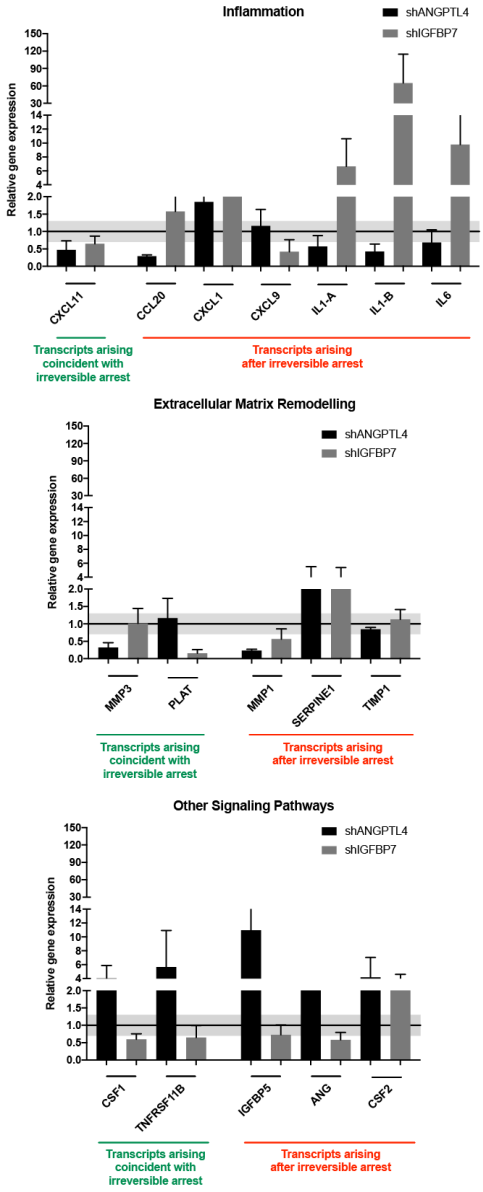

Figure 3.8 Knockdown of *ANGPTL4* affects inflammatory SASP gene expression.

Quiescent DDLS$^{tet\text{-}ONFMDM2}$ cells were treated as described in Figure 3.6. RNA was extracted and used to look at SASP gene expression. The effect of *ANGPTL4*- and *IGFBP7*-deficiency on the expression of 17 SASP-related transcripts by qRT-PCR is shown. SASP genes were broken into 3 categories based on function: inflammation-related transcripts, extracellular matrix-remodeling transcripts, and other signaling transcripts. mRNA expression is plotted as fold change compared to an shScramble control, which was normalized to 1.0. The grey shading represents the range at which values are statistically unchanged ($p>0.05$). Data shown are means ± SEM for three independent experiments.

CDK4/6i TIS and its associated SASP occur independently of DNA damage

In other senescent contexts, persistent DNA damage has been shown to be necessary for the elaboration of the SASP transcriptional program [51, 111, 112]. Given that our RNA seq data showed induction of a robust SASP, I investigated whether DNA damage occurs as part of TIS induced by CDK4/6i. DDLS cells were treated for seven days with either 1 μM palbociclib or 100 nM doxorubicin, as a positive control for DNA damage-induced senescence, and then stained against ATRX, γH2AX (a marker of double stranded breaks) and 53BP1 (a marker of DNA damage repair). As expected, cycling cells showed low levels of both γH2AX (Fig 3.9A) and 53BP1 (Fig 3.9B), consistent with normal non-homologous end joining during S-phase. Doxorubicin treatment, of course, induced high numbers of both γH2AX and 53BP1 foci. However, cells treated with palbociclib did not exhibit increases in either marker of DNA damage/repair. This was despite high levels of SA-β-gal, which were induced by both palbociclib and doxorubicin treatment (Fig 3.9C). Thus, at least in cancer cells treated with palbociclib, the elaboration of the SASP was associated with progression into stable growth arrest, not with elevated DNA damage.

Increased numbers of ATRX foci are seen in response to CDK4/6i TIS, as well as in every context of senescence we have examined thus far [31] (**Chapter 5**). ATRX is known to play a role in several DNA damage response pathways, including non-homologous end joining, homologous recombination, and the replication stress response [113]. Indeed, treatment of DDLS cells with doxorubicin caused an increase in the

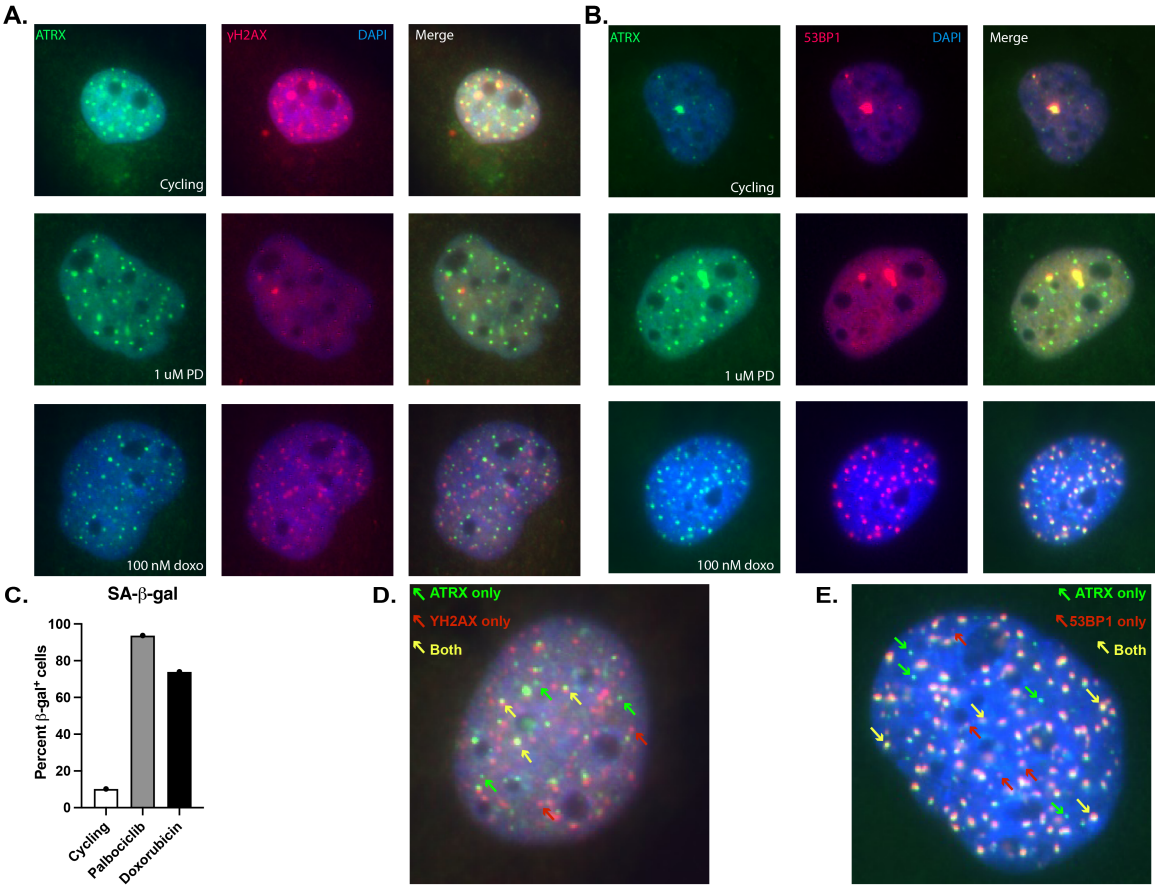

Figure 3.9 Palbociclib does not induce DNA damage in senescent liposarcoma cells.

Asynchronously growing DDLS cells were treated with either 1 μM palbociclib or 100 nM doxorubicin for seven days, at which point the subcellular distribution of **(A)** ATRX and γH2Ax, or **(B)** ATRX and 53BP1 were determined by immunofluorescence. **(C)** SA-β-gal accumulation is shown for cycling DDLS cells and for each treatment. **(D-E)** Two pools of ATRX foci are observed in doxorubicin-treated cells: those that overlap with γH2Ax (D, yellow arrows) or 53BP1 (E, yellow arrows) and those that do not (green arrows). Also observable are γH2AX and 53BP1 foci that do not overlap with ATRX (red arrows).

number of ATRX foci, many of which overlapped with γH2AX (Fix 3.9D) or 53BP1 (Fig 3.9E). However, even in cells undergoing a strong DNA damage response, there are still ATRX foci that do not colocalize with markers of DNA damage. This suggests that the role of ATRX in senescence is not limited to its role in the DNA damage response, particularly in senescence contexts like TIS, in which increased number of ATRX foci occur in the absence of a strong DNA damage response.

ANGPTL4 expression is linked with senescence in lung cancer cell lines

My work in the liposarcoma model showed that *ANGPTL4* is involved in the establishment of two foundational senescence phenotypes in CDK4/6i TIS. I next asked whether this role was unique to liposarcoma. This question was of particular importance, given that adipose tissue is one of the predominant sites of *ANGPTL4* expression in physiologically normal contexts [114]. Non-small cell lung cancer (NSCLC) is a disease in which decreased expression of INK4 proteins is common, resulting in increased signaling along the CDK4/6-Rb pathway, and therefore a number of clinical trials have looked at CDK4/6i, both as a monotherapy and in combination, for treatment of NSCLC [115]. I decided to look at the senescence response in a panel of three NSCLC cell lines – H358 (*KRAS* mutant), H1975 (*EGFR* mutant), and A549 (*KRAS* mutant).

H358 cells were treated with 1 μM palbociclib for 7, 10, and 14 days. Inhibition of CDK4/6 resulted in nearly complete growth arrest at all time points (Fig 3.10A), as well as significant increases in early senescence markers ATRX foci (Fig 3.10B) and SA-β-gal (Fig. 3.10C). H358 cells do not survive replating at single cell density, so a

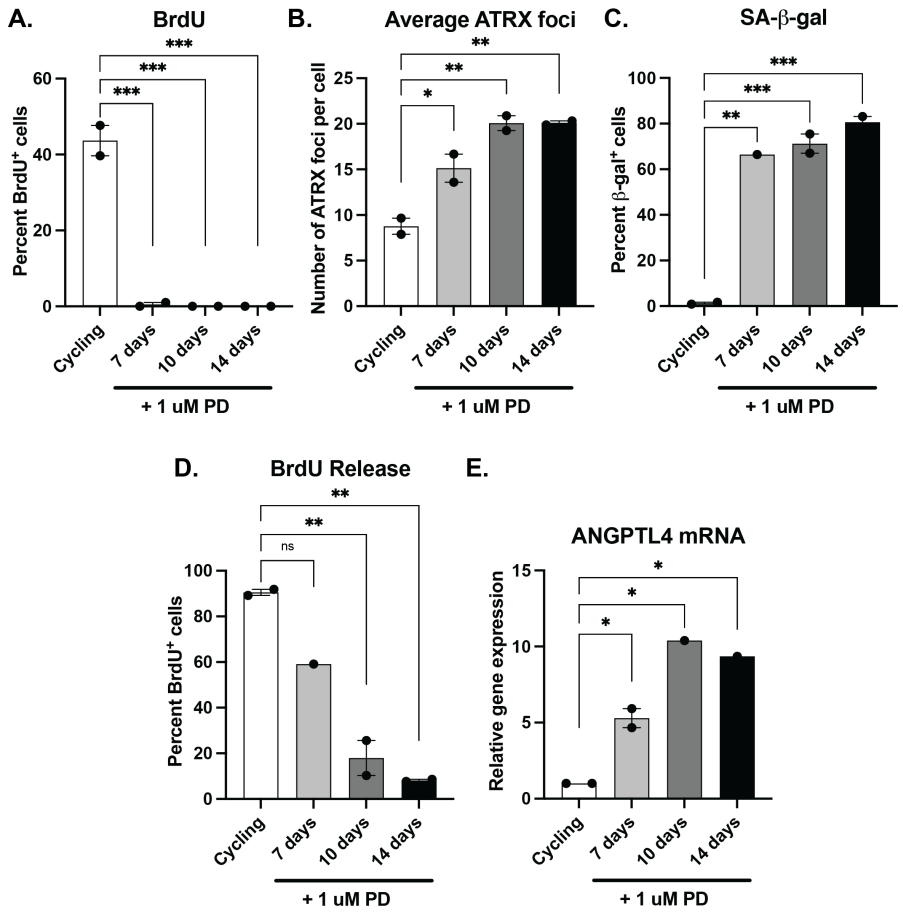

Figure 3.10 Palbociclib treatment induces senescence and *ANGPTL4* expression in H358 cells.

(A-C) H358 cells were treated with 1 μM palbociclib for 7, 10, or 14 days, at which point senescence was assessed by measuring BrdU incorporation (A), ATRX foci formation (B), and SA-β-gal accumulation (C). **(D)** Treated cells were replated in the absence of drug and presence of BrdU and allowed to grow for 48 hours, at which point BrdU incorporation was assessed using immunofluorescence. **(E)** RNA harvested from cells was used to look at expression of *ANGPTL4.* *p<0.05, **p<0.01, ***p<0.001 by one-way ANOVA.

clonogenic growth assay isn't feasible with this cell line. To determine if the cells had undergone stable growth arrest, I performed the BrdU release assay, in which treated cells are replated in the absence of drug and incubated with BrdU for 48 hours to determine the number of cells re-entering S-phase. As expected, nearly 100% of cells in the untreated control stained positive for BrdU after 48 hours of incubation (Fig. 3.10D). Treatment with 1 μM palbociclib for 7 days reduced the number of cells re-entering S-phase to ~60%, although this reduction was not significant. However, treatment for 10 or 14 days significantly reduced the number of cells retaining the ability to re-enter the cell cycle. After 14 days, only about 7% of cells stained positive for BrdU incorporation. The timing of stable growth arrest coincided with maximal expression of *ANGPTL4,* as determined by qPCR (Fig. 3.10E). Although *ANGPTL4* expression could be seen at day 7, it reached its peak at day 10, which is also the first time point at which stable growth arrest was observed. Thus, in H358 cells, as in liposarcoma cell lines, an increase in *ANGPTL4* expression is correlated with a commitment to stable growth arrest.

Similar results were seen in the *EGFR*-mutant cell line H1975. Here again, treatment with 1 μM palbociclib resulted in cell cycle exit (Fig. 3.11A), significantly increased ATRX foci (Fig. 3.11B), and SA-β-gal expression (Fig. 3.11C), at all time points of drug treatment. In this cell line, stable growth arrest was observed from day 7 onwards (Fig. 3.11D), again correlating with the induction of *ANGPTL4* expression (Fig. 3.11E). These results confirm that the expression of *ANGPTL4* during senescence is not unique to liposarcoma cell lines, that it correlates with the onset of stable growth arrest in

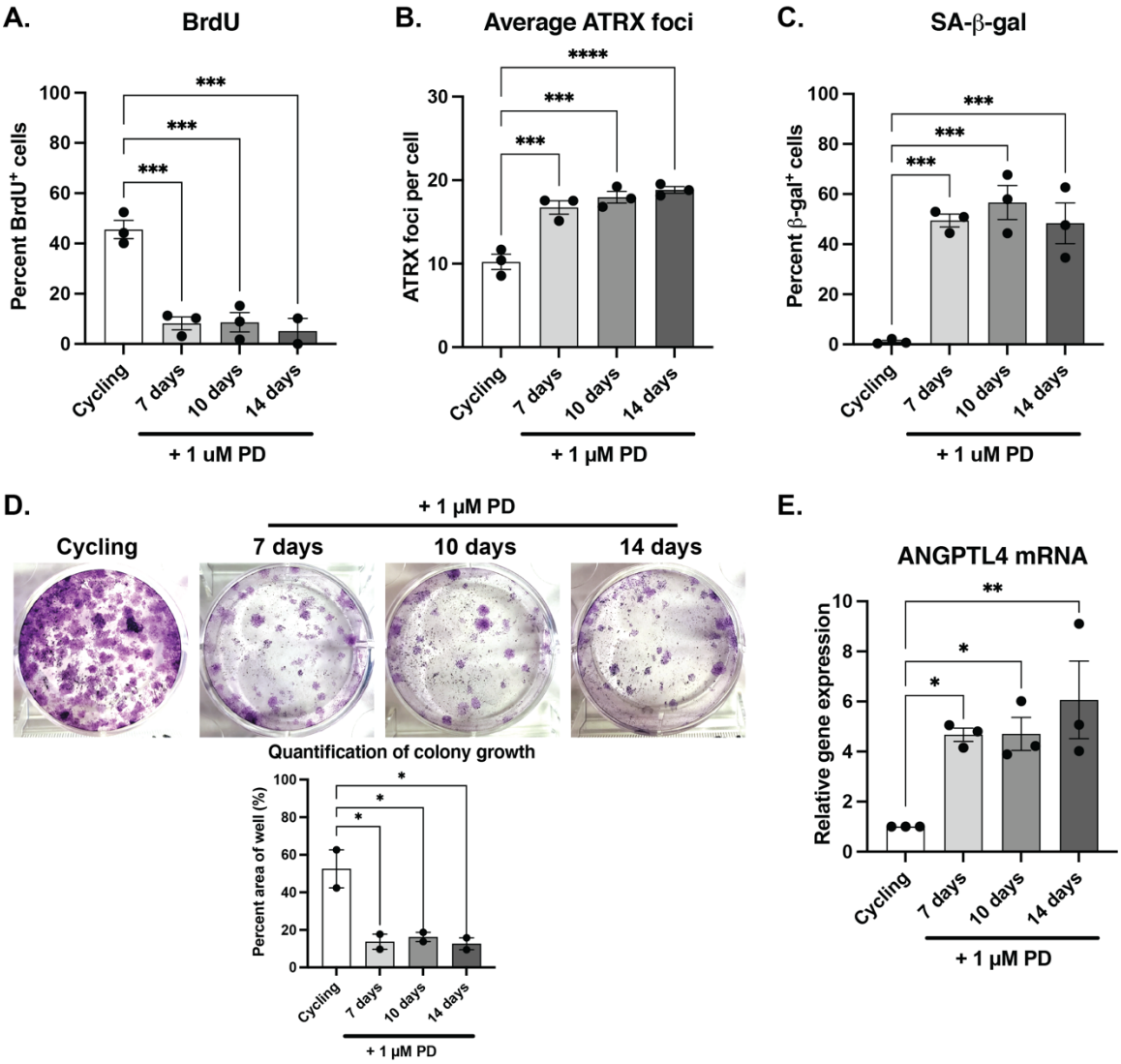

Figure 3.11 Palbociclib treatment induces senescence and *ANGPTL4* expression in H1975 cells.

(A-C) H1975 cells were treated with 1 µM palbociclib for 7, 10, or 14 days, at which point senescence was assessed by measuring BrdU incorporation (A), ATRX foci formation (B), and SA-β-gal accumulation (C). **(D)** Treated cells were replated in the absence of drug and allowed to form colonies for 3 weeks. Representative images are shown and quantified below **(E)** RNA harvested from cells was used to look at expression of *ANGPTL4.* *p<0.05, **p<0.01, ***p<0.001, ****p<0.0001 by one-way ANOVA.

NSCLC lines as it does in liposarcoma, and that it does not, within the NSCLC cell line panel, correlate with one specific mutation (e.g. *EGFR* or *KRAS)*.

Finally, I looked at the outcome of palbociclib treatment in the *KRAS* mutant A549 cell line. Unlike H358 and H1975, which are both responders to CDK4/6i, A549 is only a partial responder cell line. Previous studies have shown that A549 cells do not undergo a full senescence response when treated with CDK4/6i alone, but they can be made to senesce by treating with a combination of CDK4/6i and a MEK inhibitor [116]. Indeed, when treated with a high dose of palbociclib (2 μM) for 14 days, a proportion of A549 cells exited the cell cycle (Fig. 3.12A) and showed expression of early senescence markers like ATRX foci (Fig. 3.12B) and SA-β-gal (Fig. 3.12C), but they failed to undergo stable growth arrest (Fig. 3.12D). In line with this inability to commit fully to the senescence program, these cells also did not express *ANGPTL4* (Fig. 3.12E) and had low or no expression of most SASP factors (Fig. 3.12F-G). They are, therefore, partial responders, since they exhibit early markers of senescence, but are unable to complete the geroconversion transition into the stable senescent state.

However, when treated first with 2 μM palbociclib for 2 days to induce cell cycle exit, and then with a combination of palbociclib and 10 nM trametinib, a MEK inhibitor, for a further 8 days, A549 cells became stably growth arrested and displayed even higher levels of senescence markers like ATRX foci and SA-β-gal (Fig. 3.12 A-D). Notably, they also showed increased expression of *ANGPTL4,* as well as a number of other inflammatory SASP factors whose expression was associated with *ANGPTL4* in the liposarcoma system, including *CXCL1* and *IL6* (Fig. 3.12E-G).

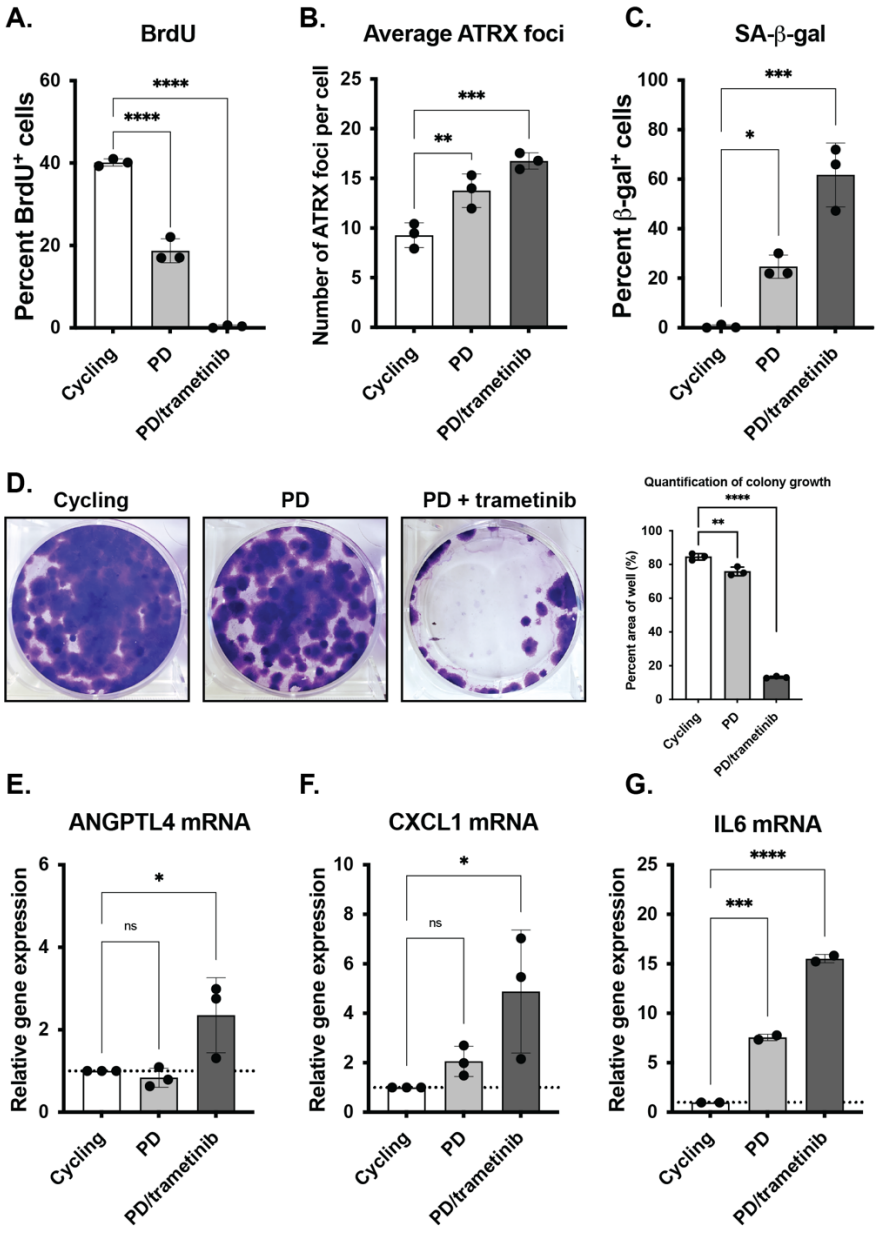

Figure 3.12 Combination palbociclib/trametinib therapy induces senescence and *ANGPTL4* expression in A549 cells.

A549 cells were treated with 2 μM palbociclib (PD) for 10 days, or with 2 μM palbociclib for 2 days, followed by 8 days of palbociclib/10 nM trametinib combination therapy. **(A-C)** After 10 days of treatment, senescence was assessed by measuring BrdU incorporation (A), ATRX foci formation (B), and SA-β-gal accumulation (C). **(D)** Treated cells were replated at low density in the absence of drug and allowed to form colonies for 2 weeks. Quantification of % area of well covered by colonies is shown. **(E-G)** RNA harvested from cells was used to look at expression of *ANGPTL4* (E), *CXCL1* (F), and *IL6* (G). *p<0.05, **p<0.01, ***p<0.001, ****p<0.0001 by one-way ANOVA.

Forced expression of ANGPTL4 *in A549 cells promotes geroconversion and SASP expression*

I noted with interest the fact that A549 cells treated with palbociclib alone developed an incomplete senescent phenotype that was similar to the one I observed in DDLS$^{\text{Tet-ON FMDM2}}$ cells in which *ANGPTL4* had been knocked down: early markers, like cell cycle exit, ATRX foci, and SA-β-gal expression, were successfully induced, but late markers, like stable growth arrest and SASP, were absent. Since these cells do not endogenously express *ANGPTL4* in response to treatment with CDK4/6i, I next asked whether forced expression of *ANGPTL4* in combination with palbociclib treatment would be sufficient to push A549 cells along the geroconversion pathway into the full senescent state. To that end, I transduced A549 cells with retrovirus containing an *ANGPTL4*-expressing plasmid or an EGFP-expressing control. After selection with puromycin, I obtained two stable cell lines: A549$^{\text{EGFP}}$ and A549$^{\text{ANGPTL4}}$. I then treated these cell lines with 2 μM palbociclib for 14 days, at which time I tested whether the cells had undergone stable growth arrest.

Using qPCR, I first confirmed the expression of both EGFP and *ANGTPL4* mRNA. As expected, EGFP levels were present and essentially equivalent in A549$^{\text{EGFP}}$ cycling cells and A549$^{\text{EGFP}}$ palbociclib-treated cells and absent in both cycling and palbociclib-treated A549$^{\text{ANGPTL4}}$ cells (Fig. 3.13A). When compared to the A549$^{\text{EGFP}}$ control, *ANGPTL4* mRNA levels in both the cycling and palbociclib-treated A549$^{\text{ANGPTL4}}$ cells were strongly elevated (Fig. 3.13B). I next assessed the onset of senescence by looking at BrdU incorporation (Fig. 3.13C), ATRX foci formation (3.13D), and SA-β-gal expression (Fig. 3.13E), and found that A549$^{\text{EGFP}}$ and A549$^{\text{ANGPTL4}}$ reacted similarly

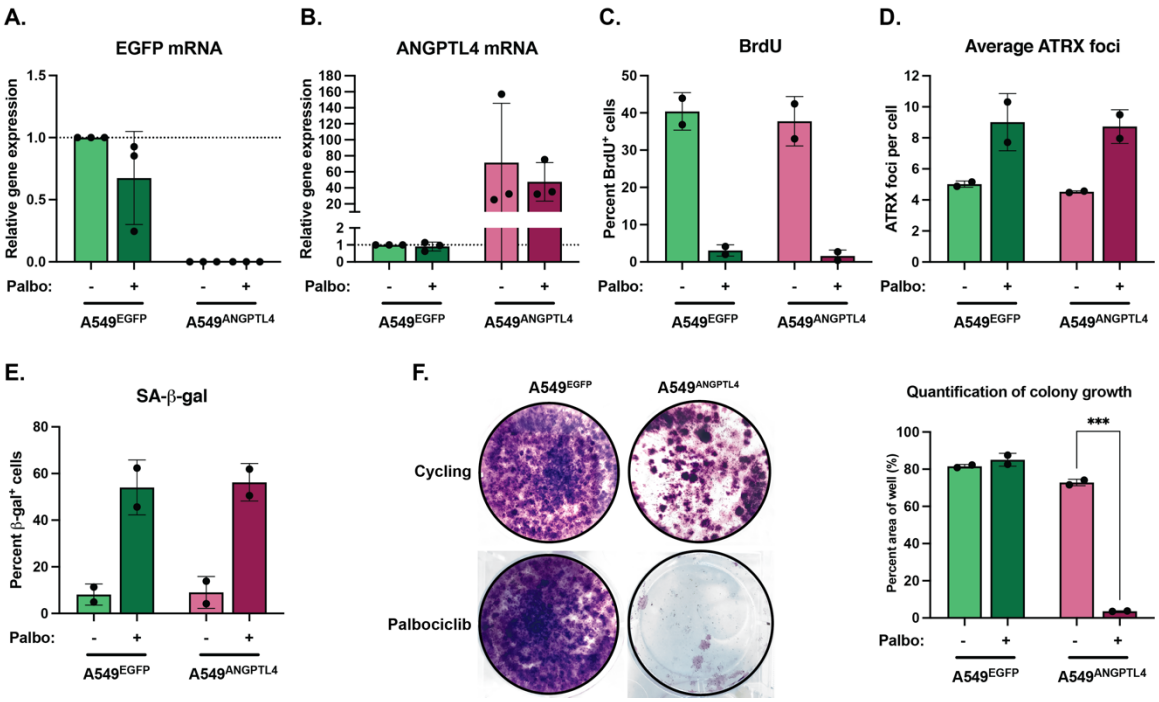

Figure 3.13 Exogenous expression of *ANGPTL4* in A549 cells drives stable growth arrest in response to palbociclib treatment.

A549 cells were engineered to express EGFP ($A549^{EGFP}$) or *ANGPTL4* ($A549^{ANGPTL4}$), then treated with 2 μM palbociclib for 14 days. **(A-B)** Expression of exogenous genes was confirmed using qPCR. All samples were normalized to cycling $A549^{EGFP}$ cells. **(C-E)** Senescence status after 14 days of treatment with 2 μM palbociclib was assessed by measuring BrdU incorporation (C), ATRX foci formation (D), and SA-β-gal expression (E). **(F)** After 14 days, cells were replated at low density in the absence of drug and allowed to grow for 2 weeks. Quantification of % area of well covered by colonies is shown.

during the first phase of palbociclib treatment. Like the parental A549 cell line, they both arrested and exhibited early phenotypes of senescence. Notably, exogenous expression of *ANGPTL4* did not cause any hallmarks of senescence in cycling cells, confirming that the role of *ANGPTL4* in senescence is specific for cells that have already exited the cell cycle. After 14 days of palbociclib treatment, the cells were plated at low density in the absence of drug and allowed to grow for a subsequent two weeks. $A549^{EGFP}$ cells, whether treated with palbociclib or not, quickly returned to the cell cycle and filled in the plate with colonies. $A549^{ANGPTL4}$ cells, on the other hand, failed to grow back following the removal of palbociclib (Fig. 3.13F).

After observing this marked increase in commitment to stable growth arrest in the presence of *ANGPTL4,* I wondered whether the $A549^{ANGPTL4}$ cells treated with palbociclib would exhibit a stronger SASP program compared to the $A549^{EGFP}$ control. Indeed, qPCR analysis confirmed that senescent $A549^{ANGPTL4}$ cells had much higher levels of a number of inflammatory SASP factors than the palbociclib-treated, but not stably growth arrested, $A549^{EGFP}$ cells (Fig. 3.14A-F). Importantly, many of these SASP factors, including *CCL20, CXCL11, IL-1A, IL-1B*, and *IL6*, were among those whose expression decreased when *ANGPTL4* was knocked down in $DDLS^{Tet\text{-}ON\ FMDM2}$ cells (Fig 3.8). Additionally, expression of the extracellular matrix remodeling protein *MMP1* was increased in $A549^{ANGPTL4}$ cells treated with palbociclib, but not in the $A549^{EGFP}$ cells, which is also in line with our findings from the sh*ANGPTL4* experiment (Fig. 3.14G). Other SASP factors, like the growth factor *IGFBP3* and the metallopeptidase inhibitor *TIMP1,* were equally unaffected by palbociclib treatment in both $A549^{EGFP}$ and

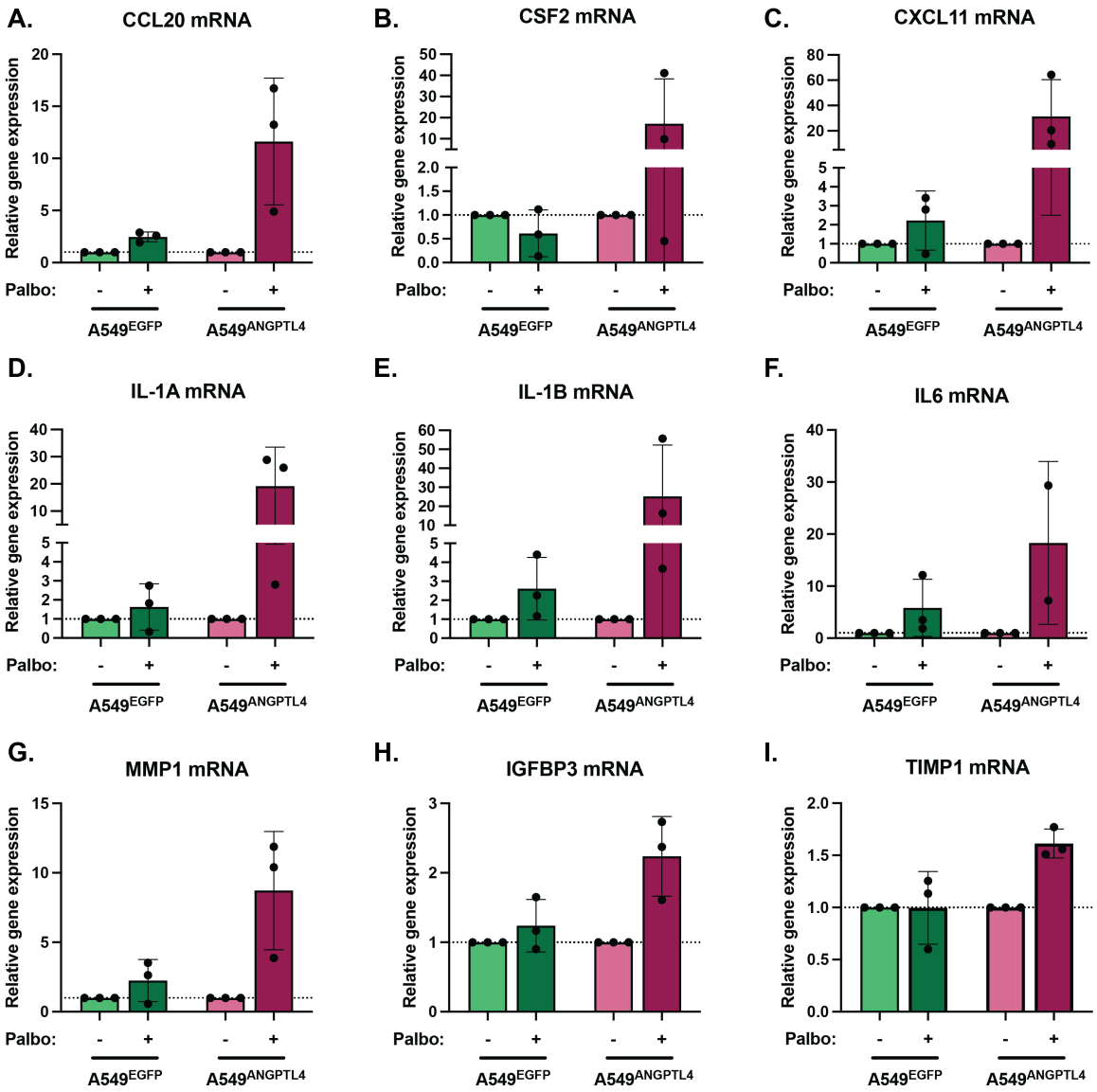

Figure 3.14 Exogenous expression of *ANGPTL4* in A549 cells drives SASP gene expression in response to palbociclib treatment.

A549 cells were engineered to express EGFP ($A549^{EGFP}$) or *ANGPTL4* ($A549^{ANGPTL4}$), then treated with 2 μM palbociclib for 14 days. **(A-I)** SASP gene expression was quantified using qPCR. Each palbociclib-treated sample is normalized to its own cycling control.

A549^{ANGPTL4} (Fig 3.14H). Thus, exogenous expression of *ANGPTL4* in quiescent cells is sufficient to stimulate the transition to stable growth arrest and to induce expression of some arms of the SASP, including the inflammatory program.

The addition of full-length ANGPTL4 protein promotes geroconversion in quiescent cells

ANGPTL4 protein is known to exist in several different isoforms (Fig. 3.15). The full-length, 406 amino acid protein consists of an N-terminal signal peptide and coiled-coil domain (CCD), which is connected by a flexible linker to the C-terminal fibrinogen-like domain (FLD). Full-length ANGPTL4 (flANGPTL4) often oligomerizes into variably sized multimers. It can also be cleaved at the RRKR linkage site into N-terminal (nANGPTL4) and C-terminal (cANGPTL4) fragments. nANGPTL4 retains the ability to form higher order structures, while cANGPTL4 does not. Each isomer has been identified in different cell/tissue types in varying ratios, and each has been associated with different signaling pathways. flANGPTL4 is involved in lipoprotein lipase (LPL) inhibition, as well as in the inhibition of endothelial cell adhesion, migration, and tubule formation. nANGPTL4 also plays a role in LPL inhibition, while cANGPTL4 has been implicated in $\alpha5\beta1$ integrin binding, wound healing, and anoikis resistance [114, 117-119].

While the previous experiments established the importance of the *ANGPTL4* gene for irreversible arrest and SASP expression in different cell lines, they could not elucidate the isoform of ANGPTL4 protein that is required for senescence. To do this, I obtained recombinant ANGPTL4 protein (rANGPTL4) and added it to the media of quiescent A549 cells to determine which isoform could promote stable growth arrest. In this

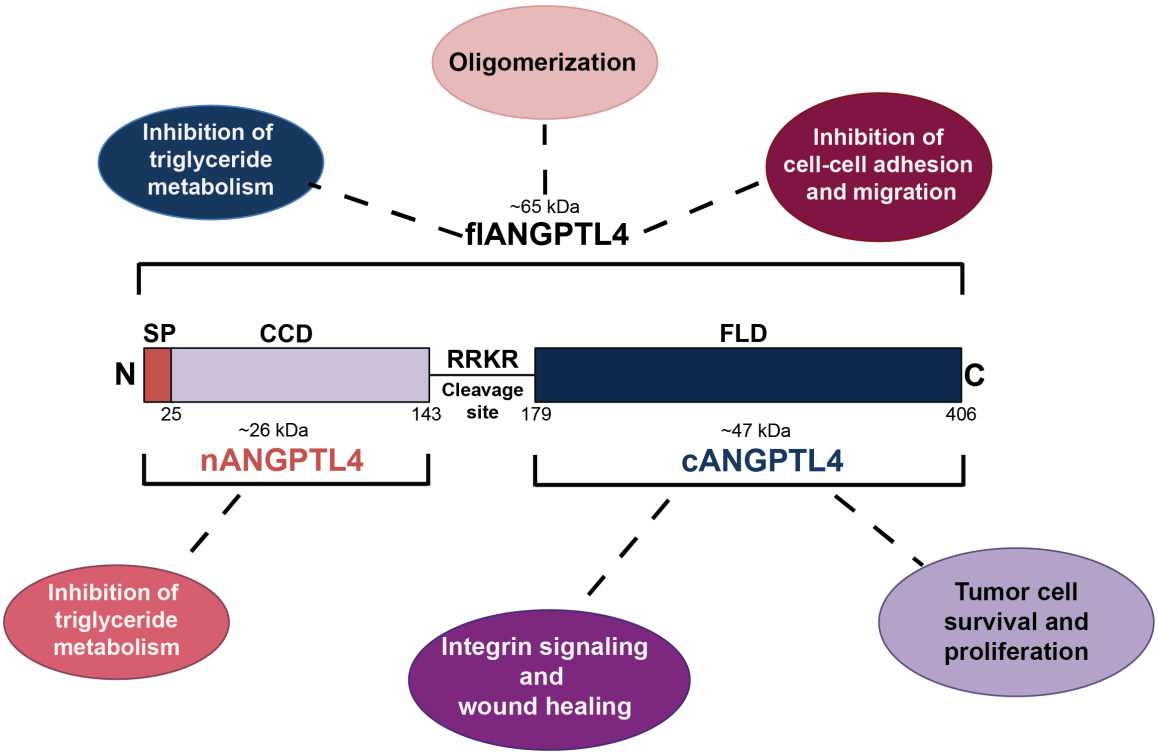

Figure 3.15 The structure and function of ANGPTL4 protein isoforms.

The structure, length, and relevant domains of full-length (flANGPTL4), N-terminal (nANGPTL4), and C-terminal (cANGPTL4) are shown. nANGPTL4 and cANGPTL4 are connected by a flexible linker containing an RRKR cleavage site. Some of the best characterized functions of each isoform are indicated in surrounding bubbles.

experiment, A549 cells were pre-treated with 2 μM palbociclib for 2 days to induce cell cycle exit, then treated with a combination of palbociclib and human rANGPTL4 protein for a further six days. I tested all three isomers of the protein (flANGPTL4, nANGPTL4, and cANGPTL4), and concentrations between 100 ng/mL and 2,000 ng/mL were added to the media, with one change of media on the third day of the treatment. At the end of the treatment, cells were plated at low density in the absence of both palbociclib and rANGPTL4 and allowed to grow for a subsequent two weeks.

As expected, A549 cells treated with palbociclib alone quickly returned to the cell cycle after removal of the drug and were able proliferate repeatedly. The addition of nANGPTL4 or cANGPTL4 to the media did not significantly affect the formation of colonies (Fig. 3.16). However, the addition of flANGPTL4 did decrease the ability of A549 cells to return to the cell cycle in a dose-dependent manner – at the highest dose tested, 2,000 ng/mL, colony formation was reduced by roughly half. This result suggests that flANGPTL4, but neither of the two truncated N- and C-terminal isoforms, is sufficient to push cells along the geroconversion pathway from a quiescent state to a stably growth arrested state.

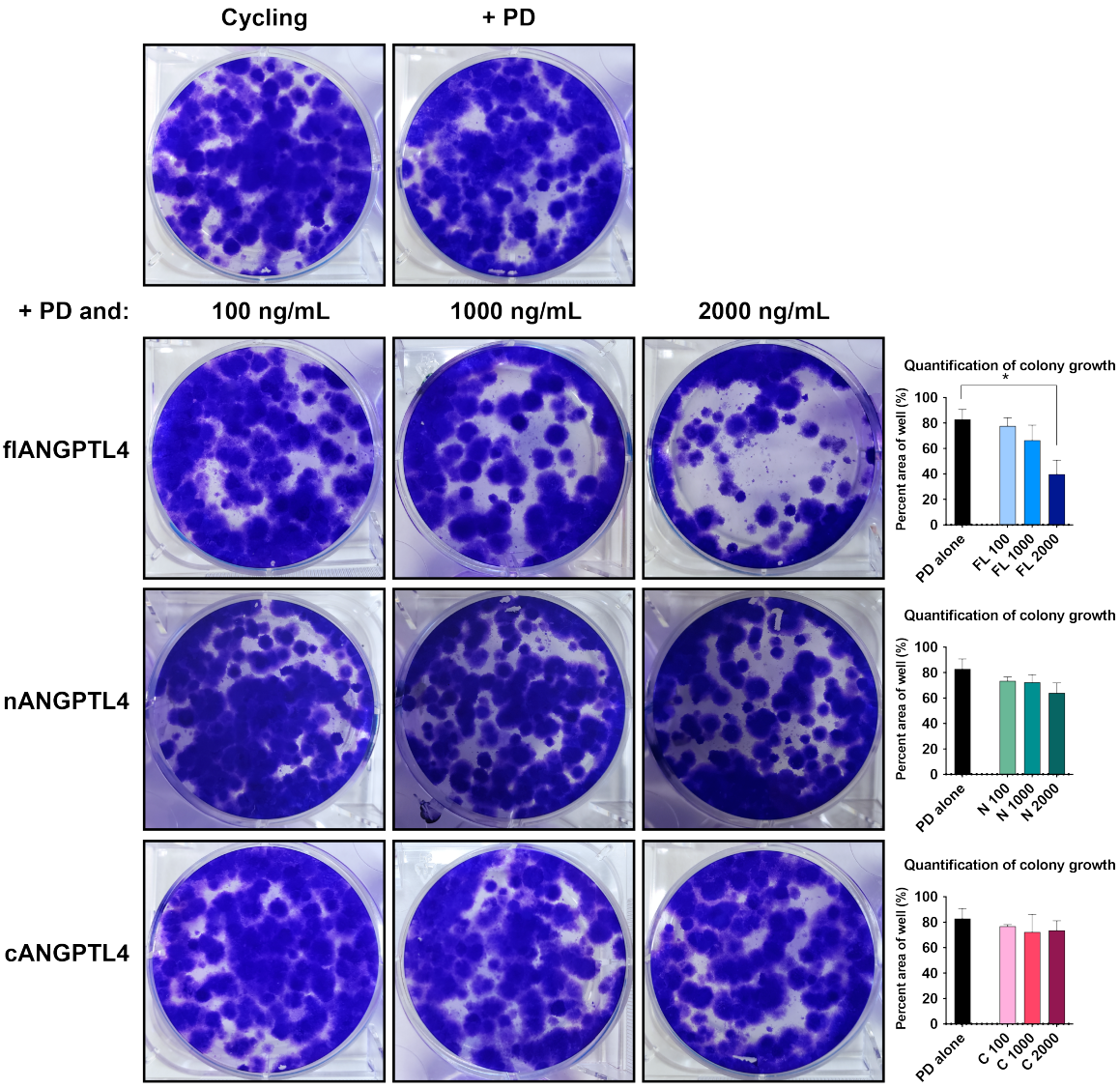

Figure 3.16 flANGPTL4 is sufficient to push cells from quiescence into stable growth arrest.

A549 cells were treated with 2 μM palbociclib for 2 days to induce cell cycle exit, followed by 6 days of palbociclib + the indicated amount of either full length (fl), N-terminal (n) or C-terminal (c) recombinant ANGPTL4 protein. After treatment, a clonogenic growth assay was performed. Data shown are means ± SEM for two independent experiments. *p<0.05 by Student's *t* test.

Discussion

ANGPTL4 as a regulator of geroconversion induced by CDK4/6 inhibitors

ANGPTL4 is a secreted factor that is neither an inflammatory cytokine nor an extra-cellular matrix remodeler, but its expression has been noted to increase in a variety of senescence contexts, including replicative senescence in bone marrow mesenchymal stromal cells [120], oncogene-induced senescence (OIS) in human fibroblasts [84], and human endothelial cells induced to senesce by knockdown of c-Myc [121]. Expression of *ANGPTL4* has also been reported to increase with aging in a number of different human and mouse tissues [122-124]. ANGPTL4 protein has been implicated in several metabolic and non-metabolic conditions, including redox regulation, glucose homeostasis, lipid metabolism, and energy homeostasis, all of which can be altered during cellular senescence [125]. But despite its frequent appearance in lists of SASP genes, to the best of my knowledge, its function during senescence has not previously been explored.

Here, I have shown that *ANGPTL4* plays an important role in regulating two of the core phenotypes of senescent cells in the context of CDK4/6 inhibition: expression of the inflammatory SASP and the onset of stable, long-term growth arrest. This role is observed regardless of the CDK4/6 inhibitor used (discussed further in **Chapter 4**) and is not unique to sarcoma cells. In this model, changes in *ANGPTL4* are observable at the RNA level. How expression of *ANGPTL4* is transcriptionally regulated remains unclear, although several transcription factors (TFs) have been implicated in this process, including PPARα, PPARγ, and HIF-1α [114]. There is evidence to suggest a role for each of these TFs in senescence. PPARγ was shown to accelerate the onset of replicative

senescence by inducing expression of p16 in human fibroblasts [126]. PPARα and HIF-1α have also been linked with senescence, although their role seems to be to suppress, rather than promote, entry into the senescent state [127-129].

One study of OIS in human fibroblasts showed a direct link between macroH2A1, a common component of the SAHF, and *ANGPTL4* expression. In wild-type fibroblasts, macroH2A1 was specifically enriched on a number of SASP genes, including *ANGPTL4.* When those fibroblasts were induced to senesce by overexpression of $HRAS^{V12}$, there was a genome-wide rearrangement of macroH2A1, including its removal from those SASP genes. Additionally, knockdown of macroH2A1 prevented the up-regulation of several inflammatory SASP factors during OIS, though it did not affect the accumulation of SA-β-gal^{+} cells [84]. These results demonstrate yet another functional link between two common senescent phenotypes, the SAHF and the SASP, whereby SAHF components are essential for the regulation of SASP gene expression during senescence.

Interestingly, one of ATRX's known functions is the removal of macroH2A from chromatin [130], prompting the fascinating possibility of a role for ATRX during senescence relating to the rearrangement of heterochromatin that allows for expression of SASP genes like *ANGPTL4*. This hypothesis is supported by fact that U2OS cells, which lack a functional ATRX protein, do not express *ANGPTL4* in response to treatment with CDK4/6 inhibitors (Fig. 3.5). Other non-responder sarcoma cell lines, like LS8107 and LS7785-1, do have intact ATRX, and they exhibit a baseline number of ATRX foci in cycling cells, but the number of foci does not increase in response to CDK4/6 inhibition [31], which is associated with failure to undergo geroconversion and lack of induction of

ANGPTL4 (Fig. 3.5). Therefore, a deeper understanding of where ATRX is being targeted during senescence, as opposed to where it is located in cycling cells, might shed light on the transcriptional regulation of *ANGPTL4* and other SASP factors.

Post-translationally, flANGPTL4 protein can undergo cleavage into N- and C-terminal fragments (Fig. 3.15), but the mechanism by which ANGPTL4 protein is cleaved remains unclear. Proprotein convertases, including furin, are capable of cleaving ANGTPL4 at the RRKR site, but cleavage continued normally in a furin-deficient cell line, showing that another protein(s) must also have the ability to cut ANGPTL4 protein [118]. One study showed that cell lysates contained only flANGPTL4, while the individual N- and C-terminal fragments, as well as flANGPTL4, could be detected in the medium, suggesting that the cleavage event occurs late in the secretory pathway, either on the cell surface or in the medium [118].

Once cleaved, the different isoforms of ANGPTL4 localize to different compartments, where they are involved in diverse signaling pathways. nANGPTL4 and flANGPTL4, which both contain the CCD, tend to localize to the extracellular matrix, while the C-terminal fragment, which lacks the CCD but contains the FLD, is more commonly found in the secretion medium [119]. flANGPTL4 binds to the extracellular matrix, where it can influence cell adhesion, migration, and tubule formation. nANGPTL4 and flANGPTL4 are both involved in lipid metabolism, while cANGPTL4 has been connected to integrin signaling, tumor promotion, and wound healing [117].

Though my work demonstrates that flANGPTL4 protein is sufficient to push reversibly arrested cells towards stable growth arrest (Fig. 3.16), it does not address the pathway through which ANGPTL4 is acting. It is also not possible to say with certainty

whether flANGPTL4 remains full-length once it is added to the media, or if it is cleaved and both the N- and C-terminal functions are simultaneously required. Future work will attempt to elucidate this further by creating a cell line in which endogenous *ANGPTL4* is knocked out, then transducing with plasmids expressing flANGPTL4, nANGPTL4 and cANGPTL4 together, or flANGPTL4^{GSGS}, a mutant form of the protein that is unable to undergo proteolytic cleavage and thus remains in its full-length form. This experiment will help narrow down the domain(s) of ANGPTL4 that is/are essential to its role in senescence, which will in turn facilitate the discovery of important binding partners or downstream pathways that are involved.

The connection between the SASP and stable growth arrest

One of the most exciting results from the DDLS$^{Tet\text{-}ON\ FMDM2}$ system was the link it established between the onset of stable growth arrest and the SASP. This is not the first time that SASP genes have been linked to irreversible growth arrest. In a model of OIS induced by *BRAF^{V600E}* in human primary foreskin fibroblasts, knockdown of *IGFBP7* prevented cells from entering senescence and enabled their continued proliferation [131]. Notably, knockdown of *IGFBP7* had no effect on any phenotype of senescence in our DDLS$^{Tet\text{-}ON\ FMDM2}$ system (Fig. 3.6). Similar results were seen in another model of BRAF^{V600E} OIS in human diploid fibroblasts, where knockdown of *IL6* allowed cells to bypass senescence and continue proliferating [53]. Another insulin-like growth-factor binding family member and SASP factor, *IGFBP3,* was shown to play a role in senescence in human umbilical vein endothelial cells (HUVECs). Knockdown of *IGFBP3* in aged HUVECs decreased the number of SA-β-gal^{+} cells and increased the

percentage of the population entering G2/M and S phases [132]. Another study showed that loss of *CXCR2,* which binds to a number of commonly reported SASP factors, delayed the onset of replicative senescence in IMR-90 cells and also permitted escape from growth arrest in a model of OIS [59].

Thus, several SASP factors have already been shown to play essential roles in the establishment of the senescent state. However, the findings presented here are unique in that loss of *ANGPTL4* specifically affected the induction of stable growth arrest and inflammatory SASP gene expression, two late-appearing markers of mature senescent cells, without affecting the earlier components of the senescent phenotype, like cell cycle exit, SA-β-gal expression or ATRX foci number. Unlike knockdown of *IGFPB3, IGFBP7, IL6,* or *CXCR2,* which allowed cells to continue to proliferate even in the presence of an inducing stressor (oncogene overexpression and/or replicative stress), loss of *ANGPTL4* did not allow cells to escape palbociclib-induced cell cycle exit. It simply prevented the full transition of geroconversion from occurring, such that the cells remained in a state of reversible growth arrest and were able to return to proliferation when palbociclib was removed. *ANGPTL4,* therefore, represents the first SASP factor to be nominated as a specific regulator of geroconversion, rather than a regulator of the cell cycle exit that is associated with senescence.

The regulation and complexity of the SASP

How SASP gene expression is activated remains a topic of debate and is probably, at least to some degree, cell-type and/or inducer specific. Induction of SASP gene expression has been commonly linked to DNA damage [51], but as shown in Fig. 3.9,

treatment with palbociclib does not activate a DNA damage response, despite resulting in robust expression of SASP genes. Some evidence suggests that senescent cells utilize components of the innate immune machinery to activate SASP expression, including, but not limited to, the inflammasome [60], the cytoplasmic RNA sensor RIG-1, which typically functions to identify and target viral RNA [133], and activation of the innate immunity cytosolic DNA-sensing cGAS/STING pathway [30, 134]. At the transcriptional level, initiation of SASP gene expression has been linked to NF-κB [52], GATA4 (which has also been shown to activate NF-κB) [54], and AP-1 [135], among many other TFs. Finally, epigenetic changes can contribute to activation of the SASP, including, as discussed previously, rearrangement of macroH2A1 [84], remodeling of the enhancer landscape to remove enhancers adjacent to the promoters of pro-proliferative genes and insert super-enhancers proximal to SASP gene promoters [136], and chromatin modifications at the site of SASP genes, including, for example, an increase in the active histone marks H3K79me2/3 [137].

Clearly, induction of the SASP is a complex process that is unlikely to be simplified to a single master regulator. However, there is evidence to suggest that one SASP factor can regulate expression of other SASP family genes: when *IL6* was knocked down in a model of OIS in human diploid fibroblasts, there was a marked decrease in transcriptional activation of the inflammatory network, including *IL-1A*, *IL-1B*, and *IL8* [53]. I observed similar results in DDLS$^{\text{Tet-ON FMDM2}}$ *ANGPTL4* knockdown cells (Fig. 3.8). The fact that loss of *ANGPTL4* abrogated expression of a number of inflammatory SASP factors, but did not affect the expression of other transcripts related to growth

factor signaling and extra-cellular matrix remodeling, suggests that there are at least two parallel SASP pathways that are differentially regulated.

As shown in the single cell sequencing data in Fig. 3.7, only a subset of D14-D21 senescent DDLS$^{\text{Tet-ON FMDM2}}$ cells express *ANGPTL4.* There are several populations of late time-point senescent cells, outlined in purple hexagons in Fig. 3.7D-F, that are positive for *CDKN2A* and at least weakly positive for other SASP factors, but lack expression of *ANGPTL4.* And yet, from day 14 onwards, these cells failed to return to the cell cycle in the absence of palbociclib, showing that they had committed to stable growth arrest, even if only some of those cells were expressing *ANGPTL4.* One intriguing hypothesis is that *ANGPTL4* is involved in the paracrine arm of the SASP program, and that expression of *ANGPTL4* from a sub-population of cells is sufficient to enforce growth arrest and drive SASP expression in neighboring cells.

This could be a direct effect, meaning that *ANGPTL4* itself regulates paracrine senescence, or an indirect effect, meaning that *ANGPTL4* drives the expression of other SASP factors that are involved in paracrine senescence. This second possibility is supported by evidence showing that *IL-1* signaling regulates paracrine senescence [60]. Expression of both *IL-1A* and *IL-1B* was reduced in *ANGPTL4* knockdown cells. The same study also found that *CCL20,* another inflammatory SASP factor whose expression was abrogated in the absence of *ANGPTL4,* plays a role in regulating paracrine senescence. Single cell sequencing comparing *ANGPTL4* knockdown or knockout cells with wild-type controls would shed a great deal of light on the effects of SASP expression in the absence of *ANGPTL4.* This could be coupled with conditioned media

experiments to test the ability of secreted factors from wild-type versus *ANGPTL4* knockout cells to induce senescence in a paracrine fashion.

Chapter 4: Abemaciclib induces inflammation associated with senescence in patients with dedifferentiated liposarcoma

Introduction

CDK4/6 inhibitors: the three main players

For more than 25 years, the idea has persisted to inhibit cyclin-dependent kinases (CDKs) as a mechanism of preventing tumor cell progression through the cell cycle. The first generation of CDK inhibitors, including flavopiridol, were developed as pan-kinase inhibitors, but their lack of specificity ultimately resulted in high levels of toxicity. Flavopiridol inhibits CDKs 1, 2, 4, 6, 7, and 9, and its cytotoxic response is likely due to the suppression of transcription that occurs as a result of CDK7 and CDK9 inhibition [138]. The second generation, including dinaciclib, a CDK1/2/5/9 inhibitor, was developed to be more specific and potent. However, while dinaciclib exhibited more efficient inhibition of RB phosphorylation than flavopiridol, it still proved to be ineffective in a number of clinical trials [138, 139].

Finally, the third generation of CDK inhibitors delivered a set of drugs with sufficiently high specificity and relatively low toxicity. Today, there are three commercially available CDK4/6 inhibitors: palbociclib was the first to gain FDA approval, followed by ribociclib, and then abemaciclib. All three drugs are approved, in combination with anti-estrogen therapy, for treatment of HR-positive, HER2-negative advanced or metastatic breast cancer, and abemaciclib is also approved for single agent use in this disease. Clinical trials of the three drugs have been conducted in a range of other cancers, including liposarcoma, neuroblastoma, glioblastoma, non-small cell lung

cancer, and melanoma [75]. Another CDK4/6 inhibitor, trilaciclib, is currently undergoing phase II clinical trials [139].

Ribociclib, palbociclib, and abemaciclib are thought to be ATP-competitive inhibitors that attach to the ATP binding site of CDK4 and CDK6. Both ribociclib and abemaciclib exhibit higher potency against CDK4 than CDK6, while palbociclib has similar potency against both kinases. Ribociclib and palbociclib are structurally similar, whereas abemaciclib is structurally unique. One of the more conspicuous differences among the three drugs is their dosing schedule. Both ribociclib and palbociclib are dosed orally once per day, but are necessarily administered in an intermittent manner, either in 2 weeks on/1 week off or 3 weeks on/1 week off cycles. This is to allow time for recovery from the most significant toxicity induced by these drugs, which is neutropenia. Abemaciclib, on the other hand, does not cause dose-limiting myelotoxicities, and thus can be taken continuously. It is also dosed orally but is given twice daily, and its main side effect is gastrointestinal distress [77]. Given the ability of CDK4/6 inhibitors to induce both quiescence and senescence in cultured cells, it is conceivable that the interrupted dosing pattern of palbociclib and ribociclib is disadvantageous, as it could allow reversibly arrested cells the opportunity to return to the cell cycle during drug withdrawal.

Proposed mechanisms of CDK4/6 inhibitors in patients

At the most basic level, CDK4/6 inhibitors are cytostatic drugs that work by inducing cell cycle exit. Any RB-positive tumor cell, when exposed to a CDK4/6 inhibitor, should theoretically enter a G_0/G_1 state of growth arrest, thus halting tumor

growth. This model of CDK4/6i function is supported by the fact that many mechanisms of resistance that arise in response to treatment with these drugs involve pathways that bypass the need for cyclin D1-CDK4/6 to promote cell cycle progression, including loss of *CDKN2A/*p16, loss of RB, and amplification and/or elevated expression of cyclin E1 or CDK6 [140-142]. However, CDK4/6 inhibitors do not result in cytostasis in all RB-positive patients, as demonstrated by liposarcoma patients who progress rapidly on palbociclib, despite evidence that the drug had decreased phosphorylation of RB and thus hit its target [20, 109, 143]. Furthermore, even long-term, stable growth arrest cannot account for the partial and complete responses that have been observed in some patients with liposarcoma, mantle cell lymphoma, HR^+ breast cancer, and non-small cell lung cancer in response to CDK4/6 inhibition [109, 143-145].

To promote tumor regression, rather than merely tumor stasis, CDK4/6 inhibitors must exert effects beyond cell cycle exit. Several mechanisms have been proposed to account for the clinical efficacy of these drugs. The first is induction of cellular senescence, which, through the pro-inflammatory effects of the SASP, results in immune cell recruitment to the tumor and subsequent clearance of tumor cells. It has been well-established that treatment with CDK4/6i can trigger senescence in cell lines and mouse models of a variety of cancer types besides liposarcoma, including breast, melanoma, and hepatocellular carcinoma, among many others [146-148]. However, it has been difficult to establish a link between CDK4/6 inhibition and senescence in human patients, due to the lack of viable markers [39].

In some cases, including a panel of ER+ breast cancer cell lines *in vitro* and patient-derived xenograft (PDX) models *in vivo*, CDK4/6 inhibitors have been shown to

induce autophagy, rather than senescence, in RB-positive cells [149]. In RB-positive gastric cancer cells, treatment with palbociclib induced both senescence and autophagy. When CDK4/6i were combined with autophagy inhibitors, senescence became the only outcome, suggesting that cells might undergo an early fate decision in which they "decide" between senescence or autophagy [150]. It is worth noting, however, that determination of senescence in this model was based completely on expression of SA-β-gal, which, apart from being an early marker of senescence, can also be a marker of autophagy [33].

CDK4/6i have also been shown to affect the immunogenicity of tumors in a manner that is not dependent on cellular senescence. *In vitro* treatment of T-cells with abemaciclib can trigger their activation, suggesting that abemaciclib has both tumor and T-cell intrinsic effects [151]. Treatment with CDK4/6 inhibitors can also increase antigen presentation on tumor cells, which promotes recruitment of the immune system and anti-tumor responses [75, 152]. One study found that the HLA ligands induced in response to CDK4/6 inhibition were peptides derived from cell cycle proteins like CDK4/6 and cyclin D1 [153]. The authors propose that the cell cycle exit induced by CDK4/6i renders many mitotic-associated proteins unnecessary, thus targeting them for degradation and subsequent presentation on HLA peptides.

Well-differentiated/dedifferentiated liposarcoma as a disease model for studying CDK4/6 inhibitors

Though liposarcoma is the most common type of soft tissue sarcoma, it is still a rare disease, with approximately 2,500 new diagnoses per year in the United States [154].

Well-differentiated (WDLS) and dedifferentiated (DDLS) liposarcoma are thought to represent two ends of the same disease spectrum, as both tumors are associated with amplification of the 12q13-15 region, which contains *MDM2* and *CDK4. MDM2* is amplified in nearly 100% of WD/DDLS tumors, while *CDK4* is amplified in more than 90%, and evidence suggests a less favorable prognosis in patients with amplification of *CDK4* [154, 155]. WDLS is usually a slow-growing, low-grade tumor that is not prone to metastasis, while DDLS tumors, which typically contain a WDLS component mixed with a higher grade, dedifferentiated sarcoma, are more aggressive and more likely to metastasize [156]. Treatment options for liposarcoma are generally limited to traditional chemotherapy, surgery, or radiotherapy [154], so there is a strong need for targeted therapies for this disease.

Given the near-universal amplification of *CDK4* observed in WD/DDLS tumors, treatment with CDK4/6 inhibitors is a reasonable therapeutic strategy. Two phase II clinical trials have previously been conducted at Memorial Sloan Kettering Cancer Center to investigate palbociclib as a single agent treatment for patients with advanced and progressive WD/DDLS. In one trial, palbociclib was dosed at 200 mg once daily for 14 days in a 21-day cycle [109], while the second trial tested a regimen in which patients received a lower dose, 125 mg once daily, for 21 days in a 28 day cycle [143].The first trial enrolled 30 patients, and the second enrolled 60, but they had similar results: progression-free survival (PFS) at 12 weeks, the primary endpoint of the trial, was approximately 60%, and the median PFS was 18 weeks. The first trial included one partial response, and the second trial had one complete response. The main side effect in both trials was neutropenia, but the regimen in which palbociclib was given at 125 mg for

21 days appeared to be less toxic, and eliminated side effects like thrombocytopenia, anemia, and febrile neutropenia [109, 143]. Although treatment with palbociclib was associated with an extension of progression-free survival in both trials, there was a broad spectrum of patient response, ranging from rapid progression before the 12-week mark, to stable disease for a year or longer, to partial or complete RECIST responses. This prompts the question of why some WD/DDLS patients did so well on palbociclib, while others did not, and what molecular responses underlie patient outcome.

To maximize the benefit of CDK4/6 inhibitors for all patients, it is essential to understand the mechanism by which they act *in vivo,* whether it be autophagy, senescence, or another process. It is also important to elucidate whether the distinct CDK4/6 inhibitors act differently, either because of their structural variances or due to differences in their dosing schedule. To that end, after completing my work on *ANGPTL4* as a regulator of senescence in cancer cell lines, I wanted to apply my findings to an *in vivo* model. This was complicated by the dearth of adequate mouse models of liposarcoma. The development of transgenic mouse liposarcoma models has been unsuccessful, due in large part to the lack of understanding of the precursor cell in which to induce the genetic lesions associated with the disease. PDX models, while more readily available, are necessarily made using immunocompromised mice, which, given the connection between the SASP and the immune system, are an insufficient model in which to study the outcomes of senescence in response to CDK4/6i [156]. Instead, I turned to a phase II clinical trial of the CDK4/6 inhibitor abemaciclib in patients with advanced and progressive DDLS, which had recently been performed at MSKCC. Since the work previously discussed in cancer cell lines in **Chapter 3** utilized palbociclib, I

first conducted a comparison test of abemaciclib and palbociclib in our liposarcoma cell line DDLS$^{\text{Tet-ON FMDM2}}$. I then employed samples from the phase II trial of abemaciclib to investigate the link among *ANGPTL4,* senescence, the immune system, and patient outcome.

Results

A head-to-head comparison shows that abemaciclib and palbociclib induce similar senescence phenotypes in DDLS$^{\text{Tet-ON FMDM2}}$ cells

To determine whether abemaciclib and palbociclib act similarly to trigger senescence in DDLS$^{\text{Tet-ON FMDM2}}$, we set up a comparison time course experiment using both drugs (Fig. 4.1). DDLS$^{\text{Tet-ON FMDM2}}$ cells were treated with 10 µg/mL doxycycline for two days in stimulate F-MDM2 expression, followed by three days of doxycycline + either 0.4 µM palbociclib or 0.2 µM abemaciclib to induce cell cycle exit. Cells at this quiescent stage are subsequently referred to as Day 0. Doxycycline was then removed from the media, and the cells continued incubation in abemaciclib or palbociclib until harvesting, which occurred at days 3, 4, 5, 6, 9, 12 ,14, 21, and 28 after release into

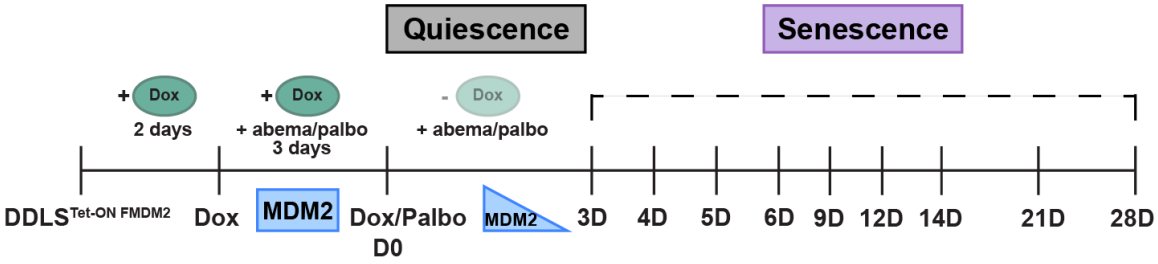

Figure 4.1 Schematic of DDLS$^{\text{Tet-ON FMDM2}}$ time course with abemaciclib and palbociclib.

CDK4/6i. At each of these time points, we assessed the appearance of several markers of senescence: ATRX foci formation, SA-β-gal, stable growth arrest, and SASP gene expression. Three replicates of this experiment were repeated, and in the third replicate, the doses were adjusted slightly to 0.5 μM palbociclib and 0.3 μM abemaciclib.

The kinetics of the induction of senescence hallmarks seen here in response to palbociclib treatment vary slightly from the results presented in **Chapter 3,** as this experiment used both a new lot of palbociclib and a different dose. However, the overall trends of the data remain the same. Treatment with both abemaciclib (Fig. 4.2A) and palbociclib (Fig. 4.2B) induced accumulation of ATRX foci. The effect was visible early, at day 3, and the average number of foci per cell continued to increase slightly throughout the remainder of the time course. Though each drug caused significant increases compared to cycling cells, there was no significant difference at any time point between the number of ATRX foci in abemaciclib- and palbociclib-treated cells (Fig. 4.2C). Similar results were seen for SA-β-gal expression. Early induction of SA-β-gal was visible in response to both drugs at days 3 and 4, and expression had more or less peaked by day 9 (Fig. 4.2D-E). Again, no significant difference in the amount of SA-β-gal expression was seen between abemaciclib- and palbociclib-treated cells at any time point (Fig. 4.2F). For both markers, as expected, no significant difference was observed in quiescent cells compared to the cycling control.

I then assessed the ability of abemaciclib and palbociclib to induce stable growth arrest by performing a clonogenic growth assay. Cells from each time point were replated at low density in the absence of drug and allowed to grow for 3 weeks. At that

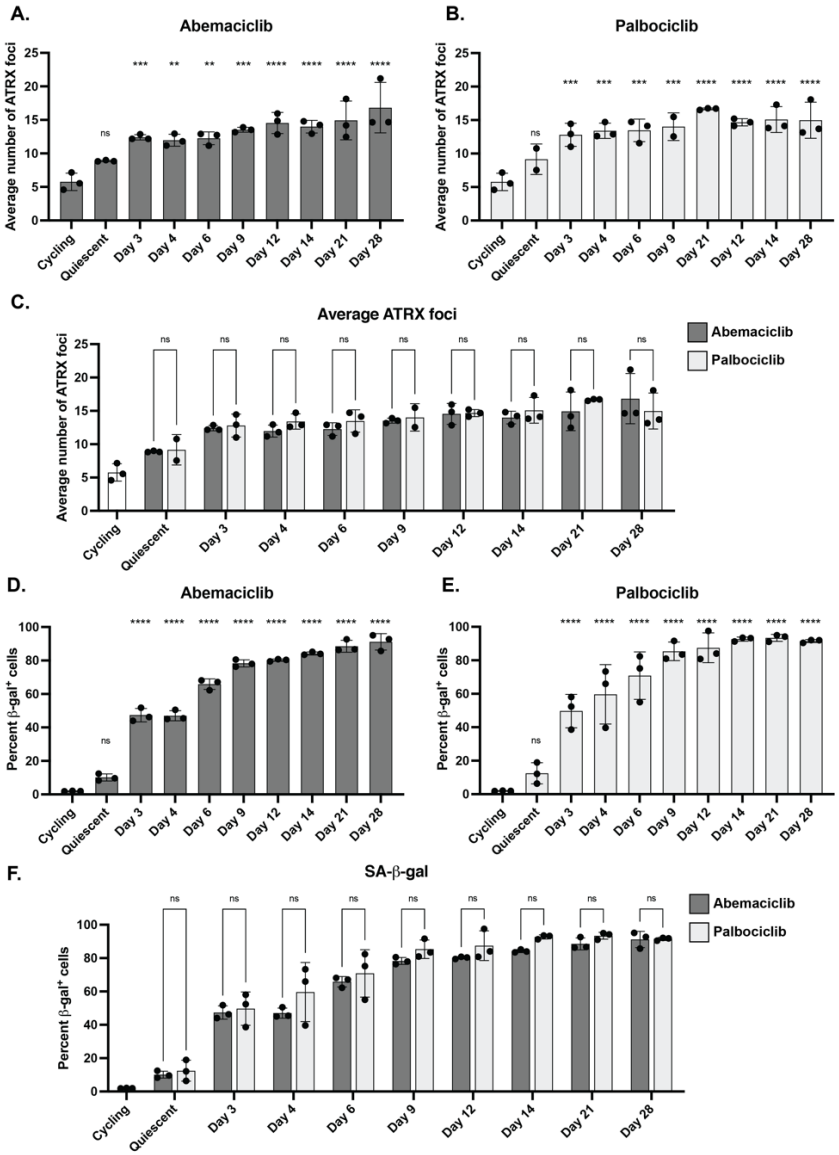

Figure 4.2 Abemaciclib and palbociclib treatment induce similar levels of early senescence markers in DDLS$^{Tet\text{-}ON\ FMDM2}$.

Cells were treated with abemaciclib or palbociclib as described in Fig. 4.1. Samples were harvested at the indicated time points and assayed for senescence markers. **(A-B)** Average number of ATRX foci/cell induced by treatment with (A) abemaciclib and (B) palbociclib are plotted. Statistics compare each time point with the cycling control. **(C)** Direct comparison of ATRX foci number in abemaciclib- and palbociclib-treated samples at each time point. **(D-E)** Percentage of SA-β-gal$^+$ cells induced by treatment with (D) abemaciclib and (E) palbociclib are plotted. Statistics compare each time point with the cycling control. **(F)** Direct comparison of SA-β-gal positivity in abemaciclib- and palbociclib-treated samples at each time point. **p<0.01, ***p<0.001, ****p<0.0001 by one-way ANOVA.

time, cells were stained with crystal violet and the area of the well containing colonies was quantified (Fig. 4.3A). For simplicity, only a subset of the time points is shown below. In both drug treatments, a significant reduction in colony growth was first visible at day 12, and the highest repression of growth occurred at day 28. Though the timing of irreversible arrest varied slightly from the time courses presented in **Chapter 3,** where irreversible arrest was first observed at day 14, there was no significant difference in colony formation between abemaciclib and palbociclib at any point in the experiment (Fig. 4.3B). Thus, abemaciclib and palbociclib also act to induce stable growth arrest with comparable kinetics.

Abemaciclib and palbociclib treatment induce similar, but not identical, SASP profiles in DDLS$^{Tet\text{-}ON\ FMDM2}$ cells

To determine if treatment with abemaciclib and palbociclib resulted in similar SASP profiles, I took RNA from cycling cells, quiescent cells, and day 6, 14, 21, and 28 senescent cells, and performed qPCR to examine the expression of SASP genes in response to each drug. I queried the expression of 21 out of the 37 SASP genes that were identified in our original DDLS$^{Tet\text{-}ON\ FMDM2}$ time course (**Chapter 3**, Table 3.2), as well as two housekeeping genes. Because the majority of the SASP genes were expected to increase in expression, I also included Cyclin E2 (*CCNE2*) as a benchmark for an E2F target gene that should be downregulated during both quiescence and senescence. Expression level was normalized to the cycling control from each time course experiment, and the results of the SASP qPCR panel are shown in an unclustered heatmap form (Fig. 4.4). Overall, the patterns of SASP gene expression appear quite

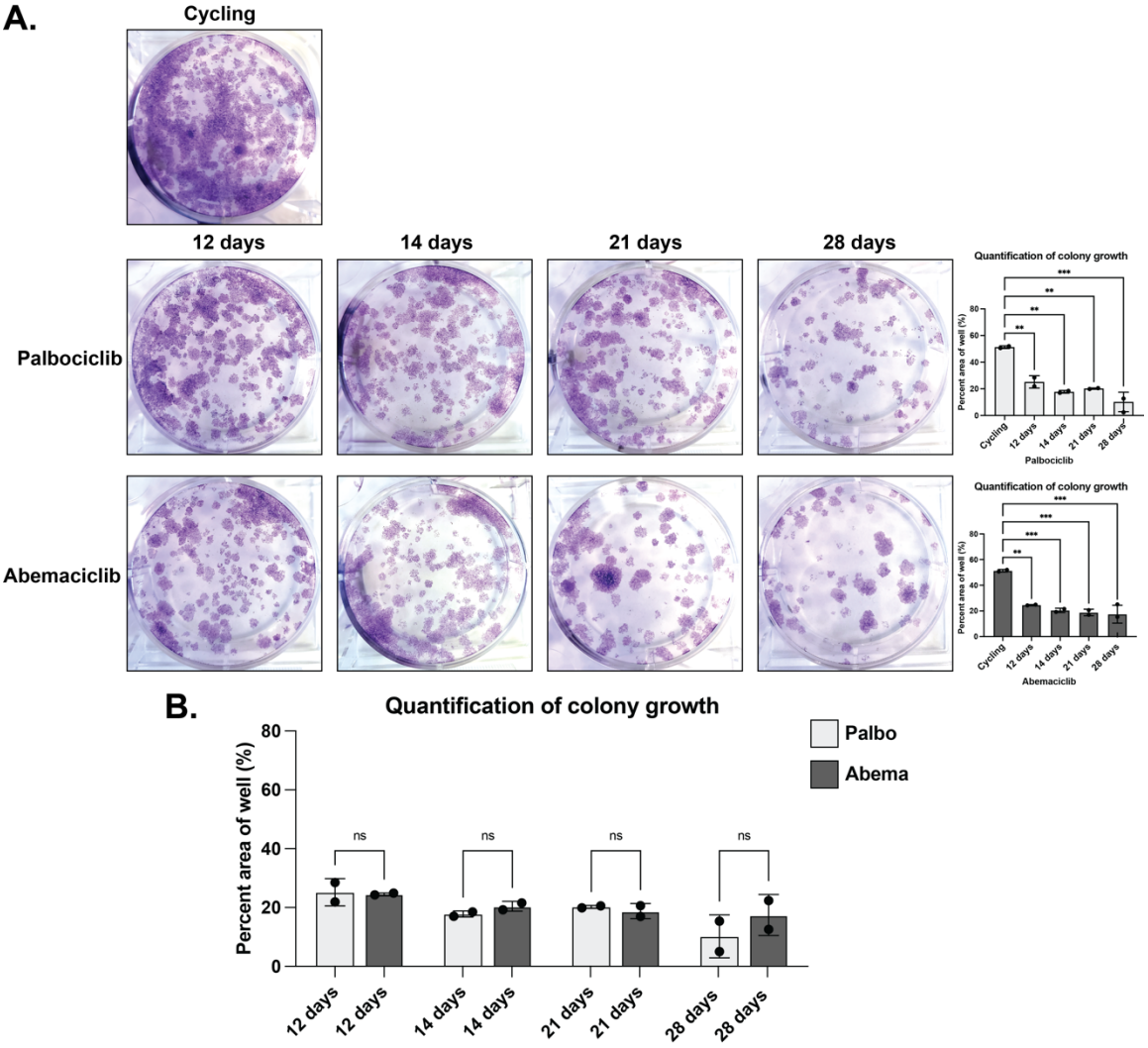

Figure 4.3 Abemaciclib and palbociclib treatment induce similar stable arrest phenotypes in DDLS$^{\text{Tet-ON FMDM2}}$ cells.

(A) After the indicated days of treatment, cells were replated at low density in the absence of drug and allowed to grow for 3 weeks. Colonies were stained with crystal violet and quantified using ImageJ. **(B)** Direct comparison of colony formation in abemaciclib- and palbociclib-treated samples at each time point. **p<0.01, ***p<0.001 by one-way ANOVA.

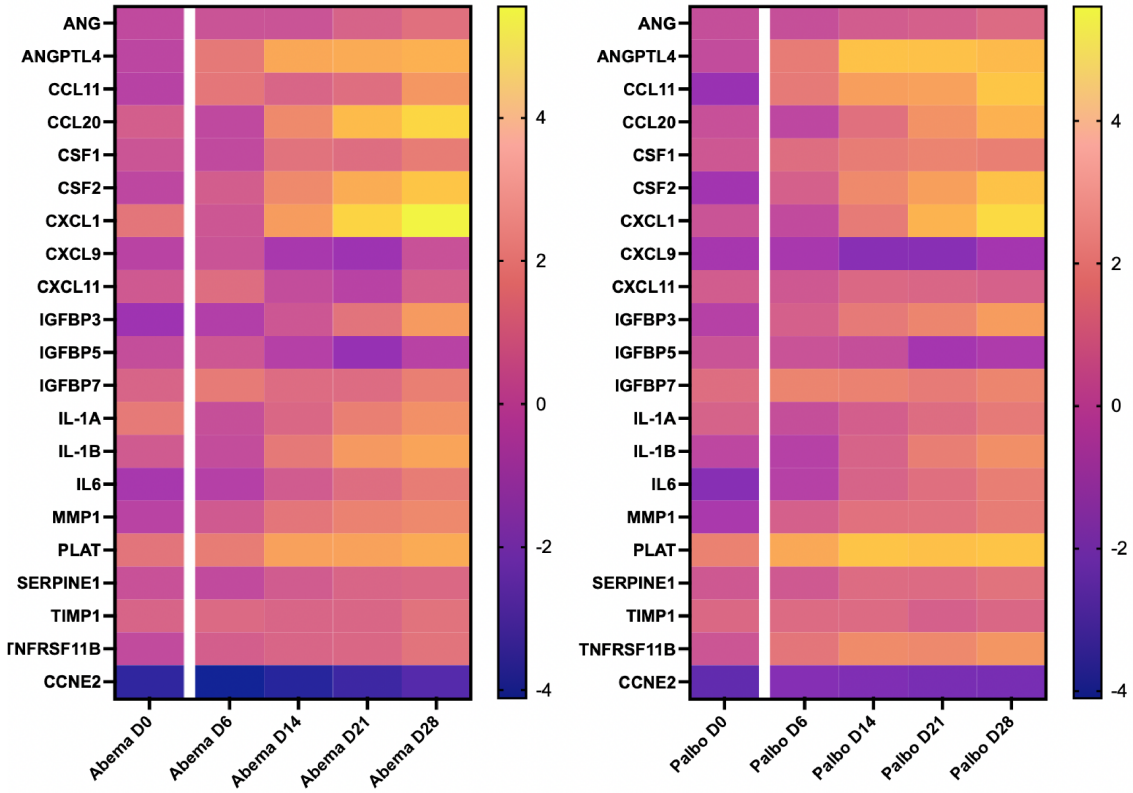

Figure 4.4 Comparison of the SASP profile of DDLS$^{\text{Tet-ON FMDM2}}$ cells treated with abemaciclib or palbociclib.

Transcript levels of 21 SASP genes were quantified using qPCR, natural log-transformed, then plotted in heatmaps where each box represents the mean ln(fold change) from the three time courses. *CCNE2* (CyclinE2) is included at the bottom of each heatmap as a control down-regulated gene.

similar, though the magnitude of gene expression varies. For example, *CXCL1* was much more strongly induced in response to abemaciclib treatment than in the palbociclib treatment, particularly at day 28. *CCNE2* expression was also more strongly suppressed in the abemaciclib-treated cells. On the other hand, *PLAT* was more highly expressed in the palbociclib samples than in abemaciclib samples.

I next took this expression data and performed unsupervised hierarchical clustering to determine how similar the SASP programs induced by abemaciclib and palbociclib truly are. Using this approach, quiescent (day 0) cells and early senescent (day 6) cells from both palbociclib and abemaciclib treatment clustered together and were most closely related to each other (Fig. 4.5). This is logical, given that SASP gene expression overall is low at these early time points. Interestingly, from day 14 onwards, the samples clustered separately based on drug treatment, and for both drugs, days 14 and 21 were more closely related than day 28. Thus, the SASP induced by abemaciclib treatment differs slightly from the SASP induced by palbociclib treatment, and this difference is especially apparent as cells move deeper and deeper into the senescent state. The results seen from this inherently biased qPCR approach are also confirmed by RNA sequencing performed on the samples from these time courses, which found that the SASP gene expression induced by these two CDK4/6 inhibitors diverges at day 28 (Eli Lilly, data not shown).

In summary, the results from these time courses show that abemaciclib and palbociclib, despite being structurally distinct, act to trigger similar senescent states in liposarcoma cells in culture. Early markers of senescence, like ATRX foci formation and SA-β-gal expression, are induced to similar degrees and with similar kinetics. Stable

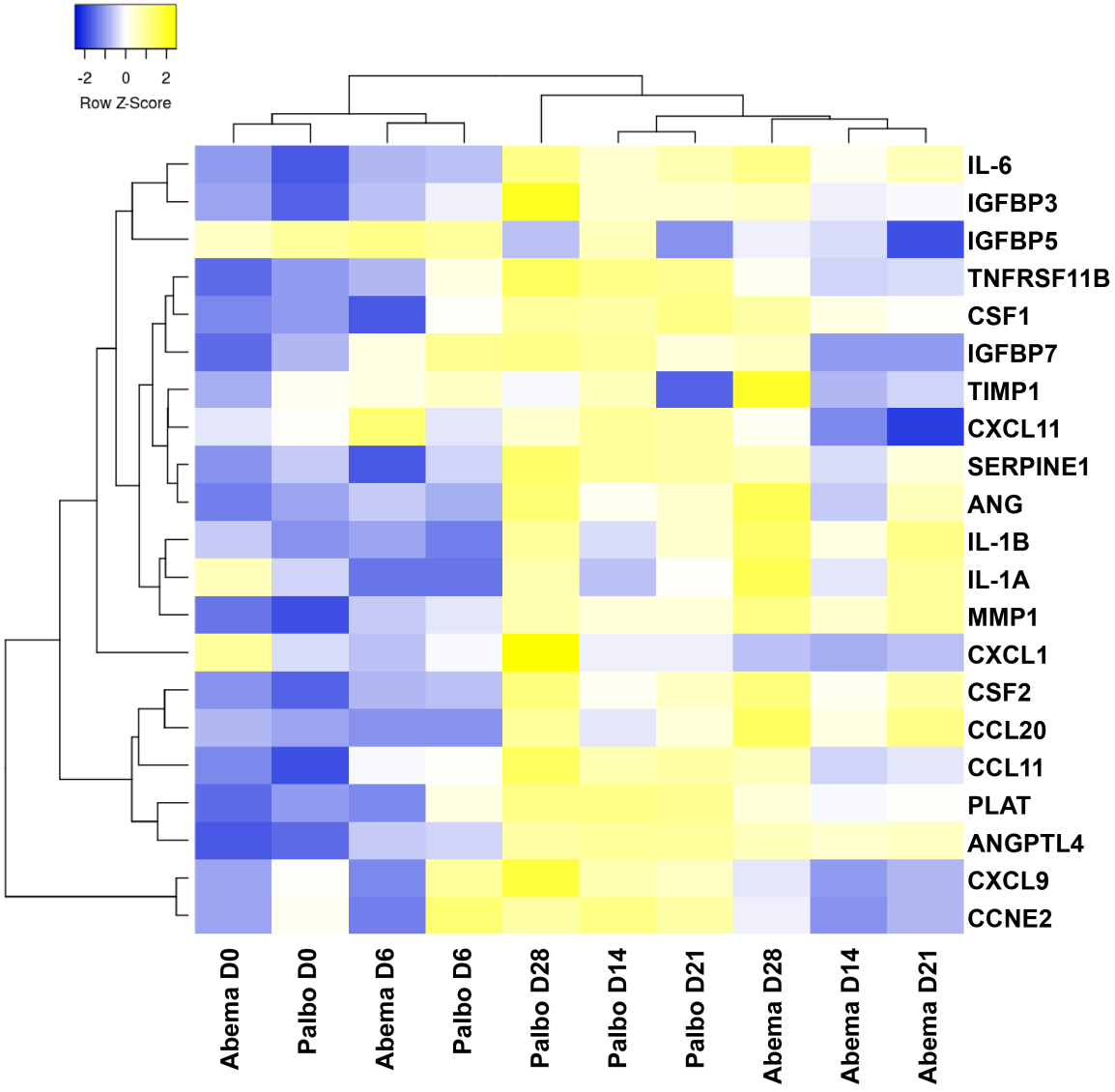

Figure 4.5 Unsupervised hierarchical clustering of the SASP profile of DDLS$^{\text{Tet-ON FMDM2}}$ cells treated with abemaciclib or palbociclib.

The mean ln(fold change) of each SASP gene is plotted and subjected to unsupervised hierarchical clustering. Values are scaled by row, and both rows and columns are clustered using the complete clustering method with Euclidean distance measuring.

growth arrest is observed at later time points in response to both drugs. SASP gene expression largely begins at day 14, and though there are differences in the expression of some SASP factors, *ANGPTL4* expression is strongly increased from day 14 onwards in response to both palbociclib and abemaciclib treatment (Fig. 4.4). Therefore, I moved forward with applying the findings from palbociclib treatment of DDLS$^{\text{Tet-ON FMDM2}}$ cells to the results of the abemaciclib clinical trial.

Abemaciclib extends median progression-free survival to 33 weeks as a single agent in patients with dedifferentiated liposarcoma

Under the supervision of Drs. William Tap and Mark Dickson, a phase II study using abemaciclib was conducted at MSKCC to determine if this drug has value for treating patients with DDLS. Between August 2016 and October 2018, thirty patients with confirmed advanced and progressive DDLS were enrolled in this single-center, non-randomized, open-label trial, during which they received 200 mg of abemaciclib orally twice daily. Image-guided needle biopsies were obtained at two time points: pre-treatment biopsies were collected within 3 weeks before starting treatment, and on-treatment biopsies were collected early in the second cycle of abemaciclib (4-6 weeks on drug). Tumor growth was assessed by an independent reference radiologist every 6 weeks for the first 36 weeks, and every 12 weeks thereafter.

One patient withdrew consent and was removed from the trial. The genomic profiles were unremarkable and were overall similar to those from previous trials with palbociclib [109, 143]. Common genomic alterations included amplification of *CDK4* and *MDM2* on chromosome 12, along with variable loss and gain of other regions and some

scattered patient-specific mutations. The patient demographics are presented in Table 4.1. Eighteen of the 30 patients were male, and the median age was 62 years. The majority of the tumors were located in the abdomen or the retroperitoneum, and the remainder were in the extremities. Half of the patients had received no prior systemic therapy. There was no

Patient demographics	**n (%)**
Total	**30**
Male	**18 (60)**
Median Age	**62**
Range	**39-88**
Prior systemic treatments (#)	
0	**15 (50)**
1	**9 (30)**
≥2	**6 (20)**
Location of primary tumor	
Abdomen/retroperitoneum	**26 (87)**
Extremity	**4 (13)**

Table 4.1 Demographics of patients enrolled in the phase II clinical trial of abemaciclib in dedifferentiated liposarcoma.

significant association of PFS with demographics, copy number variation, or prior therapy (Table 4.2). Toxicities were graded according to the National Cancer Institute's Common Terminology Criteria for Adverse Events (CTCAE) version 4.0. Gastrointestinal distress was the most common adverse effect and could be clinically managed (Table 4.3).

The primary endpoint for a single agent therapy in DDLS was PFS at 12 weeks. Twenty-three of the 30 patients were progression-free at 12 weeks (76.7%, two-sided 95% CI: 57.7% - 90.1%), and thus the study met its primary endpoint and demonstrated that

Covariate*	beta	HR (95% CI for HR)	Wald test	p.value	p.value_ FDR
Age at study entry	0.0027	1 (0.97-1)	0.02	0.89	1
Gender	0.14	1.1 (0.55-2.4)	0.13	0.71	1
# of prior lines of therapy	0.37	1.4 (1.1-2)	5.9	0.015	1

Table 4.2 Analysis of association between clinical covariates and PFS.

Univariable Cox proportional-hazards model for clinical covariate was calculated using the following model: (PFS, censored) ~ Covariate* to assess association between clinical correlates and PFS.

Toxicity (%)	G2	G3	G4
Anemia	70	37	
Thrombocytopenia	13	13	3
Neutropenia	43	17	3
Lymphocyte count decreased	23	23	3
Diarrhea	27	7	
Nausea	17	3	
Fatigue	23	3	
Vomiting	7		
Anorexia	30		

Table 4.3 Patient toxicities graded according to the National Cancer Institute's Common Terminology Criteria for Adverse Events, version 4.0.

single agent abemaciclib is useful for extending the duration of PFS in DDLS (Fig. 4.6A). With a data lock on June 1, 2021, the median PFS was 33 weeks (two-sided 95% CI: 28-72 weeks). Three patients had a partial response, and six have had stable disease for two years or longer (Fig. 4.6B). Drug treatment consistently decreased the percentage of Ki67-positive cells in the on-treatment biopsies, compared to the pre-treatment biopsies, in all but three patients (Fig. 4.6C). Patients in whom Ki67 expression did not decrease fared poorly, as expected (PFS <33 weeks, study IDs 16, 02, and 39).

Abemaciclib treatment leads to increased inflammation within tumor boundaries of patients with DDLS

To begin deciphering the mechanism by which abemaciclib extends progression-free survival, we looked at gene set enrichment analysis (GSEA) in ten of the on-treatment biopsies for which we had available tissue. Several GSEA inflammation hallmark programs were significantly increased in the three patients with a higher PFS (PFS >33 weeks) compared to the seven patients with lower PFS (PFS < 33 weeks) (Fig. 4.7, top panel). Changes in RAS signaling and metabolic pathways were also observed. Increased inflammation hallmark programs persisted even as we adjusted the stringency of the analysis parameters (Fig. 4.7, bottom panel). This suggested that an immunogenic effect might underlie the ability of abemaciclib treatment to induce senescence.

To determine whether this up-regulation of inflammatory programs resulted in recruitment of immune cells to the tumor boundaries, we performed immunohistochemistry (IHC) on serial sections from all available pre-treatment and on-treatment patient biopsy pairs using antibodies against CD4, CD8, FOXP3, or CD68.

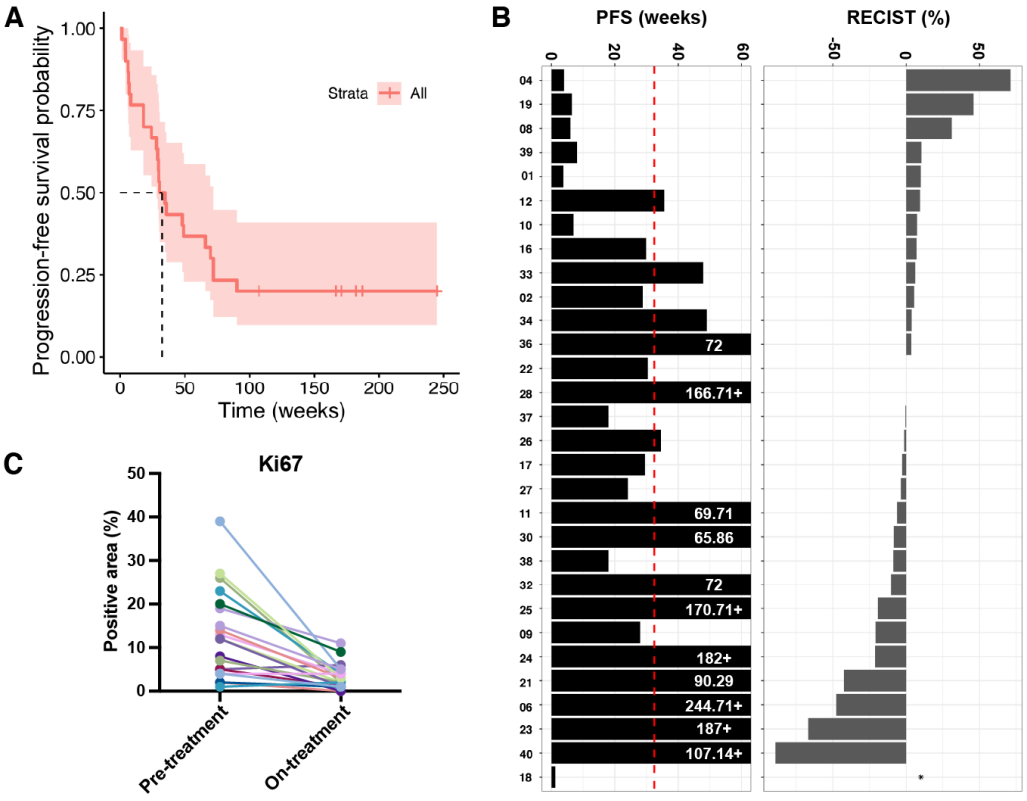

Figure 4.6 Phase II trial of the CDK4 inhibitor abemaciclib in dedifferentiated liposarcoma.

(A) Kaplan-Meier plot of progression-free survival in DDLS (n = 30). X-axis represents time in weeks, while y-axis represents progression-free survival probability. Dotted line shows median PFS (33 weeks, 95 CI=28-72 weeks). **(B)** Best RECIST changes in tumor volume observed in target lesions and corresponding PFS in patients with DDLS treated with abemaciclib**.** PFS swimplot shows patient ID (y-axis) and PFS values in weeks (x-axis), and the dotted red line illustrates median PFS values of 33. Bar chart labels show number of PFS weeks if PFS exceeded 60 weeks, and plus sign (+) represents ongoing treatment. RECIST swimplot shows 29 patients that were evaluated for response to abemaciclib (RECIST 1.1), and one patient that had no data for RECIST due to withdrawal from the study after receiving treatment for 1 week. **(C)** Ki67 expression, measured as percent positive area, for each set of matched pre- and on-treatment patient biopsies.

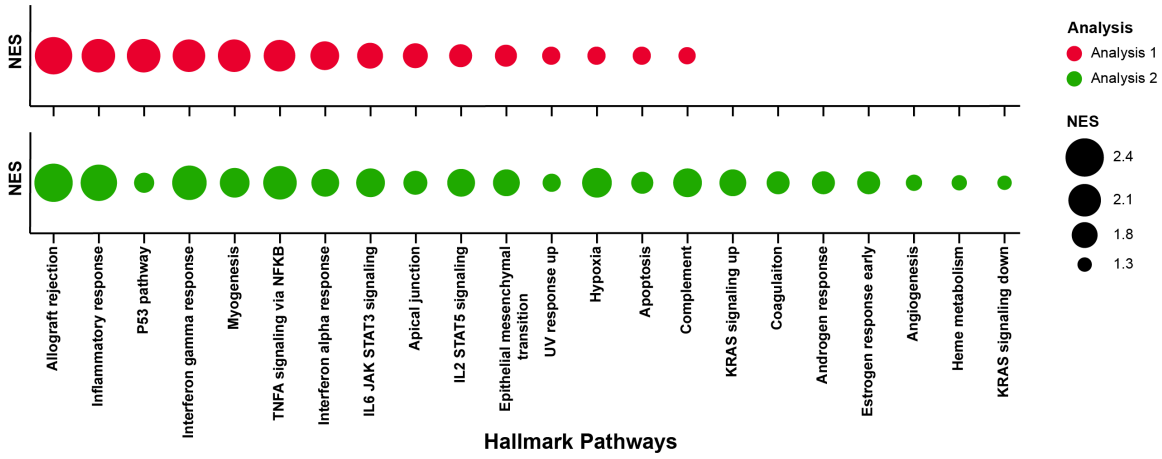

Figure 4.7 GSEA suggests inflammation in on-treatment biopsies from DDLS patients treated with abemaciclib.

Gene set enrichment analysis of pathways associated with PFS in DDLS. The results from GSEA analysis with the gene set names from Hallmark pathways and the normalized enrichment scores (NES) are shown. Genes were ranked by the effect size, which was calculated by multiplying P-value (P value based on comparison between high and low PFS) with the sign of log-fold change. These values were then used for the ranking of the genes, and weighted enrichment statistics and 100,000 gene set permutations were subsequently calculated and used for detection of significantly enriched pathways. We present two types of GSEA analysis based on the sample groups defined by PFS level. Analysis 1: Samples were divided into high and low PFS based on the median PFS values (32.5), Analysis 2: Patients 26 and 12 were moved from the high PFS group into the low PFS group to determine the effect of samples with borderline PFS values on changes in pathways analysis. Absolute value of normalized enrichment score (NES, y-axes) of only upregulated pathways in high PFS samples are shown for each Hallmark pathway (x-axes), and each dot on the plot is proportional to the size of the NES. All Hallmark pathways shown had an adjusted P value < 0.05.

Sections were then imaged, and any drug-induced changes in the number of inflammatory cells recruited into the tumors or along tumor boundaries were quantified.

Images from a representative positive and negative tumor sample are shown (Fig. 4.8A and 4.8B, respectively). We defined a significant change as ≥1.7-fold change in the number of positive cells from the baseline biopsy to the on-treatment biopsy. We also required that the distribution be significantly altered by both the Mann-Whitney and Kolmogorov-Smirnov tests, defined as $p \leq 0.05$.

Upon abemaciclib treatment, we observed an increase in tumor-associated inflammatory T-cells ($CD4^+$, $CD8^+$ or $FOXP3^+$) in most patients (15/20). All but one of these patients had an increase in $CD4^+$ cells, along with at least one other type of T-cell. The single patient who did not exhibit increased numbers of $CD4^+$ cells did have an increase in $FOXP3^+$ cells. Increases in $CD68^+$ monocytes also occurred, but we did not have sufficient tissue to explore potential changes in the M1 and M2 subtypes of such cells. A heatmap summarizing the fold change in each marker from baseline to the one-month on-treatment biopsy is shown in Fig. 4.9A.

On samples for which we were able to obtain sufficiently high-quality RNA, we also performed quanTIseq, an approach that uses RNAseq data to quantify the immune-cell fractions within tumors. Three pairs of pre- and on-treatment biopsies were included in the quanTIseq, and the data confirm that treatment with abemaciclib in liposarcoma patients resulted in significantly increased, rapid recruitment of T-cells to the tumor (Fig. 4.9B). Thus, the results of our IHC analysis are supported by results obtained from an unbiased sequencing approach, where available.

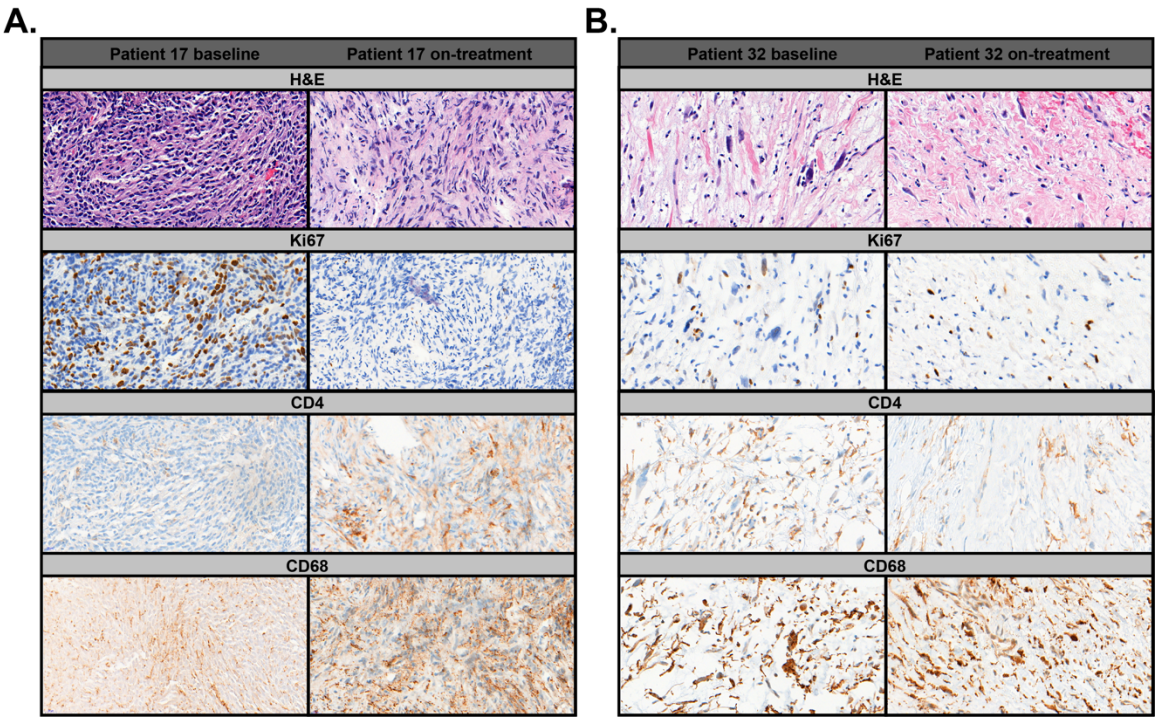

Figure 4.8 Abemaciclib treatment induces inflammation in some patients with DDLS.

Representative images of tissue stained for the indicated markers in a patient with a positive response to drug treatment **(A)** and a patient with a largely negative response **(B)**.

Despite the GSEA result (Fig. 4.7), which showed a correlation between inflammation and prolonged PFS, we found a nearly even split of inflammation$^+$ and inflammation$^-$ patients in both the low PFS and high PFS categories (not significant, p=1.0 by Fisher's exact test). Of the five patients who did not exhibit increased inflammation, two had PFS < 33 weeks and three had PFS > 33 weeks. Of the 15 patients who did experience increased inflammation, seven had PFS < 33 weeks and 8 had PFS > 33 weeks (Fig. 4.9C). This suggests that while abemaciclib acted to induce inflammation at the tumor site, and specifically, recruitment of CD4$^+$ T-cells, inflammation alone is insufficient to account for the extended PFS that was observed in liposarcoma patients treated with this drug.

Inflammation in liposarcoma patients treated with abemaciclib is associated with cellular senescence within the tumor

Given the strong senescence response observed in liposarcoma cells treated with abemaciclib in culture, we next wanted to address whether the increased inflammation observed after abemaciclib treatment in patients occurred through a senescence-dependent mechanism. We were severely limited in terms of tissue availability, and only had access to formalin-fixed, paraffin-embedded (FFPE) tissues, so we were unable to pursue markers of senescence like SA-β-gal or ATRX foci. Additionally, given the evidence shown in **Chapter 3** concerning such early phenotypes of senescence**,** we wanted to be sure that we were choosing markers that would identify fully mature senescent cells, not merely SA-β-gal$^+$ cells. To that end, we decided to assay for senescence using two markers: expression of *CDKN2A,* an early marker of cell cycle exit that is commonly associated with

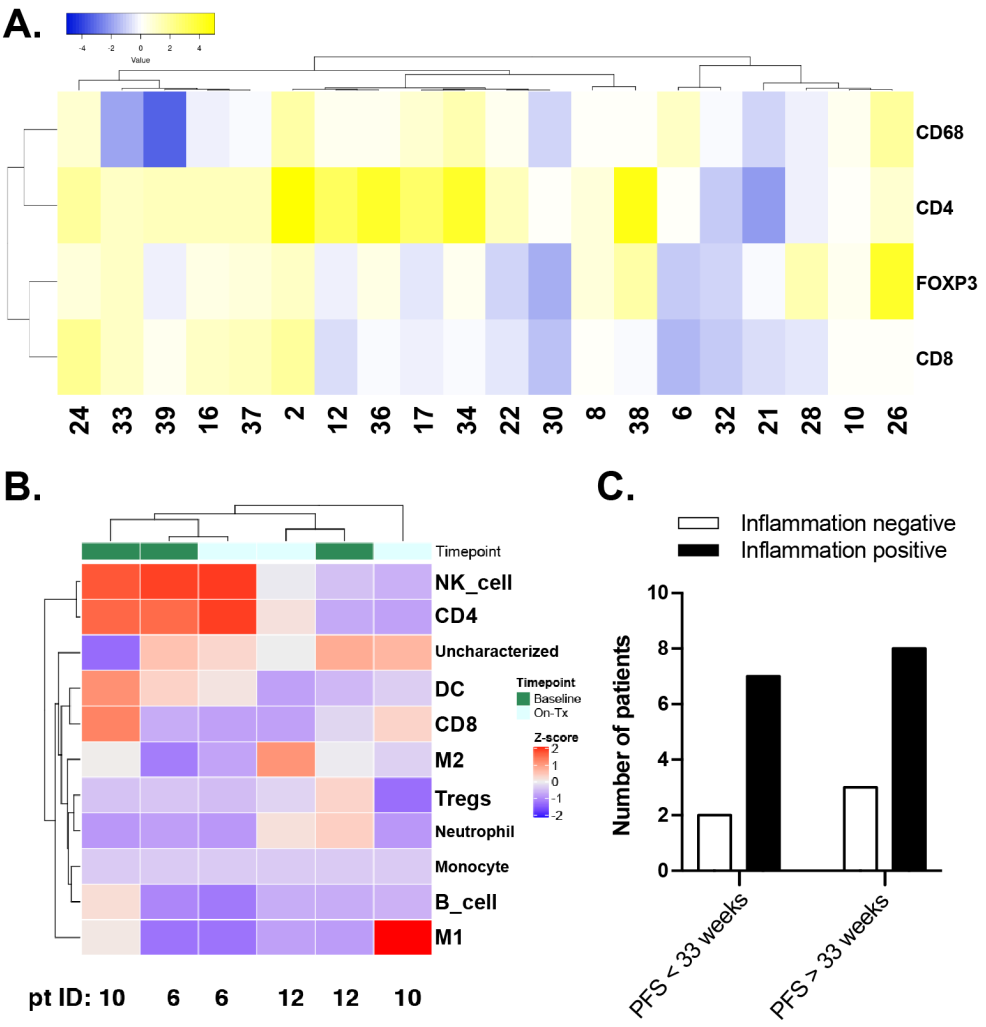

Figure 4.9 Inflammation alone cannot account for extended PFS in response to abemaciclib treatment.

(A) Unsupervised clustering of a natural log scale heat-map of the fold change in the number of positive cells (CD4, CD8, CD68, FOXP3) from pre-treatment to on-treatment biopsies. Patient IDs are listed on the x-axis. **(B)** quanTIseq of three pre- and on-treatment paired biopsies. The heatmap represents the z-score transformed immune cell fraction, estimated via the deconvolution method for paired samples. Time point of collection indicated on top (baseline, green; on-treatment, blue) and cell types on the right. **(C)** Patients were categorized as inflammation positive (≥1.7X increase in at least one of $CD4^+$, $CD8^+$, and $FOXP3^+$ cells) or inflammation negative, and plotted based on whether their PFS was greater than or less than the median (33 weeks). No significant difference was found between the groups of patients (p=1.0 (Fisher's exact test)).

senescence, and *ANGPTL4,* which I have shown to be a reliable marker of a fully senescent cell in liposarcoma cells treated both with palbociclib and abemaciclib.

We employed RNAscope, a form of in-situ hybridization that has been optimized to maximize signal to noise ratio, to look at expression of *ANGPTL4* and *CDKN2A*. Using the serial sections from the pre-treatment and one-month on-treatment patient biopsies, we measured the expression of *ANGPTL4* and *CDKN2A* mRNA and quantified the resulting fluorescent signal. We again defined a significant change as ≥1.7-fold change in the mRNA level from the baseline biopsy to the on-treatment biopsy, and we also required that the distribution be significantly altered by both the Mann-Whitney and Kolmogorov-Smirnov tests, defined as $p \leq 0.05$.

Images from a representative positive and negative tumor sample are shown (Fig. 4.10A and 4.10B, respectively), as well as a heat map summarizing all the drug-induced changes, both in the inflammatory cells and in the senescence markers (Fig. 4.11A). A kernel density estimation shows that there was a strong association between drug-induced accumulation of *ANGPTL4* mRNA and increased levels of *CDKN2A* mRNA, which is consistent with the notion that *ANGPTL4* expression can be used to identify senescent cells in tissue (Fig. 4.11B). The drug-induced senescence signature, *CDKN2A*$^+$*/ANGPTL4*$^+$, was significantly correlated with an increase in inflammatory cells, as marked by CD4, CD8, or FOXP3 positivity (Fig. 4.11C, p=0.030 by Fisher's exact test, p=0.014 by Chi-square test). The strongest association was between the senescence signature and increased levels of CD4$^+$ T-cells, such that tumors with senescence experienced, on average, 4.14-fold higher levels of CD4$^+$ cells than tumors without senescence (Fig. 4.11D). Three patients who were not *CDKN2A*$^+$*/ANGPTL4*$^+$

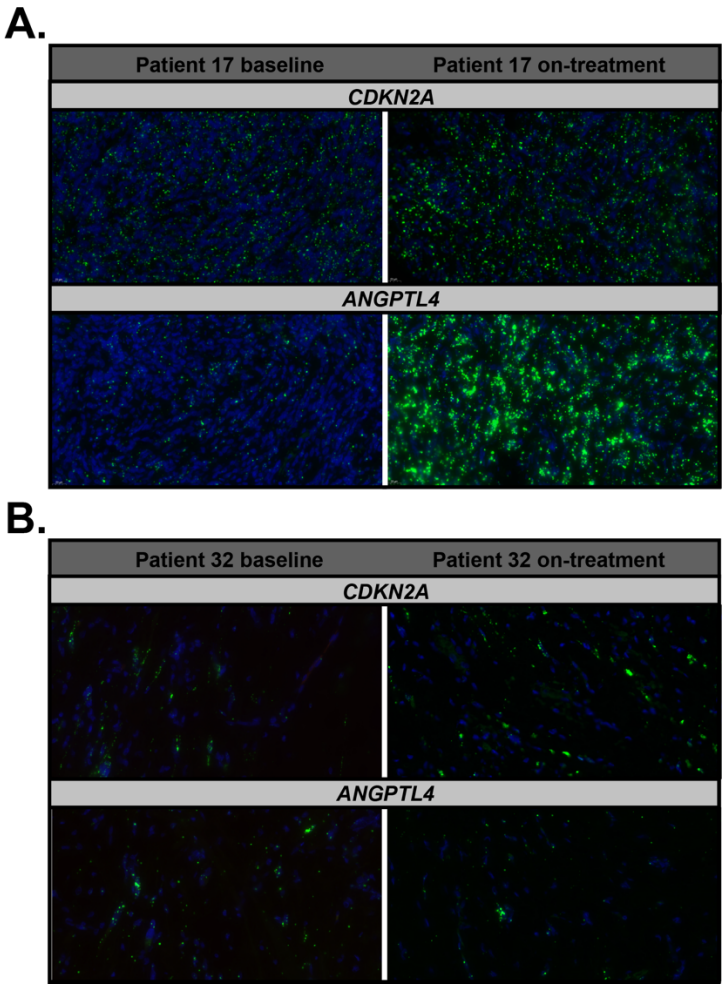

Figure 4.10 Abemaciclib treatment induces expression of senescence hallmarks in some patients.

Representative images of tissue stained for the indicated markers in a patient with a positive response to drug treatment **(A)** and a patient with a largely negative response **(B)**.

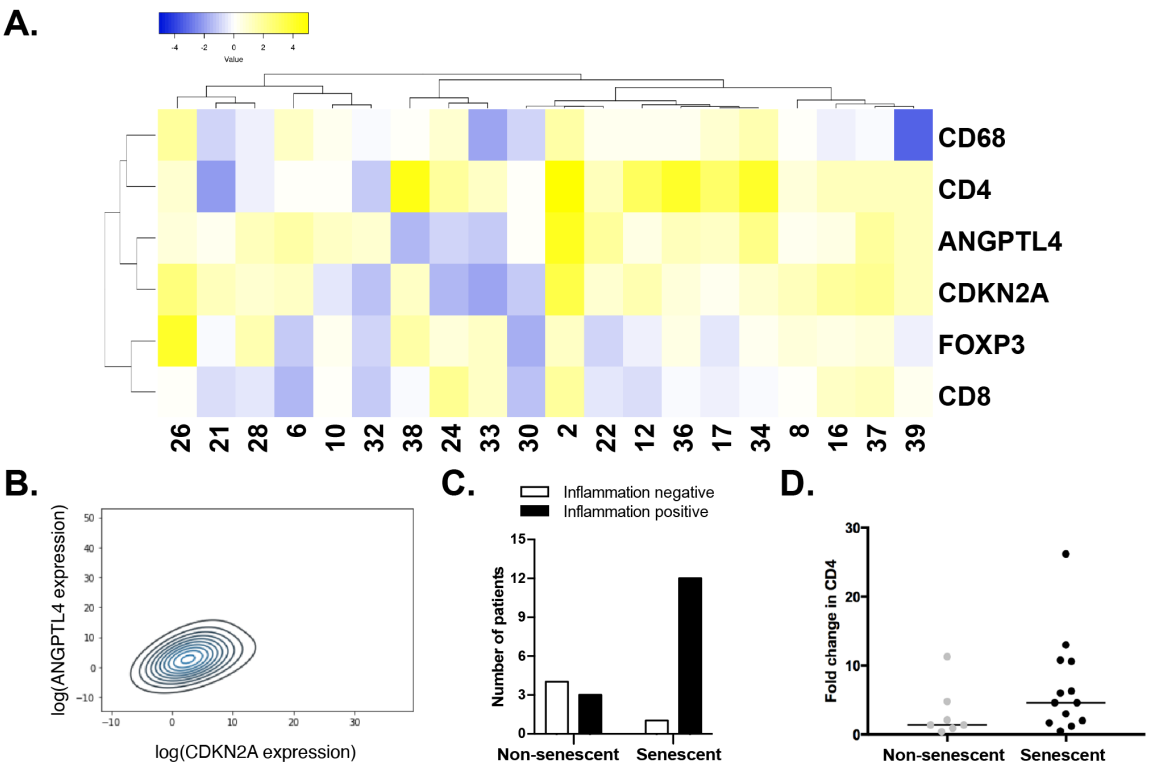

Figure 4.11 *ANGPTL4* and *CDKN2A* mRNA accumulation correlates with CD4+ cell recruitment in patients treated with abemaciclib.

(A) Unsupervised clustering of a natural log scale heat-map of the fold change in mRNA expression (*ANGPTL4* and *CDKN2A*) or the number of positive cells (CD4, CD8, CD68, FOXP3) from pre-treatment to on-treatment biopsies. Patient IDs are listed on the x-axis. **(B)** 2D kernel density plot showing the correlation between *CDKN2A* expression (x-axis) and *ANGPTL4* expression (y-axis). (**C**) Patients were categorized as senescent ($\geq$1.7X increase in *CDKN2A* and *ANGPTL4*) or non-senescent, and the overall inflammatory state of the tumors is plotted for each group. Drug-induced inflammation was defined as $\geq$1.7X in $CD4^+$, $CD8^+$, or $FOXP3^+$ cells. A significant difference was found between the groups of patients (p=0.030 (Fisher's exact test,) p=0.014 (Chi-square test)). (**D**) Plot of the magnitude of drug-induced changes in $CD4^+$ cells in the senescent and non-senescent patients (average difference in fold change=4.14, 94% CI=0.5-8.3). The line represents the median fold increase.

also exhibited low grade increases in T-cell number. Of these three, one was positive only for *CDKN2A* and the other two were double negative. The recruitment of T-cells in the absence of SASP-producing senescent cells might be due to drug-induced changes in the expression of cellular MHC receptors, as discussed previously [151-153].

Senescence and inflammation are associated with increased risk of progression over time

I next asked whether the senescence and inflammation induced by abemaciclib treatment had an impact on patient outcome. With such a small sample size, we were unable to use typical frequentist approaches to show nominal statistical significance in our clinical data, so we turned instead to Bayesian statistics. In rare diseases like liposarcoma, where clinical trials are limited to small numbers of participants, it is difficult to produce robust data. In these cases, Bayesian methods are well-suited to calculating the probability that a treatment has a clinically meaningful benefit [157-160].

Patients were broken into two groups based on whether they showed increased markers of both senescence and subsequent inflammation (*ANGPTL4*$^+$/*CDKN2A*$^+$/CD4$^+$, or ACC$^+$) or not. The second group consists of patients who had either senescence or inflammation, or neither. Bayesian inference showed that being ACC$^+$ was significantly associated with approximately a 58% increase in hazard ($p=0.0373$, Fig. 4.12A-C). In other words, patients whose tumors demonstrated signs of senescence *and* its associated inflammation were at greater risk of progression than patients whose tumors showed only signs of senescence *or* inflammation, or neither.

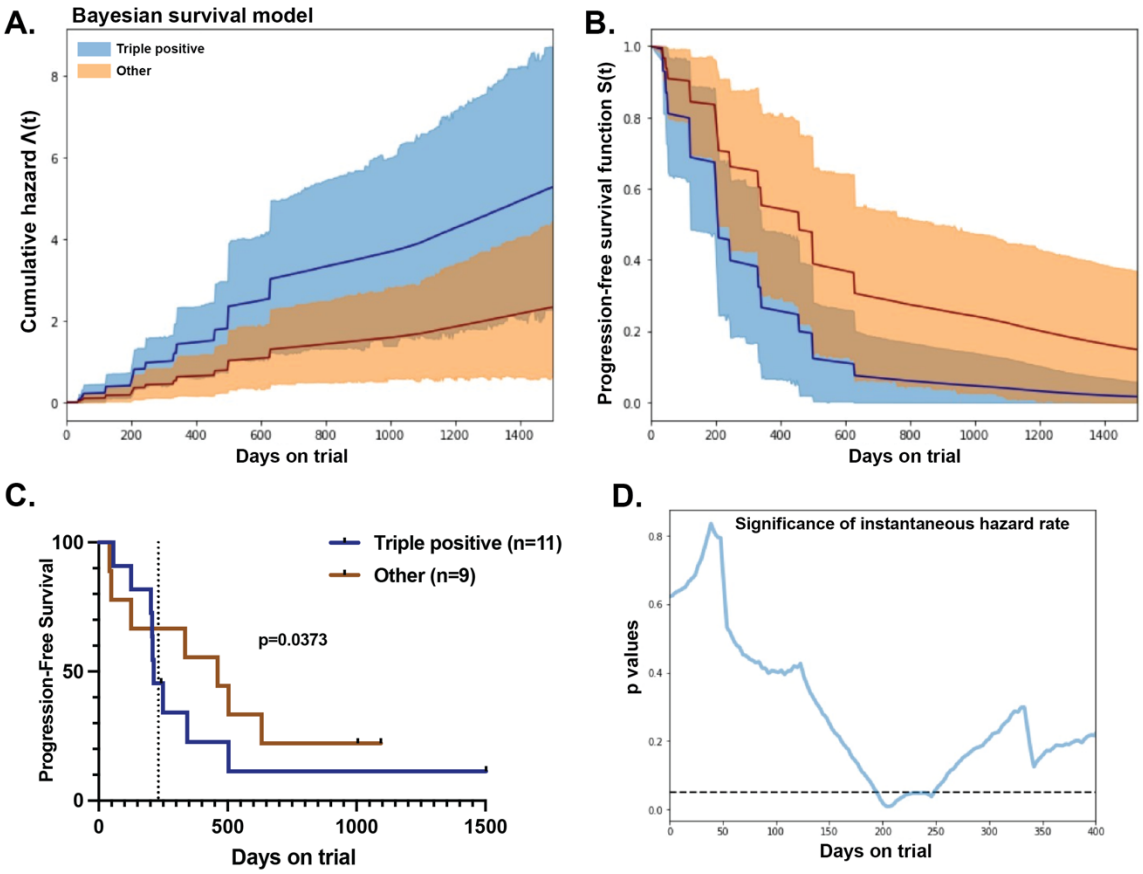

Figure 4.12 Senescence and inflammation following abemaciclib treatment correlate with increased risk of progression in patients with DDLS.

(A) The cumulative hazard function, which defines the risk accumulated over the interval (0, t), for the triple positive (*ANGPTL4*$^+$/*CDKN2A*$^+$/CD4$^+$) and non-triple positive (all other combinations) groups. **(B)** The survival function, a calculation of the probability of progression-free survival past time (t), for the two groups. For (A) and (B), the solid lines indicate the average values, and the shaded regions indicate 95% confidence intervals. **(C)** Kaplan-Meier curve showing PFS of triple positive versus other groups. Being triple positive was associated with a 58% increase in hazard rate, with significance of p = 0.0373 (measured using a ROPE null hypothesis correlate). Dotted line represents median PFS (33 weeks/231 days). **(D)** p-values, measured using a ROPE correlate, of the instantaneous hazard rate associated with being triple positive. The dashed line represents p = 0.05; p≤0.05 between days 195-246.

We next calculated the instantaneous hazard rate, which showed that the most significant risk of progression for patients in the ACC^+ group occurred between days 194 and 246, a period that encompasses the median PFS: 33 weeks, or 231 days (Fig. 4.12D, $p \leq 0.05$). Thus, having senescence and inflammation did not prevent patients from approaching or reaching the median PFS of the trial; only around the time of the median PFS did it become significantly hazardous to be ACC^+. Intriguingly, when patients were grouped based on senescence status alone, with no regard for inflammation status (*ANGPTL4*$^+$*/CDKN2A*$^+$ vs not senescent), the effect was lost (Fig. 4.13A). The cumulative hazard rate (Fig. 4.13B) and progression-free survival function (Fig. 4.13C) between the two groups were essentially equivalent. Senescence on its own, therefore, is not inherently detrimental to the patient. It is the inflammation associated with having senescence that contributes to the overall increased risk of progression.

In summary, the results from this trial show that treatment with abemaciclib can induce cellular senescence in patients with liposarcoma; that the outcome of that senescence is inflammation, driven primarily by a T-cell response; and that senescence and its associated inflammation have an overall detrimental effect on progression-free survival.

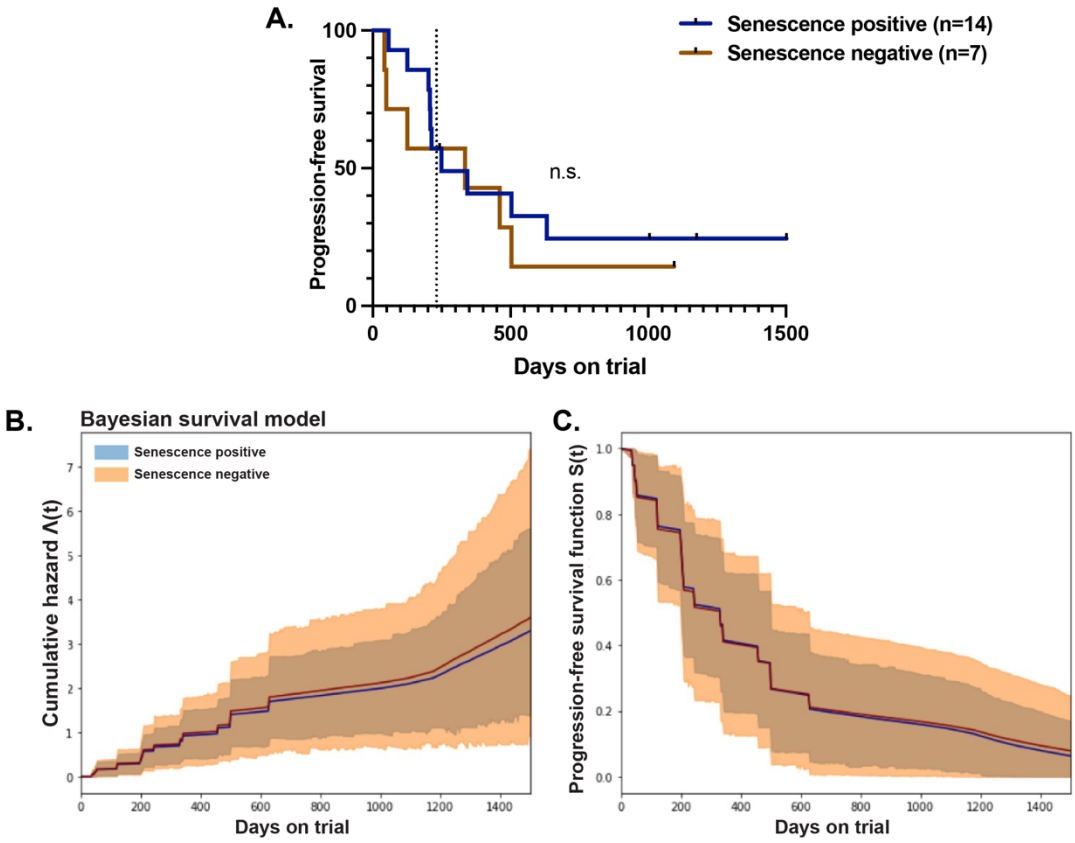

Figure 4.13 Senescence alone following abemaciclib treatment has no significant effect on risk of progression in patients with DDLS.

(A) Kaplan-Meier curve showing PFS of senescence positive (*ANGPTL4*$^{+}$/*CDKN2A*$^{+}$) and senescence negative groups. There was no significant difference in risk of progression between the two groups (measured using a ROPE null hypothesis correlate). Dotted line represents median PFS (33 weeks/231 days). **(B)** The cumulative hazard function, which defines the risk accumulated over the interval (0, t), for the senescence-positive and senescence-negative groups. **(C)** The survival function, a calculation of the probability of progression-free survival past time (t), for the two groups. For (A) and (B), the solid lines indicate the average values, and the shaded regions indicate 95% confidence intervals.

Discussion

Palbociclib versus abemaciclib: same same, but different?

Abemaciclib and palbociclib are two drugs of the same class, which theoretically function similarly and are approved to treat the same disease, but there are marked differences between them, from their structure to their dosing regimen to their specificity against CDKs. Here, I showed that palbociclib and abemaciclib induce similar senescent states in liposarcoma cells *in vitro.* I also established that *ANGPTL4* could be used as a marker of senescence in DDLS patients treated with abemaciclib. Although I was not able to obtain samples from the palbociclib clinical trials in the same disease to look at expression of *ANGPTL4* in those patients, I did show in the DDLS$^{\text{Tet-ON FMDM2}}$ cell line that abemaciclib and palbociclib both induce increased expression of *ANGPTL4* from day 14 onwards. This suggests that I might have found similar results in the palbociclib-treated patient samples.

However, there are clearly differences in how these two drugs work in patients. Firstly, the median PFS of patients on both phase II palbociclib trials at MSKCC was approximately 18 weeks [109, 143], while the median PFS resulting from abemaciclib treatment during this trial was nearly doubled, at 33 weeks (Fig. 4.6A). Although it is risky to draw conclusions from cross-study comparisons, it appears that by some mechanism, abemaciclib might extend PFS in liposarcoma patients further than palbociclib does.

Secondly, the Koff lab has previously shown that in cell lines treated with palbociclib, the down-regulation of MDM2 is dependent upon its disassociation from PDLIM7, which in turn is dependent on the intracellular availability of CDH18. When

present, CDH18 sequesters PDLIM7, thus allowing ubiquitination and degradation of MDM2 and entry into the geroconversion pathway. In the clinical samples from the two palbociclib trials, expression of CDH18 in the archival biopsies correlated with increases in both progression-free survival and overall survival, compared with patients whose archival samples lacked expression of CDH18 [110]. In the patient samples from the abemaciclib trial, we did not observe any significant correlation between CDH18 expression in the archival or pre-treatment sample and patient outcome (data not shown). This could be due to the smaller patient size in this trial, but it might also be that MDM2 regulation occurs differently in response to abemaciclib.

Although abemaciclib is five times more potent against CDK4 than palbociclib, it is also less specific for CDK4 and 6; abemaciclib is a powerful inhibitor of CDK9, and has been shown to have activity against a number of other kinases, including CDKs 1, 2, 5, 14, and 16-18, as well as GSK3α/β and PIM1 kinase [161]. It is therefore possible that abemaciclib works by targeting some of these other kinases, in addition to RB. In line with this idea, breast cancer cells that had previously developed resistance to palbociclib treatment were found to be sensitive to abemaciclib, but not to ribociclib. This effect does not appear to relate to RB, as the resistant cells already had reduced levels of phosphorylated RB compared to their parental controls prior to abemaciclib therapy [162].

One of the most significant differences between palbociclib and abemaciclib is their dosing protocol. Like ribociclib, palbociclib is dosed intermittently, while abemaciclib is dosed continuously. For drugs that are, at least theoretically, cytostatic, the week withdrawal from drug that is required for palbociclib treatment could have

significant clinical effects. If palbociclib treatment induces quiescence, as it has been shown to do in some patient-derived liposarcoma cell lines [20], cells would have the opportunity to return to the proliferative cycle during the resting week. Even if palbociclib induces senescence, our work in the DDLS$^{\text{Tet-ON FMDM2}}$ system shows that it can take time for a cell to complete the geroconversion pathway and commit to permanent growth arrest **(Chapter 3)**, and the repeated drug withdrawals required for palbociclib treatment could cause cells to backtrack, preventing or delaying their maturation into a fully senescent state.

Whether the differences between the mechanisms of abemaciclib and palbociclib are related to senescence remains to be seen. The qPCR panel I performed showed that the SASP profiles induced by the two drugs in DDLS$^{\text{Tet-ON FMDM2}}$ cells are similar, but not identical, with greater divergence at the later time points of senescence (Fig. 4.5). This finding was supported by RNA sequencing run on the same samples by our collaborators at Eli Lilly (data not shown). It is conceivable that the differential SASP expression induced by each drug results in differential PFS. This could be mediated through multiple aspects of the SASP, including the promotion of tumor clearance by the immune system or the induction of paracrine senescence in neighboring tumor cells.

At present, given that all three CDK4/6 inhibitors are approved to treat the same disease, the choice of drug is largely determined by the prescribing physician's familiarity with these compounds, hospital policy, or cost [163]. A head-to-head comparison of the three drugs would shed light on the true differences among their efficacies, toxicities, and mechanisms of action, which in turn would aid in the selection of the most optimal therapy for individual patients.

Senescence as a negative outcome of chemotherapy

Whether senescence is a positive or negative outcome of chemotherapy has long been a subject of debate, exacerbated by the difficulty of identifying and studying senescent cells in human samples [39]. In the absence of viable markers to directly measure senescent cells in human patients, some groups have used computational transcriptomic methods to attempt to retroactively quantify senescent cells in tumors [164]. One clinical study found that the presence of senescent cells in baseline tumors, based on the expression of several surrogate markers, correlated with longer PFS, but they did not examine whether drug treatment induced or altered senescence in these tumors [165]. Mouse models have also been used extensively in the attempt to determine the effect of tumor cell senescence on survival. The outcomes of these studies have been very mixed, and the applicability of results from mouse models to human patients is unclear.

Treatment with either abemaciclib or palbociclib in a mouse model of breast cancer resulted in tumor regression, which was associated with the detection of senescent cells in the tumor. However, despite the presence of SA-β-gal^{+} cells in these samples, no evidence of SASP elaboration was observed, as measured by expression of *Il6*, *Il-1a*, and *Il-1b*. In light the data generated in the DDLS$^{\text{Tet-ON FMDM2}}$ system in **Chapter 3,** this begs the question of whether these cells had truly undergone senescence. Additionally, in this model, it appeared that the mechanism of action by which CDK4/6 inhibitors induced inflammation was not related to senescence, but rather to enhanced expression of MHC class I markers, and thus increased antigen presentation on the surface of tumor cells, which resulted in recruitment of cytotoxic T cells into the tumor [152].

In a mouse model of $KRAS^{G12V}$-driven non-small cell lung cancer, ablation of Cdk4, either genetically or pharmacologically, was shown to induce a senescence response that corresponded with decreased tumor burden, suggesting that senescence was a positive outcome of chemotherapy [166] However, in this study, mice were only treated with palbociclib for a total of 30 days, at which point they were euthanized. It's possible that this period was insufficient to observe the more harmful effects of senescence. A mouse model of lymphoma also linked senescence with better prognosis [167], as did a mouse model of liver carcinoma, which connected the appearance of senescent cells to activation of the immune system and subsequent tumor regression [62].

In some cases, however, therapy-induced senescence was shown to have a negative, although often indirect, effect. For example, it has been reported that treatment with widely used chemotherapeutic drugs, like doxorubicin or paclitaxel, can induce senescence in normal, noncancerous tissue and stromal cells. In an orthotopic mouse model of breast cancer, the specific elimination of these $p16^{+}$ senescent, nonmalignant cells ameliorated some of the negative side effects of chemotherapy, and delayed relapse and metastasis [168]. Senescence in normal, peritumoral hepatocytes was also shown to promote the growth of murine hepatocellular carcinomas via an immunosuppressive mechanism [169]. In a mouse model of thyroid cancer, senescent cells located at the invasive border of the tumor created a cytokine gradient, through secretion of the SASP, that helped guide and promote cell migration [170]. There is also evidence from mouse models to suggest that senescent cancer cells have increased stem-like properties, bestowing on them highly aggressive growth potential, though this model is dependent upon the concept of senescence being a reversible state [171].

Here, I have shown that in some liposarcoma patients, abemaciclib treatment induces the formation of mature, SASP-producing senescent cells, likely resulting in a $CD4^+$ T-cell response. The finding that the senescence-associated immune response is connected to $CD4^+$ cells is consistent with previous work in a model of OIS in mouse liver [64]. We suggest that the acute formation of senescent cells by either an oncogene or drug treatment favors this initial type of inflammatory response, which is growth inhibitory in the short-term. However, chronic accumulation of such SASP-producing cells may limit this beneficial response.

Perhaps the most striking finding of the work presented here is that senescence and inflammation appear to be an overall negative outcome of chemotherapy, associated with nearly a 60% significant increase in risk of progression, compared to patients who did not exhibit senescence and inflammation (Fig. 4.12). To the best of my knowledge, this is the first time a study has directly measured the drug-induced appearance of senescent cells and subsequent inflammation in human samples, and then connected the presence or absence of those cells to patient outcome. It bears mentioning that the negative effects of senescence and inflammation were not immediate. Patients who were ACC^+ experienced the greatest risk of progression during a period of ~50 days that surrounded the median PFS mark (Fig. 4.12D). This implies that having senescence and inflammation is only a negative in the long-term and suggests that the initial beneficial aspects of senescence – namely, stable growth arrest – are ultimately outweighed by the negative aspects – likely chronic inflammation driven by the SASP.

One major caveat to the study presented here is the collection of only one on-treatment biopsy, taken at approximately 4-6 weeks on drug. This is the only time point

at which we can comment on the induction of senescence and inflammation, though some of these patients remained on the drug for months or even years after this biopsy. It is impossible to determine, with such limited information, whether the senescence and local inflammation in these tumors persisted or was resolved, or whether tumors that lacked senescent cells developed them later. What we can conclude is that there is a significant connection between having senescence and inflammation at the one-month mark and an overall increased risk of progression. In the design of future trials, it will be important to obtain multiple biopsies at later time points (within the limits of the patients' well-being) to examine the trajectory of senescence and inflammation over the course of treatment and determine how that correlates with progression and survival.

Many questions remain to be answered about the mechanism(s) of action of CDK4/6 inhibitors in patients. Why do some patients accumulate senescent cells in response to abemaciclib, while others don't? Is the same senescence response induced by treatment with other CDK4/6 inhibitors? Will these findings from liposarcoma apply to CDK4/6 inhibitor therapy in other diseases, or to other types of therapy-induced senescence? The work presented here provides a framework for how to begin to address these questions and demonstrates the power of using basic research to drive clinical discovery in a seamless fashion.

Chapter 5: *Angptl4* is required for the inflammatory response associated with senescence during excisional wound healing

Introduction

Senescence in physiologically relevant contexts

In parallel to my work on senescence in response to CDK4/6 inhibition, I became interested in the regulation of senescence in other models, as well. Senescence is not merely an outcome of treatment with a chemotherapeutic agent; it is a naturally occurring and physiologically relevant process that is involved in many different areas of organismal biology. Indeed, senescence is thought to have originally evolved, much like apoptosis, as a way of preventing damaged cells from proliferating, thus acting as a natural barrier to tumorigenesis [172]. However, in addition to their anti-proliferative properties, senescent cells also express a bioactive secretome, the effects of which can be detrimental and, paradoxically, pro-tumorigenic [65, 67, 173]. Because of this dual nature, senescence is often described as a double-edged sword, meaning that its overall effect on the organism can be positive, negative, or a balance of both, depending on the context [174].

Two physiological processes in which senescence has been shown to play a beneficial role are development and wound healing. Senescent cells have been identified during embryogenesis in a variety of structures, including the inner ear [175, 176], the mesonephros, the limbs, the neural tube, and the tail tip [177], among others. These cells were first identified based on SA-β-gal staining but have since been shown to express other senescent phenotypes as well, including p21, HP1γ foci (SAHF), and SASP, though

they lack expression of p53 and p16. The cells are visible only during certain periods of embryonic development, after which they are cleared in a macrophage-dependent manner, suggesting that senescence is a programmed mechanism during development [176]. Ablation of senescent cells, either genetically or by treatment with senolytics, results in morphological defects, implying that senescent cells make a necessary contribution to development, although it remains unclear just what that might be [178].

A similar role has been demonstrated for senescence during wound healing. In mice inflicted with full excisional wounds, senescent cells, defined as $p16^+$ cells, appeared transiently in the wound bed, arising about 3 days after injury, peaking around 6 days, and resolving after 9-12 days [56, 179]. In addition to expression of p16, senescence was detected by changes in expression of SASP factors, including *Il-1a* and *Pai-1,* with kinetics that aligned with the appearance and subsequent disappearance of the $p16^+$ cells. Using a mouse model in which these $p16^+$ cells could be selectively ablated by treating with the drug ganciclovir (GCV), the authors demonstrated that in the absence of senescence, normal wound healing was disrupted. The wounds of mice treated with GCV showed delayed wound closure, ultimately resulting in increased fibrosis.

Clearly, senescent cells are not simply bystanders in the wound healing process, but play an active role that is critical for normal, timely healing. The rate of wound closure is largely determined by the proliferative phase of healing, during which α-Sma^+ myofibroblasts expand and drive contraction of the wound [180]. Comparison of GCV-treated wounds with PBS-treated controls showed that in the absence of $p16^+$ cells, there was a strong decrease in the number of α-Sma^+ myofibroblasts. The authors connected the expansion of myofibroblasts in normal wound repair to the SASP, and in particular, to

one SASP factor: PDGF-AA. Thus, in the context of wound healing, senescence overall, and the SASP specifically, play a beneficial role for organismal health.

On the other side of the double-edged sword, senescence has also been implicated in aging, where it has a much more antagonistic role. Senescent cells, again typically defined by their expression of p16 and sometimes SA-β-gal, accumulate with age in mouse and human tissue, where they induce sterile inflammation, largely through the expression of the SASP [68]. Mouse models in which $p16^{+}$ cells are selectively ablated as they arise, thus preventing their accumulation, exhibited delayed tumorigenesis and improved the function of the kidneys, heart, and fat tissue in old mice [181, 182]. Clearance of these cells also improved cognitive function and slowed neurodegeneration in a mouse model of Alzheimer's disease [183]. However, not all senescent cells are eliminated in these models, including immune, liver, and colon cells, suggesting that identification of senescent cells cannot be simplified to p16 expression alone.

Given the many roles that senescence can play, both positive and negative, throughout an organism's lifespan, and particularly given the connection between senescent cells and aging, which causes declines in every organ system in the body, a crucial question that must be addressed is why and how senescent cells form. Since the majority of cells in the body at any time are quiescent [184], a logical hypothesis is that quiescent, reversibly arrested cells embark on the geroconversion pathway that leads them to become irreversibly arrested. Along the way, they develop other markers of the senescent phenotype. One example of naturally occurring geroconversion comes from muscle satellite cells, which are normally quiescent throughout their adult life and become activated only in response to injury. With age, de-repression of the p16 locus

costs these cells their ability to resume proliferation, pushing them instead into a state of irreversible arrest [108]. A deeper understanding of how geroconversion is regulated, therefore, could allow for the manipulation of senescence in contexts like chronic wounds and aging, which would have major implications on human health.

The conservation (or lack thereof) of senescence regulators

If geroconversion underlies senescence in naturally occurring settings, then it is essential to understand how a cell commits to transitioning into the senescent state. As shown in **Chapter 3,** *ANGPTL4* regulates two of the key hallmarks of geroconversion in multiple different cancer cell lines treated with CDK4/6 inhibitors. **Chapter 4** discusses how *ANGPTL4* can be used as a marker of senescence in samples from patients taking the same type of drug. I next wanted to investigate whether *ANGPTL4* might be involved in the regulation of senescence in normal, non-cancerous cells undergoing senescence in a variety of different contexts. Given that *ANGPTL4* has previously been published as a SASP component during replicative senescence in mesenchymal stromal cells [120] and oncogene-induced senescence (OIS) in fibroblasts [84], it seemed reasonable to predict that I might find its expression during senescence to be more broadly conserved.

Some senescence hallmarks and regulators are likely to be cell-type or inducer-specific. For example, as discussed in **Chapter 3,** downregulation of MDM2 protein is required for cells to undergo senescence in response to CDK4/6 inhibition, but this event has not been observed in other types of senescence (Koff lab, unpublished data). The SASP is another aspect of the senescence phenotype that is thought to vary greatly based on both cell type and senescence context. One recent study examined the secreted SASP

profile of human primary fibroblasts that were induced to senesce by oncogene overexpression, replicative stress, or treatment with the protease inhibitor ATV. The composition of the SASP was highly dependent on the inducer, with only about 10% overlap among the different samples [185]. This study also compared the SASPs of different cell types, fibroblasts versus endothelial cells, that were induced to senesce by the same trigger, irradiation, and again found that the majority of the SASP varied based on cell type, with only about 10-20% overlap.

However, regardless of the cell type or the inducer, senescence ultimately results in the same foundational phenotypes: long-term, stable growth arrest and the development of a pro-inflammatory secretome. It is therefore likely that there are at least some elements of the core senescence machinery that are conserved, regardless of the context in which senescence is induced. There are many examples of senescence regulators that are preserved in multiple contexts, such as the transcription factor AP-1, which has been shown to bind to enhancer regions and trigger the activation of a network of transcription factors that drive the expression of genes associated with senescence, including the SASP [135]. The initial discovery of the role of AP-1 was in the context of OIS in primary lung and skin fibroblasts, but another group has since shown similar activity of AP-1 during CDK4/6 inhibitor therapy-induced senescence in breast cancer cells [186].

Another example, discovered in our own lab, is an increase in ATRX foci number. Although this hallmark of senescence was first observed (and shown to be necessary) in the context of cancer cells undergoing therapy-induced senescence in response to CDK4/6i, ATRX foci also increase in every senescence context that has thus

far been investigated, including replicative senescence, DNA damage-induced senescence, and oncogene-induced senescence in human primary cells (Koff lab, unpublished data).

Even among the highly heterogeneous SASP, there are some genes that seem to be broadly expressed in different senescence contexts. For example, the previously described study of the SASP in different cell types/contexts identified a total of 17 SASP factors that were shared among all senescence inducers and cell types examined [185]. Another study profiled the SASP of mesenchymal stromal cells undergoing senescence in response to oxidative stress, doxorubicin treatment, irradiation, and replicative exhaustion, and found that while there was a great deal of variation among the individual SASP factors, there were three key conserved signaling pathways and 11 conserved factors found in all of the senescent secretomes, but none of the control secretomes [88].

Here, I set out to determine the extent to which markers of senescence discovered in our models of therapy-induced senescence can be applied to other contexts of senescence. I examined the use of ATRX foci as a marker of senescence in mouse cells, as previous work in the lab had only focused on human cells. I also investigated the use of *ANGPTL4* as a marker of senescence in models of senescence in human and mouse primary cells, and ultimately in an *in vivo* model of mouse wound healing.

Results

ANGPTL4 *expression correlates with senescence in human primary dermal fibroblasts*

Since *ANGPTL4'*s role in senescence was discovered in human cells, I began my study of non-cancerous cells with human primary dermal fibroblasts (HPDFs) undergoing replicative senescence. HPDFs were cultured continuously until they reached their replicative capacity, a process that took approximately 5 months (Fig. 5.1A). At various passages, cells were harvested for RNA and stained for markers of senescence. BrdU incorporation decreased gradually as cells approached their replicative limit (Fig. 5.1B). This loss of proliferative potential was accompanied by progressively higher levels of SA-β-gal (Fig. 5.1C) and ATRX foci number (Fig. 5.1D). Using qPCR, I showed that expression of *CDKN2A/*p16 was elevated the longer cells were in culture, first appearing around passage 7 and increasing to its peak at passage 13 (Fig. 5.1E). Finally, I looked at expression of *ANGPTL4* mRNA, and found that it also increased substantially in late passage HPDFs (Fig. 5.1F). Its expression arose later than *CDKN2A,* consistent with *ANGPTL4* being a later marker of senescence.

Similar results were seen during DNA damage-induced senescence (DDIS) in the HPDFs. Early passage cells were treated with a sub-lethal dose of doxorubicin (100 nM) for seven days to induce DNA damage. Nearly 100% of cells experienced DNA damage as a result of drug treatment, as indicated by accumulation of 53BP1 (Fig. 5.2A) and γH2AX (Fig. 5.2B) foci. In response to the DNA damage, HPDF cells entered senescence, as measured by almost complete loss of BrdU incorporation (Fig. 5.2C),

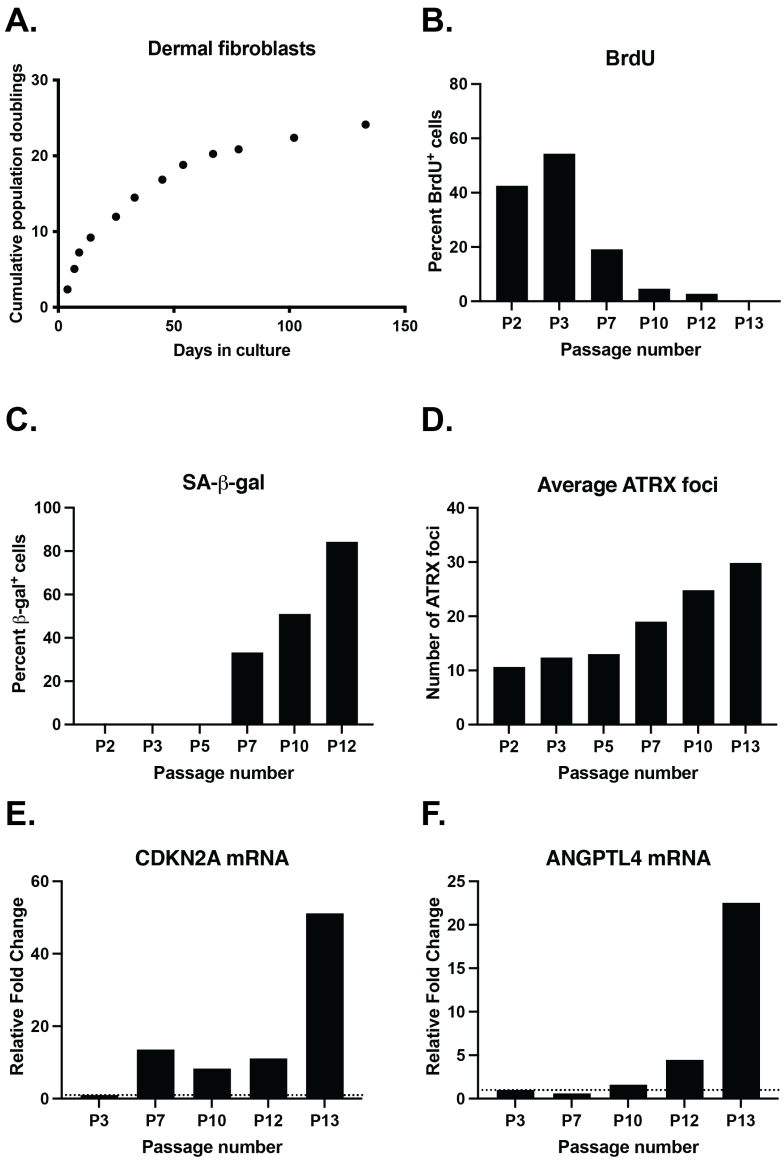

Figure 5.1 *ANGPTL4* expression correlates with senescence in HPDFs undergoing replicative senescence.

(A) HPDFs were passaged until they reached replicative senescence. At various passages, senescence phenotypes were assayed by measuring BrdU incorporation **(B),** SA-β-gal positivity **(C),** and ATRX foci formation **(D)**. RNA was collected and qPCR performed to analyze the expression of *CDKN2A/*p16 **(E)** and *ANGPTL4* **(F).**

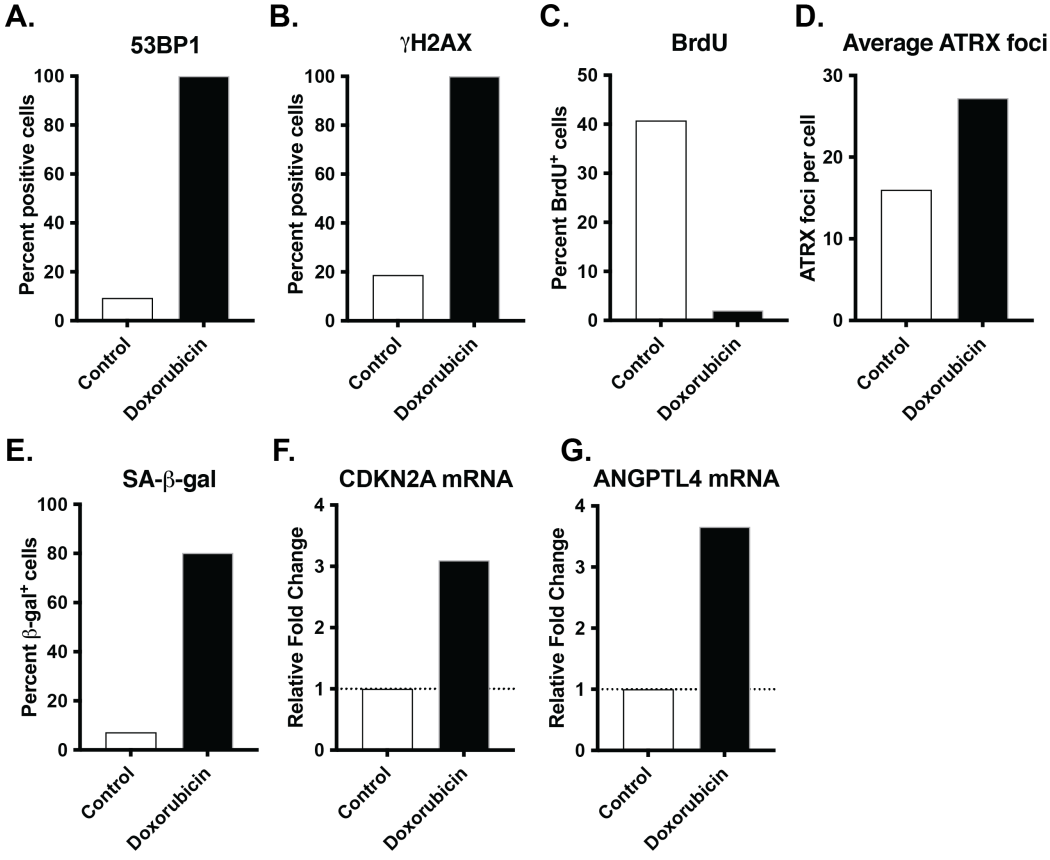

Figure 5.2 *ANGPTL4* expression correlates with senescence in HPDFs undergoing DDIS.

HPDFs were treated with 100 nM doxorubicin for 7 days, then DNA damage was assessed by 53BP1 **(A)** and γH2AX **(B)** foci formation. Cells were counted as positive for DNA damage if they had 10 or more foci. The onset of senescence was measured by BrdU incorporation **(C),** ATRX foci formation **(D),** and SA-β-gal staining **(E).** RNA was collected and qPCR performed to analyze the expression of *CDKN2A/*p16 **(F)** and *ANGPTL4* **(G).**

increased formation of ATRX foci (Fig. 5.2D), and expression of SA-β-gal (Fig. 5.2E). This entry into DDIS was accompanied, as in the replicative senescence model, by increased expression of both *CDKN2A* (Fig. 5.2F) and *ANGPTL4* mRNA (Fig. 5.2G). Thus, *ANGPTL4* expression increases during senescence in human primary dermal fibroblasts in response to two different stimuli.

Angptl4 ***expression correlates with senescence in mouse embryonic fibroblasts***

Having shown that *ANGPTL4* expression marks senescence in human primary cells, I next wanted to see if the same would hold true for mouse cells. Establishing *Angptl4* as a marker of senescence in cultured cells would be a necessary precursor to any future mouse work done in the Koff lab or elsewhere. To test whether *Angptl4* expression correlates with senescence in primary mouse cells, I grew three distinct clones of mouse embryonic fibroblasts (MEFs) into replicative senescence, a process which took approximately 30 days (Fig. 5.3A). At each passage, MEFs were tested for various phenotypes of senescent cells, and RNA was collected to look at expression of genes associated with senescence. As expected, incorporation of BrdU decreased progressively with each passage, showing the steady decline of the replicative potential of these cells (Fig. 5.3B). Compared to the earliest passage (P2), loss of BrdU positivity was significant from passage 4 onwards. This was accompanied by an increase in the number of SA-β-gal positive cells, which first began to appear around passage 5, became significantly elevated at passage 6, and reached their peak (~70%) at passage 7 (Fig. 5.3C).

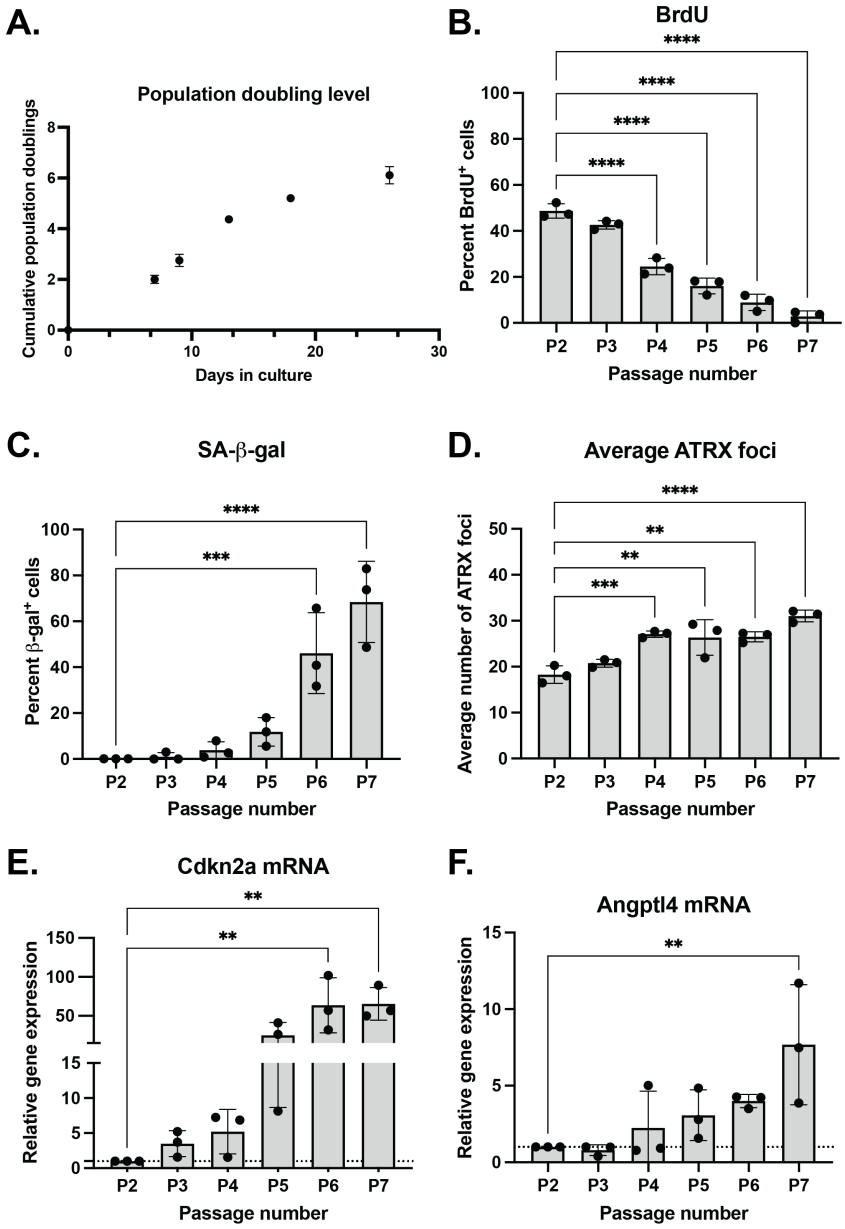

Figure 5.3 *Angptl4* expression correlates with senescence in MEFs undergoing replicative senescence.

(A) Three distinct MEF clones were passaged until they reached replicative senescence. At each passage, senescence phenotypes were assayed by measuring BrdU incorporation **(B),** SA-β-gal positivity **(C),** and ATRX foci formation **(D)**. RNA was collected and qPCR performed to analyze the expression of *Cdkn2a/*p16 **(E)** and *Angptl4* **(F).** **p<0.01, ***p<0.001, ****p<0.0001 by one-way ANOVA.

ATRX foci did indeed increase in the MEFs, first appearing elevated at passage 4 and then continuing to increase in number until passage 7 (Fig. 5.3D). This is the first evidence in mouse cells that ATRX foci can serve as a marker of senescence, as they do in human cells. Finally, I looked at gene expression throughout the lifespan of the MEFs using qPCR. Expression of *Cdkn2a/*p16 was massively increased as the cells approached their replicative limit, as anticipated (Fig. 5.3E). Excitingly, *Angptl4* RNA levels also increased as the MEF population progressed into senescence and was significantly elevated at passage 7 compared to the early passage cells (Fig. 5.3F).

These results suggest that the use of *Angptl4* expression as a marker of senescence might not be limited to human cells. To delve into this further, I also tested a model of DDIS in these MEFs. In this experiment, two distinct MEF clones at an early passage (P2) were treated with 100 nM doxorubicin for seven days, at which point the extent of DNA damage was assessed by quantifying the number of cells containing 10 or more 53BP1 (Fig. 5.4A) and γH2AX (Fig. 5.4B) foci. Greater than 80% of cells showed an elevated DNA damage response after treatment with doxorubicin. I next measured the induction of senescence by looking at BrdU incorporation (Fig. 5.4C), ATRX foci formation (Fig. 5.4D) and SA-β-gal positivity (Fig. 5.4E). Almost total loss of BrdU indicated that doxorubicin treatment had induced cell cycle exit. There was a corresponding significant increase in both ATRX foci number and SA-β-gal^{+} cells. Finally, I looked at expression of *Cdkn2a* (Fig. 5.4F) and *Angptl4* (Fig. 5.4G) and saw that both were strongly up-regulated in response to treatment with doxorubicin. Therefore, *Angptl4* expression can serve as a marker of the senescent state in mouse cells

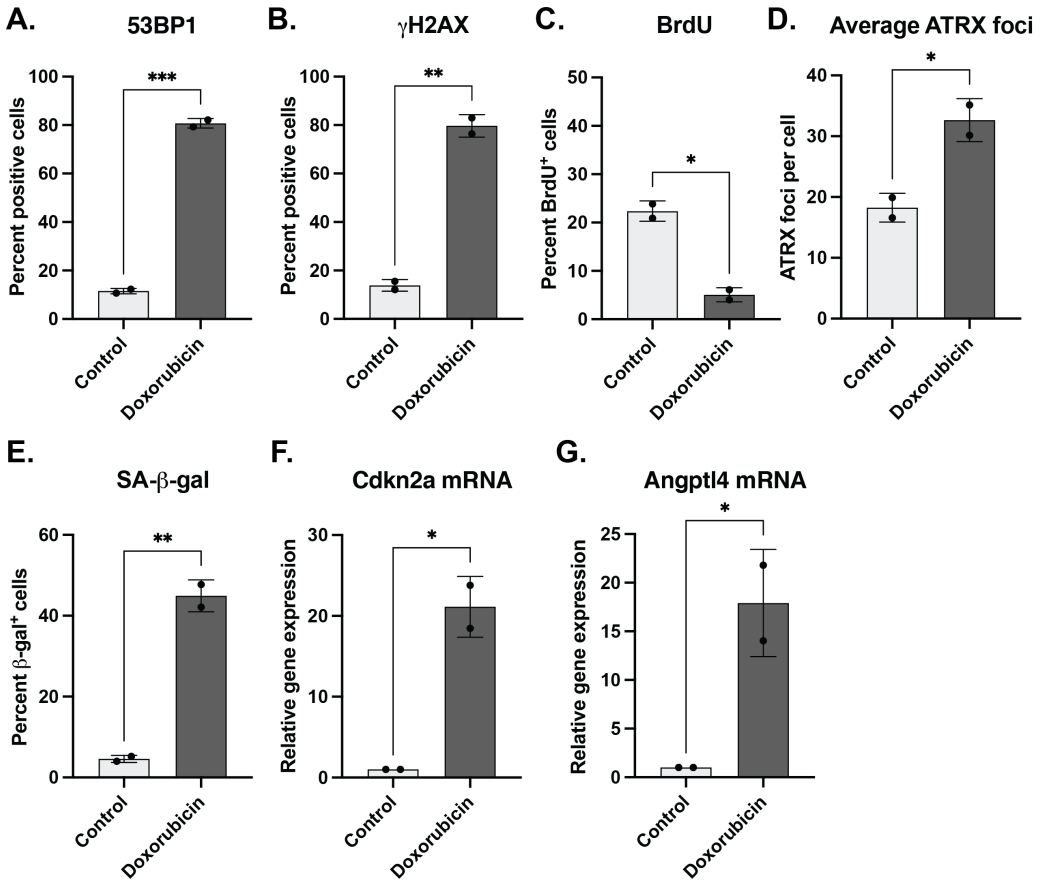

Figure 5.4 *Angptl4* expression correlates with senescence in MEFs undergoing DDIS.

Two distinct MEF clones were treated with 100 nM doxorubicin for 7 days, then DNA damage was assessed by 53BP1 **(A)** and γH2AX **(B)** foci formation. Cells were counted as positive for DNA damage if they had 10 or more foci. The onset of senescence was measured by BrdU incorporation **(C),** ATRX foci formation **(D),** and SA-β-gal staining **(E).** RNA was collected and qPCR performed to analyze the expression of *Cdkn2a/*p16 **(F)** and *Angptl4* **(G).** *p<0.05, **p<0.01, ***p<0.001 by one-way ANOVA.

that are undergoing senescence in response to two distinct stimuli. Additionally, the increase in ATRX foci observed in all senescent contexts in human cells is also observed in mouse cells.

Angptl4 *is required for normal senescent cell kinetics during excisional wound healing in mice*

The results presented above, as well as in **Chapters 3 and 4,** show that in both cancer cells and primary cells, there is a connection between *ANGPTL4* expression and senescence. In the liposarcoma model, loss of *ANGPTL4* resulted in a deficit in the ability of senescent cells to secrete pro-inflammatory SASP factors. I next wanted to use mouse models to determine whether loss of *Angptl4* would affect senescence and its associated inflammation in a different, more physiologically relevant context. I therefore turned to a model of excisional wound healing in *Angptl4*$^{+/+}$ *(*WT) and *Angptl4*$^{-/-}$ (KO) mice. Andrew Tan's lab at Nanyang Technological University Singapore has previously established that in the absence of *Angptl4*, mice experience delayed wound healing and increased fibrosis [102, 187, 188]. In fact, the results observed in *Angptl4* KO mice are strikingly similar to the results seen in mice in which p16^{+} cells are ablated during wound healing [56]. I hypothesized that the deficit in wound healing observed in *Angptl4* KO mice is due to the inability of mature, inflammation-provoking senescent cells to develop in the wound bed.

I collaborated with the Tan lab to determine whether *Angptl4'*s role during excisional wound healing is related to senescence. WT and KO male mice were inflicted

with 5 mm full-excisional wounds, and biopsies containing the wound and adjacent tissue were harvested at various time points spanning the different phases of the wound healing process: day 0 (uninjured control), day 1 (open wound), day 5 (wound filled with initial scab), and day 10 (wound closed over with early granulation tissue) (Fig. 5.5A-B). Five

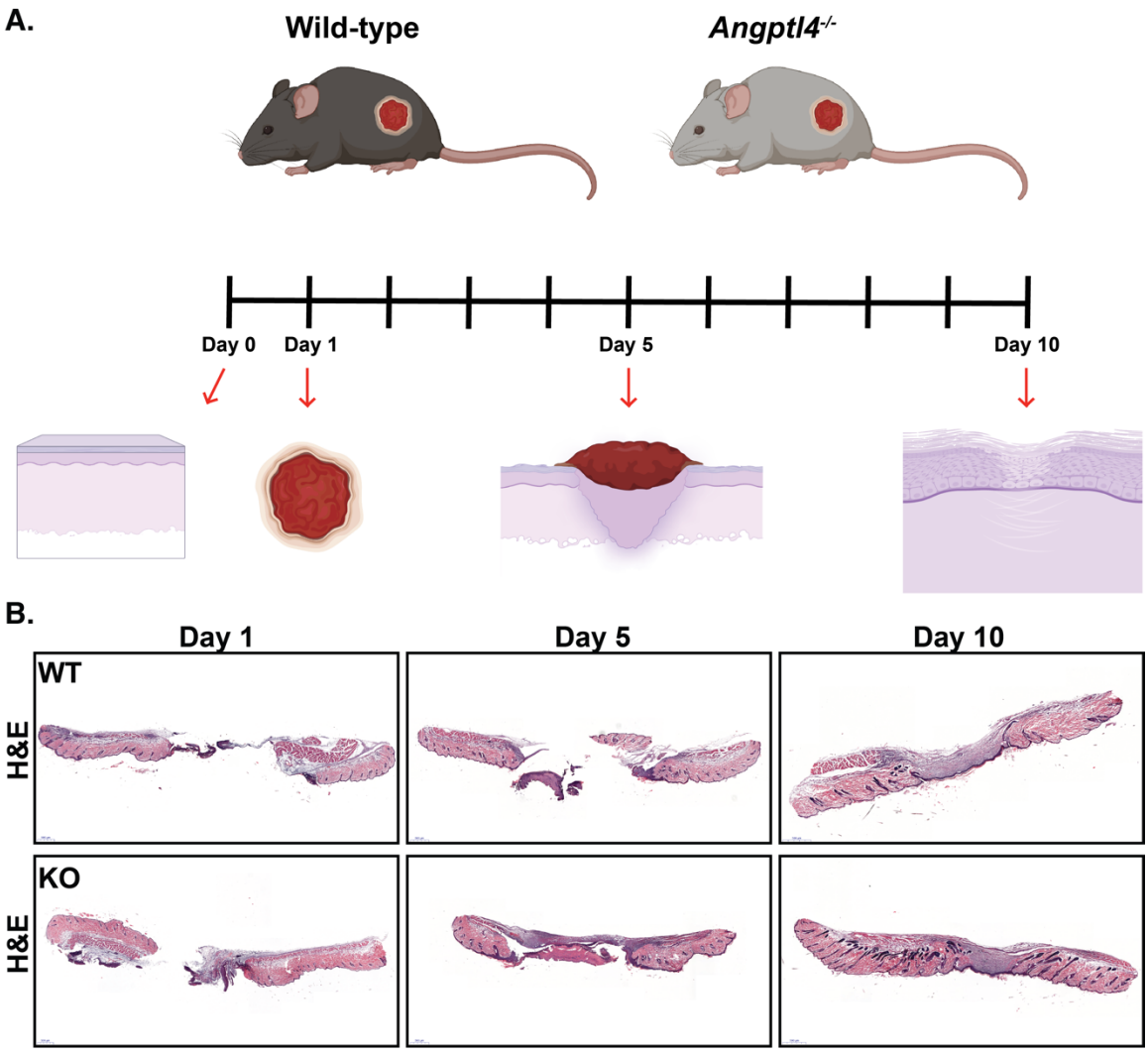

Figure 5.5 Schematic of wound healing experiment.

(A) Schematic of wound healing experiment. **(B)** Representative H&E images of WT and KO wounds at days 1, 5 and 10.

mice per genotype were assayed at each time point. Although we attempted to measure senescence by looking at ATRX foci number and SA-β-gal within the wound boundaries, we were unsuccessful (data not shown). Both assays need to be performed on frozen tissue, rather than formalin-fixed, paraffin-embedded (FFPE) sections, and frozen tissue does not retain histomorphology as well as FFPE tissue. This caused a particular challenge in the case of skin samples containing a wound, as the tissue was extremely prone to tearing during the sectioning process.

In lieu of these markers, we looked at expression of *Cdkn2a/*p16 as a marker of senescent cells. This allowed us to compare our results directly to previous work on senescence in wound healing, which also used p16 positivity to measure the kinetics of senescent cell appearance and clearance during wound healing [56]. Because *Angptl4* is a secreted protein, and because there are no effective antibodies against mouse p16, we decided against using an immunohistochemical approach. Instead, we looked at expression of both genes at the mRNA level using RNAscope, as discussed previously in **Chapter 4**.

Serial sections from both WT and KO wounds, as well as from uninjured skin controls, were stained with RNAscope probes against *Angptl4* or *Cdkn2a,* then imaged and quantified. In the WT wounds, *Angptl4* expression reached its peak at day 5, at which point it was approximately 14 times higher than at baseline. By day 10, expression was decreased, though still significantly higher than baseline (Fig. 5.6A). These kinetics of *Angptl4* induction and resolution are consistent with previously published results of *Angptl4* during wound healing, as measured by qPCR and immunoblotting [188]. In the

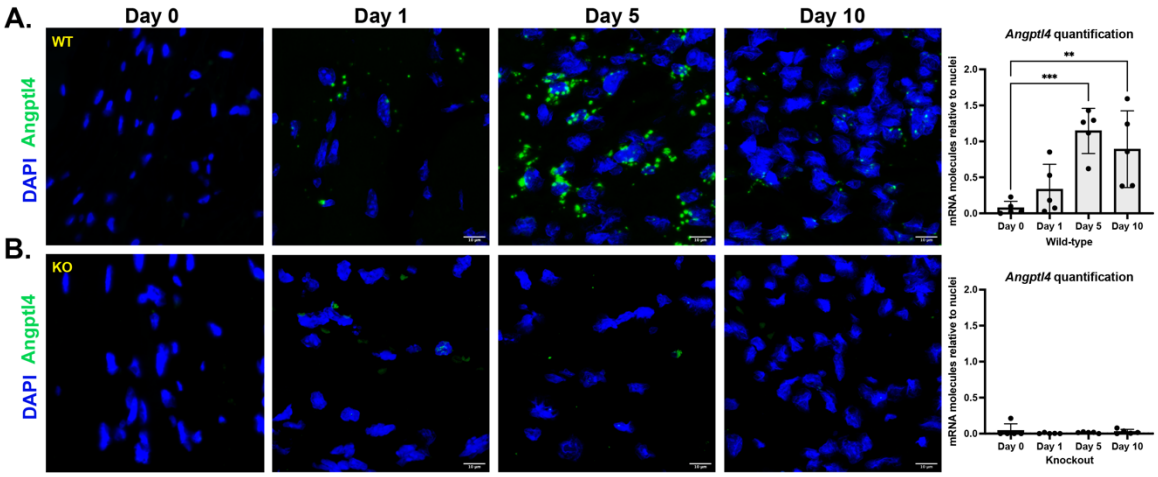

Figure 5.6 RNAscope shows *Angptl4* expression peaks at day 5 in wild-type wounds.

Wounds from *Angptl4*$^{+/+}$ (WT) and *Angptl4*$^{-/-}$ (KO) mice were harvested at day 1, 5, and 10, sectioned, and used for RNAscope, alongside control, uninjured skin (day 0). Representative confocal immunofluorescence images show expression of *Angptl4* mRNA in green. Quantification of mRNA particles relative to number of nuclei was performed using ImageJ. Each data point represents the median value of particles/nuclei counted from 10 images of each individual wound sample. n=5 mice per genotype per time-point. **p<0.01, *** p<0.001 by one-way ANOVA.

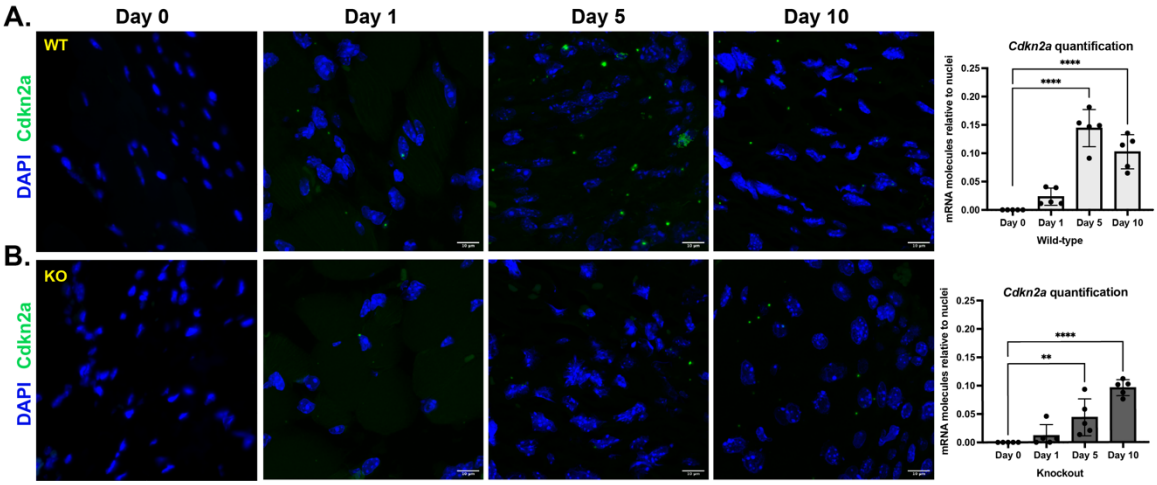

Figure 5.7 RNAscope shows *Cdkn2a* expression peaks at day 5 in wild-type wounds and is delayed in knockout wounds.

Wounds from *Angptl4*$^{+/+}$ (WT) and *Angptl4*$^{-/-}$ (KO) mice were harvested at day 1, 5, and 10, sectioned, and used for RNAscope, alongside control, uninjured skin (day 0). Representative confocal immunofluorescence images show expression of *Cdkn2a* mRNA in green. Quantification of mRNA particles relative to number of nuclei was performed using ImageJ. Each data point represents the median value of particles/nuclei counted from 10 images of each individual wound sample. n=5 mice per genotype per time-point. **p<0.01, ****p<0.0001 by one-way ANOVA.

KO wounds, as expected, *Angptl4* mRNA could not be detected above background staining, confirming that this mouse is a true knockout (Fig. 5.6B).

Using the same RNAscope technique, I next looked at expression of *Cdkn2a/*p16 as another indication of the formation of senescent cells. In the WT wounds, *Cdkn2a/*p16 expression was first significantly increased at day 5, which is also when it reached its peak. By day 10, p16 levels had dropped in WT wounds, though they were still significantly increased from baseline levels (Fig. 5.7A). These kinetics are consistent with what has previously been observed for the appearance and clearance of $p16^+$ senescent cells during wound healing [56]. In the KO wounds, *Cdkn2a* expression was also significantly increased from the baseline at day 5, but the level of expression was only about 30% of what was seen in WT wounds (Fig. 5.7B). Interestingly, at day 10, the overall expression level of *Cdkn2a* was virtually equivalent in both WT and KO wounds, but the accumulation of $p16^+$ cell was still trending upwards in KO wounds, while it was resolving in WT wounds.

Overall, the results from this section indicate that the kinetics we observed in WT mice for *Angptl4* and *Cdkn2a* expression are consistent with the appearance and resolution of senescent cells previously reported during wound healing, and that there is a defect, or at least a delay, in the accumulation of $p16^+$ senescent cells in the absence of *Angptl4.*

Loss of **Angptl4** *reduces recruitment of macrophages and T-cells during the inflammation phase of excisional wound repair*

Given the important role that *ANGPTL4* played in the establishment of an inflammatory SASP in our cell culture experiments, and given that one of the main functions of the SASP *in vivo* is thought to be interaction with the immune system, I next wanted to determine whether *Angptl4* KO mice experience a defect in the recruitment of the immune system to the site of the wound. The wound healing process occurs in three main overlapping phases: inflammation, proliferation, and remodeling. During the inflammation phase, different components of the immune system are recruited to the site of the wound, where they perform specific tasks that contribute to the healing process (Fig. 5.8).

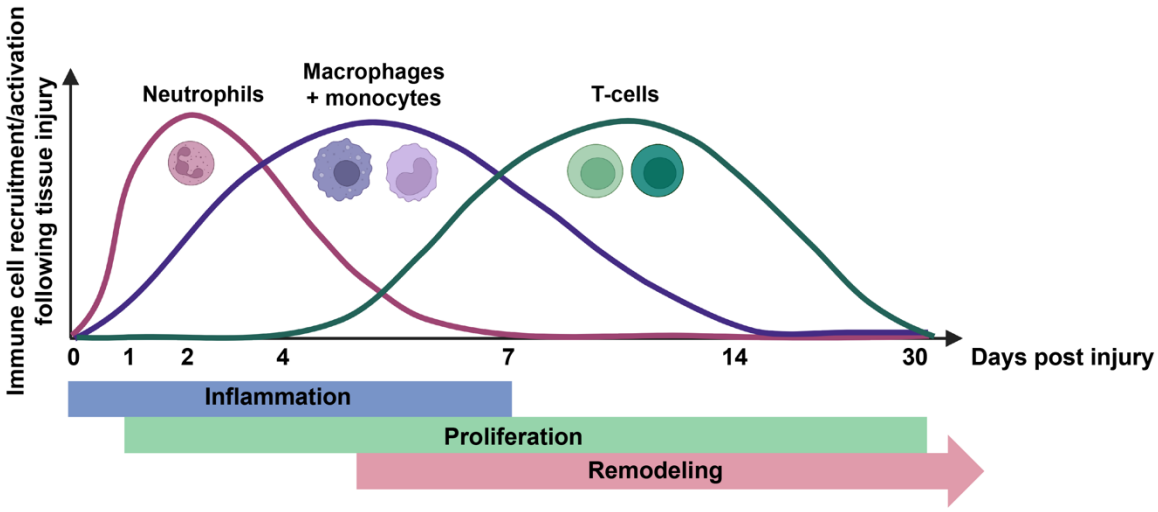

Figure 5.8 The timing of immune cell recruitment and clearance during wound healing.

Schematic showing the kinetics of the key immune system cell types during the process of excisional wound healing: neutrophils, macrophages, and T-cells. Also shown are the durations of the three main phases of wound healing: inflammation, proliferation, and remodeling.

Neutrophils, which appear within hours and peak approximately 1-2 days after injury, are among the first inflammatory cells to arrive at the wound, where they serve several important functions. They help to remove contaminants, produce antimicrobial proteases that can kill potential pathogens, and facilitate the recruitment of macrophages, which phagocytose the neutrophils. In this way, neutrophils contribute to their own clearance, and are usually absent from the site of the injury after about a week [189]. Monocytes and macrophages are the next immune cells that arrive at the wound, generally appearing between 1-3 days after the injury and peaking around 4-7 days, though they may persist in the wound for several weeks. Macrophages secrete cytokines, growth factors, and extracellular matrix components that promote tissue repair and angiogenesis. They also contribute to the healing process by engulfing necrotic cells and pathogens [189, 190]. Finally, T-cells are recruited to the site of the wound towards the end of the inflammation phase. They function both as immunological effector cells and as a source of secreted growth factors that help stimulate the proliferation and remodeling phases of wound repair [191].

To determine whether loss of *Angptl4* affects the recruitment of immune cells to the wound bed, I used serial sections of wound biopsies from each time point to look at recruitment of neutrophils (marked by Cd11b), macrophages (marked by F4/80), and T-cells (marked by Cd3). Neutrophil recruitment was unaffected by loss of *Angptl4;* both WT and KO wounds had significant populations of neutrophils present one day after wounding, and after 5 days, that population was declining. By day 10, there were virtually no neutrophils detectable in the wounds from either group of mice (Fig. 5.9).

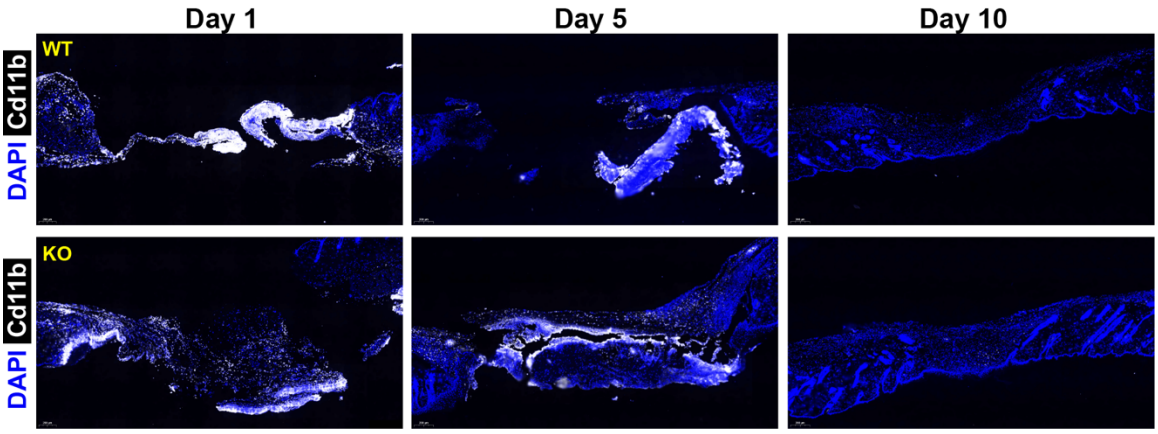

Figure 5.9 *Angptl4* knockout does not affect neutrophil recruitment to the wound bed

Representative immunofluorescence images of WT and KO wounds on days 1, 5, and 10 stained with neutrophil marker Cd11b (white) and DAPI (blue). n = 5 mice per genotype per time-point.

I next looked at macrophage recruitment using F4/80 as a monocyte-macrophage marker. The WT wounds showed the expected kinetics of macrophage entry to the wound: compared to the baseline (day 0, uninjured skin), there was a slight increase in monocytes at day 1, but they reached their peak at day 5, at which point they were significantly elevated from the control. By day 10, the macrophage population was decreasing (Fig. 5.10A). In KO wounds, on the other hand, the levels of F4/80^{+} cells remained more or less stable throughout the time course, never reaching a significant level of elevation compared to the uninjured KO skin sample (Fig. 5.10B).

Similar results were observed for the kinetics of T-cell recruitment. In the WT wounds, there was a slight increase in Cd3+ cells at day 1, which peaked and became significant at day 5, compared to the baseline levels. At day 10, the level of Cd3+ T-cells had decreased, but remained significantly elevated from the control (Fig. 5.11A). In the KO wounds, as was seen with monocytes, there was no significant change in the levels of Cd3^{+} cells throughout the wound healing process (Fig. 5.11B). Together, these results show that the loss of *Angptl4* affects the mouse's ability to engage the immune system following injury.

Loss of **Angptl4** *reduces expansion of α-Sma^{+} myofibroblasts during the proliferation phase of excisional wound repair*

Having established the effect of *Angptl4* knockout on the inflammation phase of wound healing, I looked to see if there was an effect on the next phase: proliferation (Fig. 5.8). It has already been shown that *Angptl4* KO mice exhibit delayed and impaired wound healing with higher levels of fibrosis, much like the mice in which p16^{+} cells are

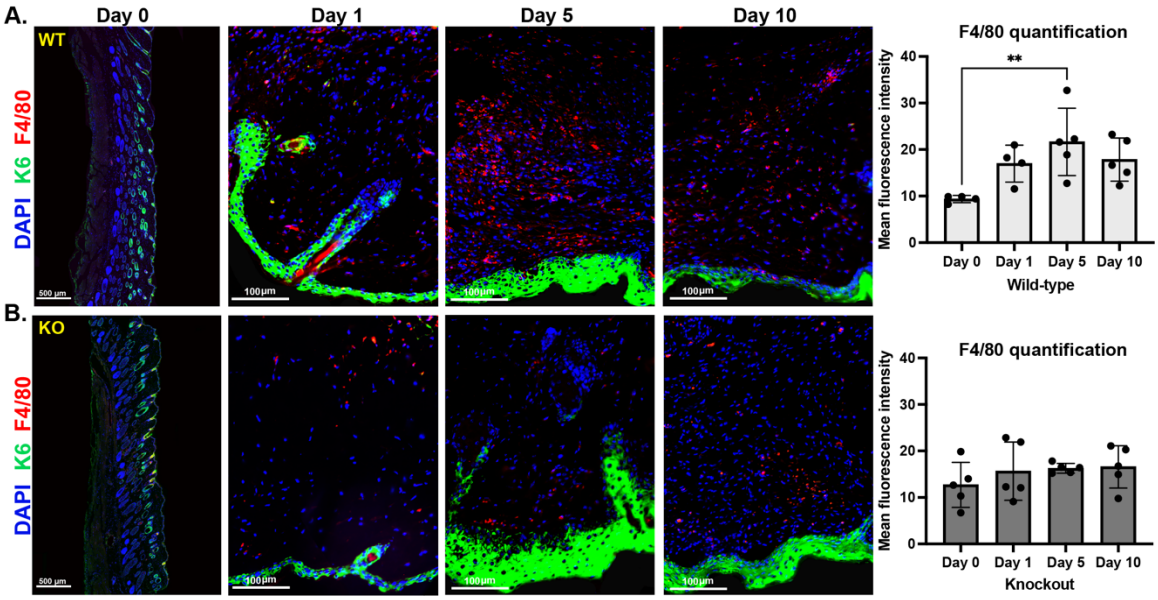

Figure 5.10 Macrophage populations increase significantly during wound healing in WT, but not KO, mice.

Representative confocal immunofluorescence images of WT and KO wounds on days 1, 5, and 10, along with uninjured control samples (day 0). Keratin6 (K6, green) marks the boundary of the wound. Macrophage infiltration was detected by F4/80 staining (red), and DAPI is in blue. n = 5 mice per genotype per time-point. **p<0.01 by one-way ANOVA.

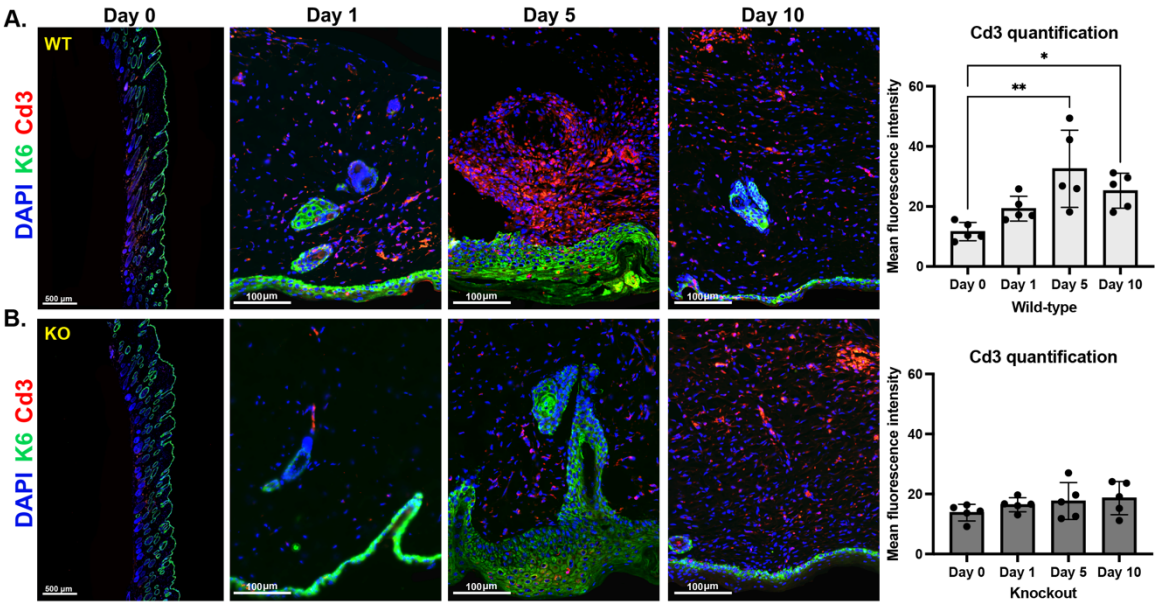

Figure 5.11 T-cell populations increase significantly during wound healing in WT mice, but not KO, mice.

Representative confocal immunofluorescence images of WT and KO wounds on days 1, 5, and 10, along with uninjured control samples (day 0). Keratin6 (K6, green) marks the boundary of the wound. T-cell infiltration was detected by Cd3 staining (red), and DAPI is in blue. n = 5 mice per genotype per time-point. **p<0.01, *p<0.05 by one-way ANOVA.

selectively killed [56, 188]. In the p16 mouse model, the observable effect that loss of senescent cells had on the wound environment was a defect in the expansion of α-Sma$^+$ myofibroblasts to fill in the wound bed. These cells play a critical role during the proliferation phase in the formation of granulation tissue, as well as promoting re-epithelialization and vascularization, and sustained loss of α-Sma$^+$ cells delays or prevents wound healing [192].

Therefore, I looked at α-Sma expression in the wound beds as a marker for myofibroblasts. In the WT mice, the day 5 wound beds were filled with α-Sma$^+$ cells, a highly significant increase from baseline levels (Fig. 5.12A). Following the same trends observed with the immune cell markers, the number of α-Sma$^+$ cells had decreased by day 10, showing that the exponential phase of wound repair had concluded, but it remained significantly elevated compared to the uninjured control. In the KO wounds, on the other hand, α-Sma levels increased slightly by day 5, but at no point in the 10-day time course were they significantly higher than the baseline level (Fig. 5.12B).

The maximal effect of **Angptl4** *loss occurs at day 5, during the exponential phase of the wound healing process*

Because every marker seemed to reach its peak at day 5 in the WT wounds compared to baseline, I used that time point to directly compare the expression of each marker in WT and KO mice, rather than comparing each genotype to its own uninjured control. There was almost a 70% reduction in *Cdkn2a* expression in KO wounds compared to WT wound at day 5, suggesting that loss of *Angptl4* reduced the overall

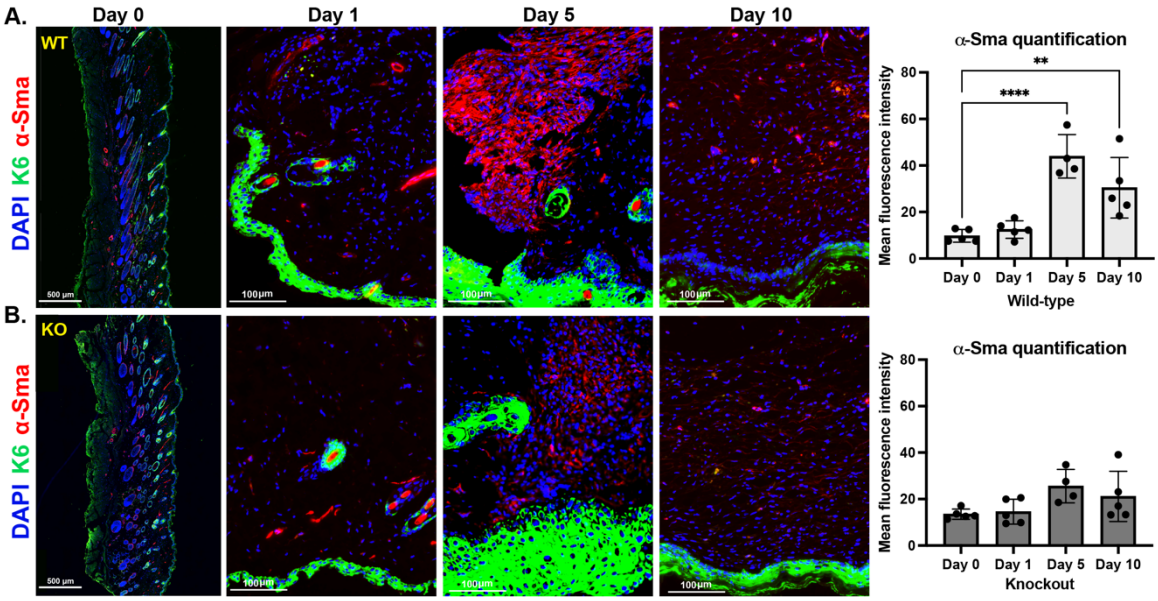

Figure 5.12 α-Sma+ myofibroblasts increase significantly during wound healing in WT mice, but not KO, mice.

Representative confocal immunofluorescence images of WT and KO wounds on days 1, 5, and 10, along with uninjured control samples (day 0). Keratin6 (K6, green) marks the boundary of the wound. The overall myofibroblast population was detected by α-Sma staining (red), and DAPI is in blue. n = 5 mice per genotype per time-point. ****p<0.0001, **p<0.01 by one-way ANOVA.

number of senescent cells present, even as measured by an early marker of senescence like p16 (Fig. 5.13A). The recruitment of F4/80$^+$ macrophages at day 5 was decreased by about 25% in KO wounds compared to WT wounds, although this change was not significant (Fig. 5.13B). There was, on average, about a 45% decrease in Cd3$^+$ T-cells present in KO wounds at day five compared to WT wounds, and this difference was significant (Fig. 5.13C). This is consistent with the results from the abemaciclib clinical trial in **Chapter 4,** in which we found that *ANGPTL4* expression correlated most strongly with recruitment of T-cells to the tumor.

Finally, there was a ~40% decrease in the number of α-Sma$^+$ myofibroblasts in the wound beds of KO mice compared to WT mice, a change that was, again, significant (Fig. 5.13D). To confirm that the difference in myofibroblast number was due to a lack of proliferation of these cells in KO wounds, we co-stained day 5 wound samples with α-SMA and Ki67. In WT wounds, many nuclei within α-Sma$^+$ cells stained positive for Ki67. In KO wounds, not only were the α-Sma$^+$ cells scarcer overall, but fewer of them were proliferating, as shown by lack of by Ki67 staining (Fig. 5.13E).

In summary, the data from these wound healing experiments in *Angptl4* KO mice show that multiple facets of the wound healing process are affected by the loss of *Angptl4.* First, senescent cells, as marked by p16, are either reduced or accumulate with severely delayed kinetics. Next, the recruitment of two different types of immune cells to the site of the injury is dampened, presumably due to a lack of pro-inflammatory SASP factors being secreted in the absence of *Angptl4.* Finally, the expansion of myofibroblasts that is essential for wound contraction and granulation tissue formation is impaired in

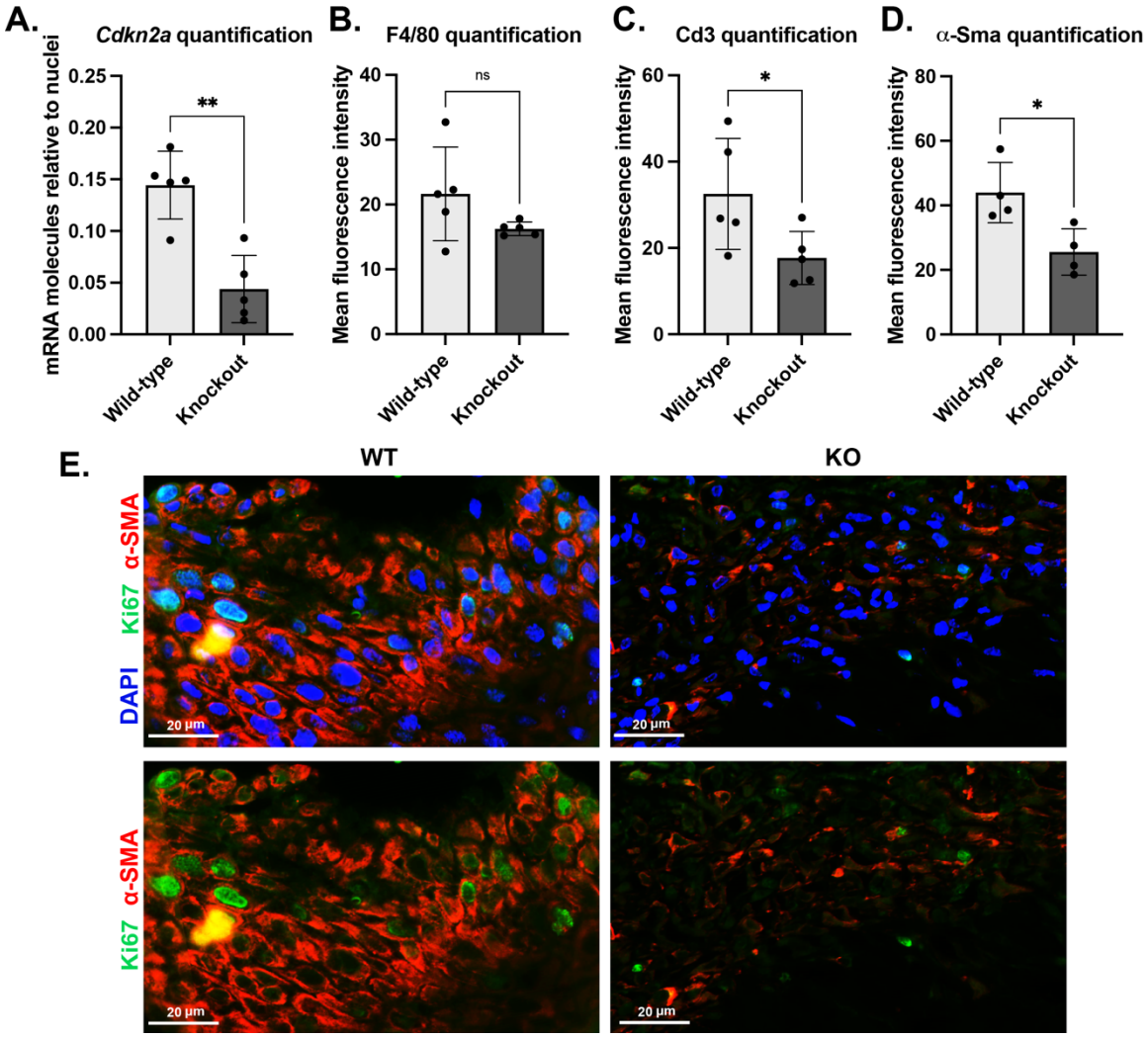

Figure 5.13 Direct comparison of senescence and inflammation markers in WT and KO wounds at day 5.

(A-D) Comparison of (A) *Cdkn2a* RNAscope expression, (B) F4/80 macrophage staining, (C) $Cd3^+$ T-cell staining, and (D) α-SMA^+ myofibroblasts in WT vs KO wounds at day 5. **p<0.01, *p<0.05 by Student's t-test. **(E)** Proliferation of α-SMA^+ myofibroblasts in WT and KO wounds, assessed by Ki67 staining. Top (with DAPI) and bottom (without DAPI) images are of the same area, allowing for visualization of nuclei number (top) and $Ki67^+$ cells (bottom).

Angptl4 KO mice, a phenotype that has previously been linked to the loss of senescent cells [56]. Collectively, these results suggest that a defect in the cellular senescence program may underlie ineffective wound healing in *Angptl4* knockout mice [102, 188].

Discussion

The role of Angptl4 *and senescence during the inflammation phase of wound healing*

Inflammation can both promote and impede wound repair, depending largely on the extent and duration of the inflammation. Normal cutaneous healing is associated with timely, acute inflammation that is rapidly eliminated, while wounds that are unable to resolve the inflammatory state often experience delayed healing, and the prolonged presence of inflammatory cytokines and immune cells exacerbates fibrosis and scarring [193]. My work here shows that in the absence of *Angptl4*, mouse wounds exhibit a low-grade level of inflammation that fails to reach statistical significance, but also does not return to baseline levels by day 10 (Figs. 5.10B and 5.11B). Similar results were seen in terms of *Cdkn2a* expression in these wounds – at day 10, in fact, *Cdkn2a* levels seemed to be increasing, whereas they were resolving in the wounds of WT mice (Fig. 5.7B).

Though it is impossible to draw definitive conclusions without looking at the levels of senescence and inflammation at later time points, the results from this study suggest that wounds in *Angptl4* KO mice might experience a prolonged state of low-grade inflammation and senescence, rather than the acute induction and rapid resolution of senescence and inflammation that is observed in normal wound healing. This phenotype has been linked to chronic wounds in diseases like diabetes [194], and indeed,

a previous study found that the wounds of *Angptl4* KO mice only reached about 60% closure by day 10, whereas WT wounds were nearly completely closed by that time [102]

A recent paper showed that there was a delay in the accumulation of senescent cells in the wounds of diabetic mice. This delay caused differential SASP gene expression compared to control wounds and a lack of myofibroblast differentiation and expansion, and ultimately resulted in the impaired healing that is often associated with chronic diabetic ulcers. However, senescent cells were identified in the wounds of diabetic patients over 60 days post-injury, suggesting that while there might be a delay in the onset of senescence in these wounds, senescent cells, once present, persist long-term, causing chronic inflammation and contributing to the pathology of diabetic wounds [195]. Our collaborators in Singapore have previously shown that topical addition of recombinant cANGPTL4 to the wounds of diabetic mice results in faster wound healing [102], which again demonstrates that *Angptl4* expression in mouse wounds is essential for the normal kinetics of transient senescence during healing.

The role of **Angptl4** *and senescence during the proliferation phase of wound healing*

One interesting, somewhat unexpected finding from this work was that there were fewer *Cdkn2a*$^{+}$ cells in *Angptl4* KO mice. Given that *Cdkn2a*/p16 is an early marker of senescent cells, we had expected that loss of *Angptl4* would not affect the accumulation of p16^{+} cells, but rather would prevent those cells from becoming fully senescent and expressing a robust secretome program. There are a few possible explanations for the decrease of p16^{+} cells in the absence of *Angptl4.* The first is that cells entering the senescent pathway turn back without *Angptl4* present to help them commit to the

transition. This hypothesis could be addressed by taking biopsies at intermediate time points (between days 1 and 5) to see if there is a higher level of $p16^+$ cells earlier on that disappear by day 5. Another possibility is that senescence in the wound bed normally acts in a paracrine way, such that early senescent cells act through the SASP to encourage neighboring cells to become senescent as well. This paracrine mechanism of senescence has been observed previously in several models of OIS, and has been linked to different SASP factors, including *IGFBP7, CXCR2,* and *IL-1A* [59, 60, 131]. In this case, we would predict that the absence of *Angptl4* abrogates the formation of a mature SASP, which in turn prevents the induction of paracrine senescence, thus reducing the overall number of $p16^+$ senescent cells in the wound. A final possibility is that the loss of *Angptl4* simply delays the accumulation of senescent cells. This is supported by the fact that p16 expression increases at day 10 in KO wounds, compared to day 5. Future experiments could look at later time points to determine whether the accumulation of $p16^+$ cells is truly reduced in *Angptl4* KO cells, or if it is simply delayed.

Previous work has demonstrated that the immediate outcome of a paucity of senescent cells during wound repair is a defect in the proliferation of α-Sma+ myofibroblasts [56]. Thus, my results showing a strong deficit in both the total number of these cells (Fig. 5.12B) and in their active proliferation (Fig. 5.13D) in *Angptl4* KO wounds are in line with *Angptl4* playing a role in senescence during wound healing. Historically, it was believed that α-Sma^+ myofibroblasts are critical for wound healing because they are a major source of collagen I [196], but a recent study showed that specific deletion of collagen I in αSMA+ fibroblasts did not affect wound closure, re-

epithelialization, or vascularization. Loss of integrin β1 in myofibroblasts, however, caused a significant delay in wound closure, specifically during the early phases, which resulted in reduced epithelialization and vascularization [192]. The lack of α-Sma^{+} cells in *Angptl4* KO wounds shows that *Angptl4* acts either directly or indirectly to stimulate myofibroblast proliferation. However, given the established connection between cAngptl4 and β1 integrin signaling during wound healing [197], it's possible that *Angptl4* is also involved in re-epithelialization and vascularization downstream of myofibroblast proliferation, through its interaction with β1 integrin in these cells.

The role of **Angptl4** *and senescence during the remodeling phase of wound healing*

In the original study of senescent cells during wound healing, DeMaria and his colleagues linked the wound repair response with a specific SASP factor: PDGF-AA. In that model, topical application of PDGF-AA restored the kinetics of normal wound healing but failed to prevent the fibrosis and scarring that occurred in the absence of senescent cells. The authors hypothesized that the proteases that are present in the SASP, which function to modulate the extracellular environment, are critical to restraining fibrosis, and thus the addition of inflammatory SASP factors alone, while sufficient to restore normal wound closure kinetics, cannot compensate for the presence of a complete and functional SASP [56, 198]. Interestingly, in *Angptl4* KO mice, topical application of recombinant cAngptl4 protein can restore both the normal rate of wound closure and prevent scarring and fibrosis, suggesting that the presence of Angptl4 protein is sufficient

to trigger the necessary ECM remodeling that is abrogated when senescent cells are eliminated [102].

Although we found in our liposarcoma model that loss of *ANGPTL4* expression resulted mainly in decreased expression of pro-inflammatory SASP factors, we did also observe effects in the other SASP categories as well – namely, loss of *MMP1* and *MMP3* expression when *ANGPTL4* was knocked down (**Chapter 3,** Fig. 3.8). Additionally, exogenous expression of *ANGPTL4* in A549 cells resulted in increased expression of *MMP1* in response to palbociclib treatment (Fig. 3.14G). Together, these pieces of data suggest that *ANGPTL4* might be involved in the regulation of *MMP* factor expression.

Intriguingly, the timing and level of MMP protein activation is vital for normal wound healing, particularly in remodeling of the scar tissue, where MMPs are involved in degradation of excessive collagen [102, 199]. In normal tissue, MMPs are present at low levels, if at all, but their expression is quickly activated when there is a need for tissue remodeling, such as during wound healing. They are secreted in an inactive form and must be activated by other proteases, including furin, plasminogen, or other MMPs. Both MMP1 and MMP3 are important factors during wound repair, where they regulate chemokine signaling, either by directly degradation or by increasing chemokine activity, and function as collagenases and degraders of other non-collagenous connective tissue. MMP1 and MMP3 are expressed during the re-epithelialization phase of wound healing and turn off once the wound has closed, which is consistent with the kinetics of *Angptl4* expression in the wound beds of WT mice (Fig. 5.6A) [199-201].

The fact that topical cAngptl4 alone both restores the kinetics of normal wound healing *and* reduces scar-associated collagen deposition could indicate that *Angptl4* is

necessary for induction of multiple arms of the SASP during wound healing. The decrease in pro-inflammatory SASP factors that we observed in the liposarcoma model corresponds with the decreased recruitment of the immune system to the wound beds of *Angptl4* KO mice, while the increased fibrosis and scarring associated with the wounds of *Angptl4* KO mice suggests a potential loss of matrix metalloproteinase expression and/or activation when *Angptl4* is missing.

Based on the results of our wound healing experiments and the data from other groups discussed above, I propose a model in which *Angptl4*$^{+}$ senescent cells are critical contributors to the three main phases of wound healing: inflammation, proliferation, and remodeling. During the inflammation phase, pro-inflammatory SASP factors secreted by *Cdkn2a*$^{+}$*/Angptl4*$^{+}$ senescent cells work to recruit the immune system to the wound bed in a timely fashion. During the proliferation phase, *Angptl4* contributes to re-epithelialization by facilitating the expansion of α-Sma^{+} fibroblasts, which form the granulation tissue and contribute to wound contraction. Finally, during the remodeling phase, *Angptl4* prevents excessive collagen secretion from wound fibroblasts, which it likely achieves through regulation of the ECM-component of the SASP. In the absence of *Angptl4,* all of these processes are blunted or lost.

Future work should focus on further characterization of the secretome of senescent cells in WT wounds and determine how that profile is altered in the absence of *Angptl4*. A particularly illuminating experiment would be a single cell seq-based comparison of *Cdkn2a*$^{+}$ cells in KO wounds with *Cdkn2a*$^{+}$*/Angptl4*$^{+}$ cells in WT wounds. Though such an experiment might be technically difficult to perform, particularly regarding the isolation of the desired cell populations in large enough numbers to perform

single cell sequencing, it would shed a great deal of light on the differences in the SASP profiles of these two populations of "senescent" cells, which in turn could help determine the mechanism(s) by which senescence and the SASP contribute to the various phases of wound repair.

Chapter 6: Discussion

Overview

Although much is known about the contexts in which senescence occurs, critical questions remain as to how cells achieve this state. Senescent cells undergo a durable, theoretically irreversible, cell cycle arrest and produce a bioactive secretome, the SASP, that can remodel the microenvironment and engage the immune response to promote cell removal. Senescence has applications in naturally occurring physiological processes, such as aging and wound healing, but it is also a potential outcome of chemotherapy, including treatment with CDK4/6 inhibitors, and the extent to which the regulatory mechanisms controlling senescence in these various contexts is unclear.

Current research on CDK4/6i spans the pre-clinical and clinical spaces and is concerned with a better understanding of treatment response, identification of biomarkers that predict resistance or sensitivity, and nomination of effective combination therapies [202]. To capitalize and improve upon the efficacy of CDK4/6i, we must understand how they act clinically. A significant clinical challenge has been determining whether the source of inflammation following treatment with these drugs is due to cancer cell senescence or some other mechanism [77]. However, the study of senescence has been hampered by the lack of viable markers for detecting senescent cells in tissues.

To address whether senescence contributes to CDK4/6i response in patients, I aimed to identify gene products that could be used to mark mature, inflammation-provoking senescent cells. Using therapy-induced senescence (TIS) as a model in which to study the regulation of senescence, I showed that *ANGPTL4,* a commonly observed

SASP factor, is necessary for geroconversion in response to CDK4/6i in two cell lines arising from different lineages and was also essential for the downstream expression of other SASP genes. I was able to use *ANGPTL4* expression as a marker to identify inflammation-provoking senescent cells in patients with liposarcoma treated with abemaciclib. Additionally, *Angptl4* was necessary for the generation of mature senescent cells arising during excisional wound repair in mice.

In **Chapter 1,** I discussed several questions that remained unanswered, despite 60 years of work in the field of senescence. The first question is whether senescence is truly irreversible. The second is whether senescence, in its myriad contexts, is a single state, or whether each trigger of senescence in each unique cell type results in a distinct form of senescence, all of which happen to share some common properties. And finally, in the realm of chemotherapy, the third question is whether CDK4/6 inhibitors act by inducing senescence in patients, as they have been shown to do in cultured cells and mouse models, and if so, whether senescence is a desirable outcome. Here, I will reflect on how the work from my thesis studies can be applied to begin to answer these elusive questions.

Senescence as a developmental pathway

Although it is commonly described as a permanent state of growth arrest, numerous observations have suggested that “irreversible” might be too strong a descriptor for senescence. Ablation of p53 allows fibroblasts that have undergone replicative senescence to re-enter S phase, as least in cells with low levels of p16 [203]. Acute loss of Rb in senescent MEFs also promotes cell proliferation [204]. These studies,

among others, claim to show the reversible nature of senescence, and have led some scientists to conclude that senescence is not a truly permanent state. Based on the work discussed in **Chapter 3**, I propose an alternative model. While it is formally possible that extraordinary measures, like the use of Yamanaka factors or genetic ablation of pro-senescence pathways, might allow senescent cells to escape from their growth arrested state, the extent to which this finding is physiologically relevant is unclear. The ability to "undo" senescence in a laboratory context is only truly meaningful if similar events occur in a natural setting, whether in normal physiology or in pathological circumstances. I suggest instead that senescence is often oversimplified and reduced to its end state, characterized by a panel of static markers, when in fact it is a developmental pathway upon which cells embark, and during which they evolve through several states.

The data from our DDLS$^{\text{Tet-ON FMDM2}}$ synchronized system show that cells can express many commonly used hallmarks of senescence without having reached the point of commitment to stable growth arrest or the SASP. These cells should be considered "pre-senescent," meaning that they only express the earlier markers of senescence, like activation of p53, induction of p16, and accumulation of ATRX foci, SA-β-gal, and/or SAHF. As these cells have started along the geroconversion pathway, but have not yet committed to irreversible growth arrest, this state might well explain observations that senescence is "reversible." For instance, one recent study of TIS in lymphoma showed that "senescent" cells can escape from growth arrest, and that they subsequently return to the cell cycle having acquired stem-like characteristics and hyperproliferative potential [171]. However, in this work, cells were treated with the chemotherapeutic drug Adriamycin for only 5 days, at which point senescence status was determined using SA-

β-gal and SAHF expression. In the context of our findings from the DDLS$^{\text{Tet-ON FMDM2}}$ system, we can surmise that these cells might never have completed the senescence transition to begin with, and thus did not truly "escape" from it.

After the pre-senescent state, cells progress to the pro-senescent state, at which point they become irreversibly arrested, but do not yet express a fully developed SASP. In our synchronized system, pro-senescence corresponds to day 14, at which point the cells have induced expression *ANGPTL4* and other early SASP factors, and have become stably arrested, but lack the inflammatory branch of the SASP. Such a state was recently observed in primary fibroblasts that were treated with abemaciclib. These cells entered a permanent growth arrested state that was dependent on p53 signaling, and while they activated expression of a subset of SASP genes regulated by p53, including growth factors like *Igfbp3* and *Gdf15*, they lacked expression of pro-inflammatory SASP genes normally regulated by NF-κB [205].

Finally, pro-senescent cells continue their maturation into the senescent state by developing a robust inflammatory SASP. Only at this point, when a cell has committed to irreversible arrest and induced expression of the inflammatory arm of the SASP, should a cell be considered truly senescent. In the context of CDK4/6i, we have shown that this transition is dependent on *ANGPTL4*. We suspect that once cells reach this final stage, further epigenetic remodeling over time [135] might explain how the secretome is sculpted and switches from its "good" cell autonomous, anti-tumorigenic state to a "bad" growth-promoting stage.

CDK4/6 inhibition as a model system for identifying conserved markers of senescence

In the work presented in this dissertation, I have used the CDK4/6i TIS system to attempt to gain a better understanding of how senescence is regulated, primarily because it has several advantages: first, cancer cell lines are significantly easier to work with in culture than primary cells, allowing for bulk production and easy manipulation without repeated isolation or specialized growth conditions or technologies. Second, this system can be engineered to permit a single inducer, palbociclib, to trigger both quiescence and senescence, thus minimizing confusion from using different signals to generate such cells for comparative analysis. Lastly, it uncouples senescence from cell cycle exit, which is already well understood, allowing for the identification of phenotypes and regulators that are essential specifically for geroconversion. Expression of p16, for instance, has frequently been associated with senescence, and indeed p16 is one of the most commonly used markers of senescent cells [206]. However, p16 is a regulator of cell cycle arrest, and while exit from the cell cycle is, of course, a fundamental requirement for the senescent phenotype, it is also the very first step that a cell makes towards becoming senescent. As the single cell sequencing data from the $DDLS^{Tet\text{-}ON\ FMDM2}$ cell line demonstrated, expression of *CDKN2A* was broadly observed in most quiescent cells, as well as in early senescent cells that had not yet committed to stable growth arrest, and in senescent cells that did not exhibit expression of SASP genes (Fig. 3.7).

The CDK4/6i TIS model has successfully been used to identify two different types of markers of senescence, one intrinsic, one extrinsic, that appear to be widely (though perhaps not universally) applicable in other cell types and other models of

senescence. The first is ATRX foci, initially implicated in TIS by Marta Kovatcheva, who showed that ATRX plays a necessary role in geroconversion in human cancer cells [20, 31], as well as in human primary cells undergoing replicative senescence, OIS, and DDIS (Marta Kovatcheva, unpublished data). Here, I have extended Marta's work to show that ATRX foci increase during senescence in mouse primary cells undergoing replicative senescence and DDIS (Figs. 5.3 and 5.4). I have also found that ATRX foci increase in mouse cancer cells treated with CDK4/6 inhibitors, and based on preliminary data, that they increase with age in mouse tissue (data not shown). To date, we are not aware of any model of senescence in which ATRX foci have *not* been found to increase.

The second marker, of course, is *ANGPTL4,* which was first identified in the $DDLS^{Tet\text{-}ON\ FMDM2}$ system discussed in **Chapter 3,** but which has also previously been published in lists of SASP factors in several studies of different senescence models, though its role in senescence had never been investigated [84, 120, 121]. I have demonstrated that *ANGPTL4* expression increases in human primary cells undergoing replicative senescence and DDIS, and in a number of different human cancer cell lines treated with CDK4/6 inhibitors. Its expression also correlates with replicative senescence and DDIS in mouse embryonic fibroblasts. Finally, I showed that *Angptl4* was essential to the normal function of senescent cells during excisional wound healing, and that *ANGPTL4* expression was connected to senescence in liposarcoma patients *in vivo.*

Taken together, these results support the conclusion that there are likely to be at least some elements of the senescence machinery that are broadly conserved, regardless of cell type or inducer. They also confirm that the CDK4/6i model is useful for the identification of such markers, since at least two regulators of senescence discovered in

the context of cancer cells have now been successfully applied to other cell types and other models of senescence.

Cellular senescence: many different states, or just a matter of timing?

Despite the fact that many phenotypes of senescence are observed regardless of cell type or inducer, there exists in the field a pervasive notion that each individual trigger in each individual cell type might result in a unique 'senescence' program. Such a view finds support in the evidence that different stimuli rely upon different mechanisms to cause cell cycle exit; the fact that many, but not all, of the components of the SASP are inducer and cell-type dependent; and the fact that commonly used markers, such as SA-β-gal and SAHF, are not observed in some models. However, if a senescent cell has truly entered a cellular state defined, at minimum, by the acquisition of an anti-apoptotic program of gene expression, the establishment of permanent growth arrest, and the development of a bioactive secretome, there is likely to be a conserved molecular mechanism responsible for achieving and integrating these phenotypes to ensure their coordination.

Collectively, the evidence presented here supports the conclusion that *ANGPTL4* is necessary to regulate the onset of senescence in multiple systems and plays a role in establishing two foundational phenotypes of a senescent cell: stable growth-arrest and elaboration of the inflammatory SASP. This supports a model in which the regulation of senescence, or at least certain components of that regulation, are indeed conserved in

different contexts. I propose that *ANGPTL4* is part of a central, conserved regulatory node associated with geroconversion.

Interestingly, in the context of wound healing, the contribution of *Angptl4* expression had a net beneficial effect for the organism, while in the liposarcoma patients, the contribution of *ANGPTL4* expression and its ensuing inflammation had a net negative effect for the organism. If senescence is regulated by the same core machinery in different contexts, then how can its pleotropic effects be explained? In part, this is likely due to the components of the senescence program that *are* context-specific – for example, members of the SASP that are differentially expressed in contexts in which senescence has beneficial and antagonistic effects.

However, another possible interpretation is that the pleiotropy associated with senescence is not related to differential regulators of the process, but rather the kinetics of its induction and clearance. In the wound healing model, normal wound healing was accompanied by acute induction and then rapid resolution of *Cdk2na*$^{+}$/*Angptl4*$^{+}$ senescent cells, macrophages, and T-cells. Loss of *Angptl4* appeared to delay and dampen the senescence and immune responses, potentially leading to a prolonged state of low-grade senescence and inflammation, and resulting in impaired healing. In the sarcoma model, the timing of the biopsies makes it impossible to conclude how long senescent cells and the inflammatory response persisted, but the highest risk of progression associated with having senescence and inflammation occurred around the 6-month mark (Fig. 4.12). This suggests that the abemaciclib-induced senescence and inflammation we observed in biopsies at the one-month mark might have lingered in the tumor, rather than being cleared. In both models, then, *ANGPTL4* plays a role in the regulation of

senescence, and in both models, chronic senescence and inflammation are problematic. There is evidence to suggest that the SASP secreted by senescent cells becomes more inflammatory with time, which likely contributes to the negative effects of prolonged senescence [55]. My work supports the idea that senescence in different contexts is a conserved state, and that its positive or negative effects are related to the longevity of senescent cells in their environment.

The utility of *ANGPTL4* as a marker of senescence

One major tool that has come out of my thesis work is the identification of *ANGPTL4* expression as a marker of SASP-producing senescent cells that have already committed to stable growth arrest. As I have established throughout this thesis, there is a strong need for markers that can be broadly used to identify senescent cells – markers that are unrelated to cell cycle exit and that are specific for mature senescent cells, rather than pre- or pro-senescent cells. I have demonstrated that *ANGPTL4* expression is associated with senescence in both human and mouse primary and cancer cells in response to a variety of different triggers, and measurement of *ANGPTL4* expression is easily done in cultured cells and tissue samples. The fact that quantification of *ANGPTL4* expression via RNAscope can be performed on FFPE samples, and does not require fresh or frozen tissue, is a huge benefit, as it opens the possibility of utilizing this marker on archival samples. All of these factors make *ANGPTL4* expression a useful and applicable hallmark of a senescent cell.

One caveat of *ANGPTL4* expression as a marker of senescence is that it is not exclusive to senescent cells, but this is the case for most phenotypes typically used to

identify senescent cells. The utility of *ANGPTL4* as a marker is therefore dependent on its ability to be associated with other known markers of senescence. Fortunately, *ANGPTL4* expression was well-correlated with *CDKN2A* expression in two *in vivo* models of senescence: CDK4/6 inhibitor therapy-induced senescence in liposarcoma patients, and senescence during excisional wound healing. In the abemaciclib trial, two patients had increased *CDKN2A* but not *ANGPTL4* in the on-treatment biopsies, but since *CDKN2A* expression precedes *ANGPTL4* expression, it is conceivable that these cells were embarking on the geroconversion pathway, and that a later biopsy would have shown positivity in both senescent markers. Only one patient had increased expression of *ANGPTL4* without a corresponding increase in *CDKN2A* expression (Fig. 4.6), suggesting that increased expression of *ANGPTL4* is generally a reliable way to identify senescent cells.

The use of *ANGPTL4* allowed us to demonstrate that senescent cells do accumulate in the tumors of patients treated with a CDK4/6 inhibitor, and that those cells were associated with an increase in tumoral inflammation. Thus, at least in the case of DDLS, we are able to conclude that the mechanism of action of CDK4/6 inhibitors is indeed connected to senescence *in vivo,* as it is *in vitro* and in mouse models. Since *ANGPTL4* expression is observed after drug treatment, it cannot be used as a prognostic biomarker to predict whether a patient will benefit from treatment with CDK4/6i. However, increased expression of *ANGPTL4* (or lack thereof) as a marker of senescent cells in an early on-treatment biopsy may predict a patient's trajectory and help inform whether they should continue taking CDK4/6i. Additionally, a deeper understanding of

how *ANGPTL4* expression is induced and how it is regulated at the transcriptional level may eventually lead to the identification of pre-treatment biomarkers.

Using senescence status to inform clinical decisions

The final question I hoped to address in my thesis work concerns the effect of senescence as an outcome to chemotherapy. Senescence is often described in the literature as a double-edged sword, given that it is beneficial to the organism in some settings and detrimental in others. Ten to twenty years ago, the prevailing view in the literature was that the durability of growth arrest and immune recruitment as a result of SASP expression would make senescence an overall positive outcome of chemotherapy [39, 62, 167]. This view perhaps stemmed from the idea that senescence evolved as a natural barrier to tumor suppression [172]. However, in recent years, as more evidence has accumulated regarding the potential pro-tumorigenic and pro-inflammatory effects of the SASP, there has been a shift towards thinking that the ability of the SASP to induce chronic inflammation and to promote tumor proliferation, invasion, and metastasis might actually make senescence a harmful outcome of treatment [74, 134, 207].

The results from our clinical trial of abemaciclib show that patients who experience senescence and inflammation after one month on treatment have increased risk of progression. Thus, when treatment with CDK4/6 inhibitors results in senescence, it would be beneficial to the patient for those senescent cells to be removed. This suggests that combining CDK4/6 inhibitors with senotherapeutics, drugs that target senescent cells, might be advantageous. Since the first two senolytics, dasatinib and quercetin, were discovered in 2015, senotherapeutic drugs have been the subject of preclinical studies and

clinical trials, generally with the goal of ameliorating age-related pathologies. Senotherapeutic drugs are broadly broken down into two categories: senolytics, which aim to selectively kill senescent cells, and senomorphics, which aim to modulate the senescent phenotype to suppress the harmful aspects of SASP expression, without actively eliminating senescent cells [208, 209].

Based on our findings about abemaciclib therapy in DDLS patients, both types of drugs could prove successful in combination with CDK4/6 inhibitors. Treatment with a senolytic to remove senescent cells early on could help resolve the inflammation we observed in most patients who exhibited senescent cell formation upon abemaciclib treatment. Senomorphic drugs would likely also be viable options in these patients. Our analysis showed that senescence alone had no significant effect, either positive or negative, on progression (Fig. 4.13). Only when senescence overlapped with signs of inflammation were patients at increased risk of progression (Fig. 4.12). Thus, a therapy that could specifically block the inflammatory aspects of senescence could be highly effective in these patients.

A deeper understanding of the mechanism by which *ANGPTL4* regulates senescence could ultimately provide the blueprint for a senomorphic drug approach. Assuming that the two components of the senescent phenotype are independently regulated, an intriguing possibility would be to uncouple the onset of irreversible arrest from the expression of the inflammatory SASP. Targeting the mechanism by which *ANGPTL4* drives SASP expression, without affecting the mechanism by which it induces geroconversion, would allow patients to benefit from the “good” effects of senescent

cells – the permanent exit of tumor cells from the cell cycle – without the "bad" effects – the chronic inflammation induced by certain SASP factors.

Existing senolytics target various aspects of the senescence phenotype, including p53 inhibitors and Bcl-2 family inhibitors, which work by undoing the inherent resistance to apoptosis that is commonly observed in senescent cells [208]. Based on our idea that pre-senescent cells evolve through several progressive stages before reaching the pinnacle senescent state, we would predict that a senolytic targeting late-stage senescence phenotypes would be the most effective option. *ANGPTL4* itself is an unlikely target for a senolytic drug, as it is expressed, at least at low levels, in most cycling cells we have examined in culture. However, further study of the mechanism by which *ANGPTL4* functions during senescence could identify viable senolytic targets either upstream or downstream of *ANGPTL4* itself, including binding partners or transcriptional regulators. In terms of nominating additional candidate targets for senotherapeutic drugs, the CDK4/6i TIS system is again a useful model for discovery. The synchronicity of the $DDLS^{Tet\text{-}ON\ FMDM2}$ cell line allows for temporal separation of senescent markers, which simplifies the task of linking a gene or protein to a specific phenotype. This model could thus be used as a system in which to identify more regulators of various components of the SASP, or other aspects of the senescence program, which could then become targets for senotherapeutic drugs.

Additionally, we have previously shown that down-regulation of MDM2 is a necessary step for embarkation on the geroconversion pathway in other types of cancer cell lines in which MDM2 is not amplified [20], and thus the Tet-inducible MDM2 construct can be broadly applied. Indeed, we have already created and begun to

characterize the H358$^{\text{Tet-ON FMDM2}}$ (non-small cell lung cancer) and the MCF7$^{\text{Tet-ON FMDM2}}$ (ER+ breast cancer) cell lines (data not shown). If *ANGPTL4,* or any other target generated from the liposarcoma model, is not found to be involved in senescence in a particular type of cancer, a Tet-ON FMDM2 cell line can be created to facilitate the identification of disease-specific regulators and hallmarks of senescent cells.

Undoubtedly, a great deal of work remains to be done to fully understand the senescent state and the ways in which it contributes to organismal biology, and my thesis work has created as many questions as it has answered. What is the mechanism by which *ANGPTL4* regulates stable growth arrest and SASP gene expression? Can that mechanism be exploited for drug development? Will *ANGPTL4* prove to be a reliable marker of senescence in other disease models, or in other contexts of senescence not investigated here? If not, can other factors upstream or downstream of *ANGPTL4* itself be used instead? Will future clinical trials of CDK4/6 inhibitors, which will enroll higher numbers of patients and collect a wider spread of biopsies for correlative analysis, confirm the finding that CDK4/6i induce senescence and inflammation in human patients, and that this outcome has a detrimental effect on tumor progression? Can that effect be ameliorated by combination therapy with senotherapeutic drugs? Only by developing a detailed, mechanistic understanding of the triggers that drive entry into, maturation of, and maintenance of the senescent state can we hope to one day successfully manipulate this complex process to our benefit.

Chapter 7: References

1. Hayflick, L. and P.S. Moorhead, *The serial cultivation of human diploid cell strains.* Exp Cell Res, 1961. **25**: p. 585-621.
2. Hayflick, L., *The Limited in Vitro Lifetime of Human Diploid Cell Strains.* Exp Cell Res, 1965. **37**: p. 614-36.
3. Shay, J.W. and W.E. Wright, *Hayflick, his limit, and cellular ageing.* Nat Rev Mol Cell Biol, 2000. **1**(1): p. 72-6.
4. Der, C.J., T.G. Krontiris, and G.M. Cooper, *Transforming genes of human bladder and lung carcinoma cell lines are homologous to the ras genes of Harvey and Kirsten sarcoma viruses.* Proc Natl Acad Sci U S A, 1982. **79**(11): p. 3637-40.
5. Serrano, M., et al., *Oncogenic ras provokes premature cell senescence associated with accumulation of p53 and p16INK4a.* Cell, 1997. **88**(5): p. 593-602.
6. Michaloglou, C., et al., *BRAFE600-associated senescence-like cell cycle arrest of human naevi.* Nature, 2005. **436**(7051): p. 720-4.
7. McHugh, D. and J. Gil, *Senescence and aging: Causes, consequences, and therapeutic avenues.* J Cell Biol, 2018. **217**(1): p. 65-77.
8. Blomen, V.A. and J. Boonstra, *Cell fate determination during G1 phase progression.* Cell Mol Life Sci, 2007. **64**(23): p. 3084-104.
9. Campisi, J., *The biology of replicative senescence.* Eur J Cancer, 1997. **33**(5): p. 703-9.
10. Wright, W.E. and J.W. Shay, *Telomere dynamics in cancer progression and prevention: fundamental differences in human and mouse telomere biology.* Nat Med, 2000. **6**(8): p. 849-51.
11. Parrinello, S., et al., *Oxygen sensitivity severely limits the replicative lifespan of murine fibroblasts.* Nat Cell Biol, 2003. **5**(8): p. 741-7.
12. Di Leonardo, A., et al., *DNA damage triggers a prolonged p53-dependent G1 arrest and long-term induction of Cip1 in normal human fibroblasts.* Genes Dev, 1994. **8**(21): p. 2540-51.
13. Courtois-Cox, S., S.L. Jones, and K. Cichowski, *Many roads lead to oncogene-induced senescence.* Oncogene, 2008. **27**(20): p. 2801-9.
14. Wiley, C.D. and J. Campisi, *The metabolic roots of senescence: mechanisms and opportunities for intervention.* Nat Metab, 2021. **3**(10): p. 1290-1301.
15. Wiley, C.D., et al., *Mitochondrial Dysfunction Induces Senescence with a Distinct Secretory Phenotype.* Cell Metab, 2016. **23**(2): p. 303-14.
16. Velarde, M.C., et al., *Mitochondrial oxidative stress caused by Sod2 deficiency promotes cellular senescence and aging phenotypes in the skin.* Aging (Albany NY), 2012. **4**(1): p. 3-12.
17. Kaplon, J., et al., *A key role for mitochondrial gatekeeper pyruvate dehydrogenase in oncogene-induced senescence.* Nature, 2013. **498**(7452): p. 109-12.

18. Zhu, X., et al., *Inflammation, epigenetics, and metabolism converge to cell senescence and ageing: the regulation and intervention.* Signal Transduct Target Ther, 2021. **6**(1): p. 245.
19. Qian, Y. and X. Chen, *Tumor suppression by p53: making cells senescent.* Histol Histopathol, 2010. **25**(4): p. 515-26.
20. Kovatcheva, M., et al., *MDM2 turnover and expression of ATRX determine the choice between quiescence and senescence in response to CDK4 inhibition.* Oncotarget, 2015. **6**(10): p. 8226-43.
21. Coller, H.A., L. Sang, and J.M. Roberts, *A new description of cellular quiescence.* PLoS Biol, 2006. **4**(3): p. e83.
22. Sang, L., H.A. Coller, and J.M. Roberts, *Control of the reversibility of cellular quiescence by the transcriptional repressor HES1.* Science, 2008. **321**(5892): p. 1095-100.
23. Harris, L. and F. Guillemot, *HES1, two programs: promoting the quiescence and proliferation of adult neural stem cells.* Genes Dev, 2019. **33**(9-10): p. 479-481.
24. Dimri, G.P., et al., *A biomarker that identifies senescent human cells in culture and in aging skin in vivo.* Proc Natl Acad Sci U S A, 1995. **92**(20): p. 9363-7.
25. Narita, M., et al., *Rb-mediated heterochromatin formation and silencing of E2F target genes during cellular senescence.* Cell, 2003. **113**(6): p. 703-16.
26. Mannava, S., et al., *Depletion of deoxyribonucleotide pools is an endogenous source of DNA damage in cells undergoing oncogene-induced senescence.* Am J Pathol, 2013. **182**(1): p. 142-51.
27. Aird, K.M., et al., *Suppression of nucleotide metabolism underlies the establishment and maintenance of oncogene-induced senescence.* Cell Rep, 2013. **3**(4): p. 1252-65.
28. Quijano, C., et al., *Oncogene-induced senescence results in marked metabolic and bioenergetic alterations.* Cell Cycle, 2012. **11**(7): p. 1383-92.
29. Hernandez-Segura, A., J. Nehme, and M. Demaria, *Hallmarks of Cellular Senescence.* Trends Cell Biol, 2018. **28**(6): p. 436-453.
30. Dou, Z., et al., *Cytoplasmic chromatin triggers inflammation in senescence and cancer.* Nature, 2017. **550**(7676): p. 402-406.
31. Kovatcheva, M., et al., *ATRX is a regulator of therapy induced senescence in human cells.* Nat Commun, 2017. **8**(1): p. 386.
32. Lee, B.Y., et al., *Senescence-associated beta-galactosidase is lysosomal beta-galactosidase.* Aging Cell, 2006. **5**(2): p. 187-95.
33. Young, A.R., et al., *Autophagy mediates the mitotic senescence transition.* Genes Dev, 2009. **23**(7): p. 798-803.
34. Severino, J., et al., *Is beta-galactosidase staining a marker of senescence in vitro and in vivo?* Exp Cell Res, 2000. **257**(1): p. 162-71.
35. Cho, S. and E.S. Hwang, *Status of mTOR activity may phenotypically differentiate senescence and quiescence.* Mol Cells, 2012. **33**(6): p. 597-604.
36. Prieur, A., et al., *p53 and p16(INK4A) independent induction of senescence by chromatin-dependent alteration of S-phase progression.* Nat Commun, 2011. **2**: p. 473.

37. Dorr, J.R., et al., *Synthetic lethal metabolic targeting of cellular senescence in cancer therapy.* Nature, 2013. **501**(7467): p. 421-5.
38. Gitenay, D., et al., *Glucose metabolism and hexosamine pathway regulate oncogene-induced senescence.* Cell Death Dis, 2014. **5**: p. e1089.
39. Ewald, J.A., et al., *Therapy-induced senescence in cancer.* J Natl Cancer Inst, 2010. **102**(20): p. 1536-46.
40. Wyld, L., et al., *Senescence and Cancer: A Review of Clinical Implications of Senescence and Senotherapies.* Cancers (Basel), 2020. **12**(8).
41. Campisi, J., *Cellular Senescence and Lung Function during Aging. Yin and Yang.* Ann Am Thorac Soc, 2016. **13 Suppl 5**: p. S402-S406.
42. Kuilman, T., et al., *The essence of senescence.* Genes Dev, 2010. **24**(22): p. 2463-79.
43. Lee, S. and C.A. Schmitt, *The dynamic nature of senescence in cancer.* Nat Cell Biol, 2019. **21**(1): p. 94-101.
44. Chakradeo, S., L.W. Elmore, and D.A. Gewirtz, *Is Senescence Reversible?* Curr Drug Targets, 2016. **17**(4): p. 460-6.
45. Ryu, S.J., Y.S. Oh, and S.C. Park, *Failure of stress-induced downregulation of Bcl-2 contributes to apoptosis resistance in senescent human diploid fibroblasts.* Cell Death Differ, 2007. **14**(5): p. 1020-8.
46. Pasillas, M.P., et al., *Proteomic analysis reveals a role for Bcl2-associated athanogene 3 and major vault protein in resistance to apoptosis in senescent cells by regulating ERK1/2 activation.* Mol Cell Proteomics, 2015. **14**(1): p. 1-14.
47. Wang, E., *Senescent human fibroblasts resist programmed cell death, and failure to suppress bcl2 is involved.* Cancer Res, 1995. **55**(11): p. 2284-92.
48. Jackson, J.G. and O.M. Pereira-Smith, *p53 is preferentially recruited to the promoters of growth arrest genes p21 and GADD45 during replicative senescence of normal human fibroblasts.* Cancer Res, 2006. **66**(17): p. 8356-60.
49. Coppe, J.P., et al., *The senescence-associated secretory phenotype: the dark side of tumor suppression.* Annu Rev Pathol, 2010. **5**: p. 99-118.
50. Coppe, J.P., et al., *Tumor suppressor and aging biomarker p16(INK4a) induces cellular senescence without the associated inflammatory secretory phenotype.* J Biol Chem, 2011. **286**(42): p. 36396-403.
51. Rodier, F., et al., *Persistent DNA damage signalling triggers senescence-associated inflammatory cytokine secretion.* Nat Cell Biol, 2009. **11**(8): p. 973-9.
52. Chien, Y., et al., *Control of the senescence-associated secretory phenotype by NF-kappaB promotes senescence and enhances chemosensitivity.* Genes Dev, 2011. **25**(20): p. 2125-36.
53. Kuilman, T., et al., *Oncogene-induced senescence relayed by an interleukin-dependent inflammatory network.* Cell, 2008. **133**(6): p. 1019-31.
54. Kang, C., et al., *The DNA damage response induces inflammation and senescence by inhibiting autophagy of GATA4.* Science, 2015. **349**(6255): p. aaa5612.
55. Hoare, M., et al., *NOTCH1 mediates a switch between two distinct secretomes during senescence.* Nat Cell Biol, 2016. **18**(9): p. 979-92.
56. Demaria, M., et al., *An essential role for senescent cells in optimal wound healing through secretion of PDGF-AA.* Dev Cell, 2014. **31**(6): p. 722-33.

57. Mosteiro, L., et al., *Tissue damage and senescence provide critical signals for cellular reprogramming in vivo.* Science, 2016. **354**(6315).
58. Orjalo, A.V., et al., *Cell surface-bound IL-1alpha is an upstream regulator of the senescence-associated IL-6/IL-8 cytokine network.* Proc Natl Acad Sci U S A, 2009. **106**(40): p. 17031-6.
59. Acosta, J.C., et al., *Chemokine signaling via the CXCR2 receptor reinforces senescence.* Cell, 2008. **133**(6): p. 1006-18.
60. Acosta, J.C., et al., *A complex secretory program orchestrated by the inflammasome controls paracrine senescence.* Nat Cell Biol, 2013. **15**(8): p. 978-90.
61. Iannello, A., et al., *p53-dependent chemokine production by senescent tumor cells supports NKG2D-dependent tumor elimination by natural killer cells.* J Exp Med, 2013. **210**(10): p. 2057-69.
62. Xue, W., et al., *Senescence and tumour clearance is triggered by p53 restoration in murine liver carcinomas.* Nature, 2007. **445**(7128): p. 656-60.
63. Lujambio, A., et al., *Non-cell-autonomous tumor suppression by p53.* Cell, 2013. **153**(2): p. 449-60.
64. Kang, T.W., et al., *Senescence surveillance of pre-malignant hepatocytes limits liver cancer development.* Nature, 2011. **479**(7374): p. 547-51.
65. Krtolica, A., et al., *Senescent fibroblasts promote epithelial cell growth and tumorigenesis: a link between cancer and aging.* Proc Natl Acad Sci U S A, 2001. **98**(21): p. 12072-7.
66. Yoshimoto, S., et al., *Obesity-induced gut microbial metabolite promotes liver cancer through senescence secretome.* Nature, 2013. **499**(7456): p. 97-101.
67. Coppe, J.P., et al., *Senescence-associated secretory phenotypes reveal cell-nonautonomous functions of oncogenic RAS and the p53 tumor suppressor.* PLoS Biol, 2008. **6**(12): p. 2853-68.
68. van Deursen, J.M., *The role of senescent cells in ageing.* Nature, 2014. **509**(7501): p. 439-46.
69. Franceschi, C., et al., *Inflamm-aging. An evolutionary perspective on immunosenescence.* Ann N Y Acad Sci, 2000. **908**: p. 244-54.
70. Di Micco, R., et al., *Cellular senescence in ageing: from mechanisms to therapeutic opportunities.* Nat Rev Mol Cell Biol, 2021. **22**(2): p. 75-95.
71. Karin, O., et al., *Senescent cell turnover slows with age providing an explanation for the Gompertz law.* Nat Commun, 2019. **10**(1): p. 5495.
72. Chang, B.D., et al., *A senescence-like phenotype distinguishes tumor cells that undergo terminal proliferation arrest after exposure to anticancer agents.* Cancer Res, 1999. **59**(15): p. 3761-7.
73. te Poele, R.H., et al., *DNA damage is able to induce senescence in tumor cells in vitro and in vivo.* Cancer Res, 2002. **62**(6): p. 1876-83.
74. Wagner, V. and J. Gil, *Senescence as a therapeutically relevant response to CDK4/6 inhibitors.* Oncogene, 2020. **39**(29): p. 5165-5176.
75. Goel, S., et al., *CDK4/6 Inhibition in Cancer: Beyond Cell Cycle Arrest.* Trends Cell Biol, 2018. **28**(11): p. 911-925.

76. Knudsen, E.S. and J.Y. Wang, *Targeting the RB-pathway in cancer therapy.* Clin Cancer Res, 2010. **16**(4): p. 1094-9.
77. Klein, M.E., et al., *CDK4/6 Inhibitors: The Mechanism of Action May Not Be as Simple as Once Thought.* Cancer Cell, 2018. **34**(1): p. 9-20.
78. Barretina, J., et al., *Subtype-specific genomic alterations define new targets for soft-tissue sarcoma therapy.* Nat Genet, 2010. **42**(8): p. 715-21.
79. Durkin, M.E., et al., *Isolation of Mouse Embryo Fibroblasts.* Bio Protoc, 2013. **3**(18).
80. Dobin, A., et al., *STAR: ultrafast universal RNA-seq aligner.* Bioinformatics, 2013. **29**(1): p. 15-21.
81. Love, M.I., W. Huber, and S. Anders, *Moderated estimation of fold change and dispersion for RNA-seq data with DESeq2.* Genome Biol, 2014. **15**(12): p. 550.
82. Mootha, V.K., et al., *PGC-1alpha-responsive genes involved in oxidative phosphorylation are coordinately downregulated in human diabetes.* Nat Genet, 2003. **34**(3): p. 267-73.
83. Subramanian, A., et al., *Gene set enrichment analysis: a knowledge-based approach for interpreting genome-wide expression profiles.* Proc Natl Acad Sci U S A, 2005. **102**(43): p. 15545-50.
84. Chen, H., et al., *MacroH2A1 and ATM Play Opposing Roles in Paracrine Senescence and the Senescence-Associated Secretory Phenotype.* Mol Cell, 2015. **59**(5): p. 719-31.
85. Coppe, J.P., et al., *A human-like senescence-associated secretory phenotype is conserved in mouse cells dependent on physiological oxygen.* PLoS One, 2010. **5**(2): p. e9188.
86. Kuilman, T. and D.S. Peeper, *Senescence-messaging secretome: SMS-ing cellular stress.* Nat Rev Cancer, 2009. **9**(2): p. 81-94.
87. Lackner, D.H., et al., *A genomics approach identifies senescence-specific gene expression regulation.* Aging Cell, 2014. **13**(5): p. 946-50.
88. Ozcan, S., et al., *Unbiased analysis of senescence associated secretory phenotype (SASP) to identify common components following different genotoxic stresses.* Aging (Albany NY), 2016. **8**(7): p. 1316-29.
89. Pribluda, A., et al., *A senescence-inflammatory switch from cancer-inhibitory to cancer-promoting mechanism.* Cancer Cell, 2013. **24**(2): p. 242-56.
90. La Manno, G., et al., *RNA velocity of single cells.* Nature, 2018. **560**(7719): p. 494-498.
91. Stuart, T., et al., *Comprehensive Integration of Single-Cell Data.* Cell, 2019. **177**(7): p. 1888-1902 e21.
92. Hafemeister, C. and R. Satija, *Normalization and variance stabilization of single-cell RNA-seq data using regularized negative binomial regression.* Genome Biol, 2019. **20**(1): p. 296.
93. Cao, J., et al., *The single-cell transcriptional landscape of mammalian organogenesis.* Nature, 2019. **566**(7745): p. 496-502.
94. Ritchie, M.E., et al., *limma powers differential expression analyses for RNA-sequencing and microarray studies.* Nucleic Acids Res, 2015. **43**(7): p. e47.

95. Tirosh, I., et al., *Dissecting the multicellular ecosystem of metastatic melanoma by single-cell RNA-seq.* Science, 2016. **352**(6282): p. 189-96.
96. Alquicira-Hernandez, J. and J.E. Powell, *Nebulosa recovers single cell gene expression signals by kernel density estimation.* Bioinformatics, 2021.
97. Yu, G., et al., *clusterProfiler: an R package for comparing biological themes among gene clusters.* OMICS, 2012. **16**(5): p. 284-7.
98. Yates, A.D., et al., *Ensembl 2020.* Nucleic Acids Res, 2020. **48**(D1): p. D682-D688.
99. Bray, N.L., et al., *Near-optimal probabilistic RNA-seq quantification.* Nat Biotechnol, 2016. **34**(5): p. 525-7.
100. Sturm, G., et al., *Comprehensive evaluation of transcriptome-based cell-type quantification methods for immuno-oncology.* Bioinformatics, 2019. **35**(14): p. i436-i445.
101. Plattner, C., F. Finotello, and D. Rieder, *Deconvoluting tumor-infiltrating immune cells from RNA-seq data using quanTIseq.* Methods Enzymol, 2020. **636**: p. 261-285.
102. Teo, Z., et al., *Angiopoietin-like 4 induces a beta-catenin-mediated upregulation of ID3 in fibroblasts to reduce scar collagen expression.* Sci Rep, 2017. **7**(1): p. 6303.
103. Gur-Cohen, S., et al., *Stem cell-driven lymphatic remodeling coordinates tissue regeneration.* Science, 2019. **366**(6470): p. 1218-1225.
104. Shihan, M.H., et al., *A simple method for quantitating confocal fluorescent images.* Biochem Biophys Rep, 2021. **25**: p. 100916.
105. Pignolo, R.J., et al., *The pathway of cell senescence: WI-38 cells arrest in late G1 and are unable to traverse the cell cycle from a true G0 state.* Exp Gerontol, 1998. **33**(1-2): p. 67-80.
106. Blagosklonny, M.V., *Geroconversion: irreversible step to cellular senescence.* Cell Cycle, 2014. **13**(23): p. 3628-35.
107. Leontieva, O.V., et al., *Hyper-mitogenic drive coexists with mitotic incompetence in senescent cells.* Cell Cycle, 2012. **11**(24): p. 4642-9.
108. Sousa-Victor, P., et al., *Geriatric muscle stem cells switch reversible quiescence into senescence.* Nature, 2014. **506**(7488): p. 316-21.
109. Dickson, M.A., et al., *Phase II trial of the CDK4 inhibitor PD0332991 in patients with advanced CDK4-amplified well-differentiated or dedifferentiated liposarcoma.* J Clin Oncol, 2013. **31**(16): p. 2024-8.
110. Klein, M.E., et al., *PDLIM7 and CDH18 regulate the turnover of MDM2 during CDK4/6 inhibitor therapy-induced senescence.* Oncogene, 2018. **37**(37): p. 5066-5078.
111. Hewitt, G., et al., *Telomeres are favoured targets of a persistent DNA damage response in ageing and stress-induced senescence.* Nat Commun, 2012. **3**: p. 708.
112. Rodier, F., et al., *DNA-SCARS: distinct nuclear structures that sustain damage-induced senescence growth arrest and inflammatory cytokine secretion.* J Cell Sci, 2011. **124**(Pt 1): p. 68-81.
113. Garbarino, J., et al., *Loss of ATRX confers DNA repair defects and PARP inhibitor sensitivity.* Transl Oncol, 2021. **14**(9): p. 101147.

114. Ge, H., et al., *Differential regulation and properties of angiopoietin-like proteins 3 and 4.* J Lipid Res, 2005. **46**(7): p. 1484-90.
115. Pacheco, J. and E. Schenk, *CDK4/6 inhibition alone and in combination for non-small cell lung cancer.* Oncotarget, 2019. **10**(6): p. 618-619.
116. Ruscetti, M., et al., *NK cell-mediated cytotoxicity contributes to tumor control by a cytostatic drug combination.* Science, 2018. **362**(6421): p. 1416-1422.
117. Tan, M.J., et al., *Emerging roles of angiopoietin-like 4 in human cancer.* Mol Cancer Res, 2012. **10**(6): p. 677-88.
118. Yin, W., et al., *Genetic variation in ANGPTL4 provides insights into protein processing and function.* J Biol Chem, 2009. **284**(19): p. 13213-22.
119. Chomel, C., et al., *Interaction of the coiled-coil domain with glycosaminoglycans protects angiopoietin-like 4 from proteolysis and regulates its antiangiogenic activity.* FASEB J, 2009. **23**(3): p. 940-9.
120. Andre, T., et al., *Evidences of early senescence in multiple myeloma bone marrow mesenchymal stromal cells.* PLoS One, 2013. **8**(3): p. e59756.
121. Florea, V., et al., *c-Myc is essential to prevent endothelial pro-inflammatory senescent phenotype.* PLoS One, 2013. **8**(9): p. e73146.
122. Zahn, J.M., et al., *AGEMAP: a gene expression database for aging in mice.* PLoS Genet, 2007. **3**(11): p. e201.
123. Yang, J., et al., *Synchronized age-related gene expression changes across multiple tissues in human and the link to complex diseases.* Sci Rep, 2015. **5**: p. 15145.
124. Plank, M., et al., *A meta-analysis of caloric restriction gene expression profiles to infer common signatures and regulatory mechanisms.* Mol Biosyst, 2012. **8**(4): p. 1339-49.
125. Aird, K.M. and R. Zhang, *Metabolic alterations accompanying oncogene-induced senescence.* Mol Cell Oncol, 2014. **1**(3): p. e963481.
126. Gan, Q., et al., *PPAR{gamma} accelerates cellular senescence by inducing p16INK4{alpha} expression in human diploid fibroblasts.* J Cell Sci, 2008. **121**(Pt 13): p. 2235-45.
127. Welford, S.M., et al., *HIF1alpha delays premature senescence through the activation of MIF.* Genes Dev, 2006. **20**(24): p. 3366-71.
128. Alique, M., et al., *Hypoxia-Inducible Factor-1alpha: The Master Regulator of Endothelial Cell Senescence in Vascular Aging.* Cells, 2020. **9**(1).
129. Chen, Y., et al., *PPARalpha regulates tumor cell proliferation and senescence via a novel target gene carnitine palmitoyltransferase 1C.* Carcinogenesis, 2017. **38**(4): p. 474-483.
130. Ratnakumar, K., et al., *ATRX-mediated chromatin association of histone variant macroH2A1 regulates alpha-globin expression.* Genes Dev, 2012. **26**(5): p. 433-8.
131. Wajapeyee, N., et al., *Oncogenic BRAF induces senescence and apoptosis through pathways mediated by the secreted protein IGFBP7.* Cell, 2008. **132**(3): p. 363-74.
132. Kim, K.S., et al., *Regulation of replicative senescence by insulin-like growth factor-binding protein 3 in human umbilical vein endothelial cells.* Aging Cell, 2007. **6**(4): p. 535-45.

133. Liu, F., et al., *Klotho suppresses RIG-I-mediated senescence-associated inflammation.* Nat Cell Biol, 2011. **13**(3): p. 254-62.
134. Birch, J. and J. Gil, *Senescence and the SASP: many therapeutic avenues.* Genes Dev, 2020. **34**(23-24): p. 1565-1576.
135. Martinez-Zamudio, R.I., et al., *AP-1 imprints a reversible transcriptional programme of senescent cells.* Nat Cell Biol, 2020. **22**(7): p. 842-855.
136. Tasdemir, N., et al., *BRD4 Connects Enhancer Remodeling to Senescence Immune Surveillance.* Cancer Discov, 2016. **6**(6): p. 612-29.
137. Leon, K.E., et al., *DOT1L modulates the senescence-associated secretory phenotype through epigenetic regulation of IL1A.* J Cell Biol, 2021. **220**(8).
138. Asghar, U., et al., *The history and future of targeting cyclin-dependent kinases in cancer therapy.* Nat Rev Drug Discov, 2015. **14**(2): p. 130-46.
139. Ammazzalorso, A., et al., *Development of CDK4/6 Inhibitors: A Five Years Update.* Molecules, 2021. **26**(5).
140. Yang, C., et al., *Acquired CDK6 amplification promotes breast cancer resistance to CDK4/6 inhibitors and loss of ER signaling and dependence.* Oncogene, 2017. **36**(16): p. 2255-2264.
141. Herrera-Abreu, M.T., et al., *Early Adaptation and Acquired Resistance to CDK4/6 Inhibition in Estrogen Receptor-Positive Breast Cancer.* Cancer Res, 2016. **76**(8): p. 2301-13.
142. Li, Z., et al., *Loss of the FAT1 Tumor Suppressor Promotes Resistance to CDK4/6 Inhibitors via the Hippo Pathway.* Cancer Cell, 2018. **34**(6): p. 893-905 e8.
143. Dickson, M.A., et al., *Progression-Free Survival Among Patients With Well-Differentiated or Dedifferentiated Liposarcoma Treated With CDK4 Inhibitor Palbociclib: A Phase 2 Clinical Trial.* JAMA Oncol, 2016. **2**(7): p. 937-40.
144. Patnaik, A., et al., *Efficacy and Safety of Abemaciclib, an Inhibitor of CDK4 and CDK6, for Patients with Breast Cancer, Non-Small Cell Lung Cancer, and Other Solid Tumors.* Cancer Discov, 2016. **6**(7): p. 740-53.
145. Leonard, J.P., et al., *Selective CDK4/6 inhibition with tumor responses by PD0332991 in patients with mantle cell lymphoma.* Blood, 2012. **119**(20): p. 4597-607.
146. Torres-Guzman, R., et al., *Preclinical characterization of abemaciclib in hormone receptor positive breast cancer.* Oncotarget, 2017. **8**(41): p. 69493-69507.
147. Yoshida, A., E.K. Lee, and J.A. Diehl, *Induction of Therapeutic Senescence in Vemurafenib-Resistant Melanoma by Extended Inhibition of CDK4/6.* Cancer Res, 2016. **76**(10): p. 2990-3002.
148. Bollard, J., et al., *Palbociclib (PD-0332991), a selective CDK4/6 inhibitor, restricts tumour growth in preclinical models of hepatocellular carcinoma.* Gut, 2017. **66**(7): p. 1286-1296.
149. Vijayaraghavan, S., et al., *CDK4/6 and autophagy inhibitors synergistically induce senescence in Rb positive cytoplasmic cyclin E negative cancers.* Nat Commun, 2017. **8**: p. 15916.
150. Valenzuela, C.A., et al., *Palbociclib-induced autophagy and senescence in gastric cancer cells.* Exp Cell Res, 2017. **360**(2): p. 390-396.

151. Schaer, D.A., et al., *The CDK4/6 Inhibitor Abemaciclib Induces a T Cell Inflamed Tumor Microenvironment and Enhances the Efficacy of PD-L1 Checkpoint Blockade.* Cell Rep, 2018. **22**(11): p. 2978-2994.
152. Goel, S., et al., *CDK4/6 inhibition triggers anti-tumour immunity.* Nature, 2017. **548**(7668): p. 471-475.
153. Charles, A., et al., *l.* Oncoimmunology, 2021. **10**(1): p. 1916243.
154. Conyers, R., S. Young, and D.M. Thomas, *Liposarcoma: molecular genetics and therapeutics.* Sarcoma, 2011. **2011**: p. 483154.
155. Italiano, A., et al., *Clinical and biological significance of CDK4 amplification in well-differentiated and dedifferentiated liposarcomas.* Clin Cancer Res, 2009. **15**(18): p. 5696-703.
156. Codenotti, S., et al., *Animal models of well-differentiated/dedifferentiated liposarcoma: utility and limitations.* Onco Targets Ther, 2019. **12**: p. 5257-5268.
157. Kidwell, K.M., et al., *Application of Bayesian methods to accelerate rare disease drug development: scopes and hurdles.* Orphanet J Rare Dis, 2022. **17**(1): p. 186.
158. Berry, D.A., *Interim analyses in clinical trials: classical vs. Bayesian approaches.* Stat Med, 1985. **4**(4): p. 521-6.
159. Tudur Smith, C., P.R. Williamson, and M.W. Beresford, *Methodology of clinical trials for rare diseases.* Best Pract Res Clin Rheumatol, 2014. **28**(2): p. 247-62.
160. Lee, J.J. and C.T. Chu, *Bayesian clinical trials in action.* Stat Med, 2012. **31**(25): p. 2955-72.
161. George, M.A., et al., *Clinical and Pharmacologic Differences of CDK4/6 Inhibitors in Breast Cancer.* Front Oncol, 2021. **11**: p. 693104.
162. Hafner, M., et al., *Multiomics Profiling Establishes the Polypharmacology of FDA-Approved CDK4/6 Inhibitors and the Potential for Differential Clinical Activity.* Cell Chem Biol, 2019. **26**(8): p. 1067-1080 e8.
163. Braal, C.L., et al., *Inhibiting CDK4/6 in Breast Cancer with Palbociclib, Ribociclib, and Abemaciclib: Similarities and Differences.* Drugs, 2021. **81**(3): p. 317-331.
164. Zhou, L., et al., *Senescence as a dictator of patient outcomes and therapeutic efficacies in human gastric cancer.* Cell Death Discov, 2022. **8**(1): p. 13.
165. Haugstetter, A.M., et al., *Cellular senescence predicts treatment outcome in metastasised colorectal cancer.* Br J Cancer, 2010. **103**(4): p. 505-9.
166. Puyol, M., et al., *A synthetic lethal interaction between K-Ras oncogenes and Cdk4 unveils a therapeutic strategy for non-small cell lung carcinoma.* Cancer Cell, 2010. **18**(1): p. 63-73.
167. Schmitt, C.A., et al., *A senescence program controlled by p53 and p16INK4a contributes to the outcome of cancer therapy.* Cell, 2002. **109**(3): p. 335-46.
168. Demaria, M., et al., *Cellular Senescence Promotes Adverse Effects of Chemotherapy and Cancer Relapse.* Cancer Discov, 2017. **7**(2): p. 165-176.
169. Eggert, T., et al., *Distinct Functions of Senescence-Associated Immune Responses in Liver Tumor Surveillance and Tumor Progression.* Cancer Cell, 2016. **30**(4): p. 533-547.
170. Kim, Y.H., et al., *Senescent tumor cells lead the collective invasion in thyroid cancer.* Nat Commun, 2017. **8**: p. 15208.

171. Milanovic, M., et al., *Senescence-associated reprogramming promotes cancer stemness.* Nature, 2018. **553**(7686): p. 96-100.
172. Childs, B.G., et al., *Senescence and apoptosis: dueling or complementary cell fates?* EMBO Rep, 2014. **15**(11): p. 1139-53.
173. Cahu, J., S. Bustany, and B. Sola, *Senescence-associated secretory phenotype favors the emergence of cancer stem-like cells.* Cell Death Dis, 2012. **3**: p. e446.
174. Campisi, J., *Aging and cancer: the double-edged sword of replicative senescence.* J Am Geriatr Soc, 1997. **45**(4): p. 482-8.
175. Munoz-Espin, D. and M. Serrano, *Cellular senescence: from physiology to pathology.* Nat Rev Mol Cell Biol, 2014. **15**(7): p. 482-96.
176. Munoz-Espin, D., et al., *Programmed cell senescence during mammalian embryonic development.* Cell, 2013. **155**(5): p. 1104-18.
177. Storer, M., et al., *Senescence is a developmental mechanism that contributes to embryonic growth and patterning.* Cell, 2013. **155**(5): p. 1119-30.
178. Gibaja, A., et al., *TGFbeta2-induced senescence during early inner ear development.* Sci Rep, 2019. **9**(1): p. 5912.
179. Demaria, M., et al., *Cell Autonomous and Non-Autonomous Effects of Senescent Cells in the Skin.* J Invest Dermatol, 2015. **135**(7): p. 1722-1726.
180. Darby, I.A., et al., *Fibroblasts and myofibroblasts in wound healing.* Clin Cosmet Investig Dermatol, 2014. **7**: p. 301-11.
181. Baker, D.J., et al., *Clearance of p16Ink4a-positive senescent cells delays ageing-associated disorders.* Nature, 2011. **479**(7372): p. 232-6.
182. Baker, D.J., et al., *Naturally occurring p16(Ink4a)-positive cells shorten healthy lifespan.* Nature, 2016. **530**(7589): p. 184-9.
183. Bussian, T.J., et al., *Clearance of senescent glial cells prevents tau-dependent pathology and cognitive decline.* Nature, 2018. **562**(7728): p. 578-582.
184. Yao, G., *Modelling mammalian cellular quiescence.* Interface Focus, 2014. **4**(3): p. 20130074.
185. Basisty, N., et al., *A proteomic atlas of senescence-associated secretomes for aging biomarker development.* PLoS Biol, 2020. **18**(1): p. e3000599.
186. Watt, A.C., et al., *CDK4/6 inhibition reprograms the breast cancer enhancer landscape by stimulating AP-1 transcriptional activity.* Nat Cancer, 2021. **2**(1): p. 34-48.
187. Goh, Y.Y., et al., *Angiopoietin-like 4 interacts with matrix proteins to modulate wound healing.* J Biol Chem, 2010. **285**(43): p. 32999-33009.
188. Chong, H.C., et al., *Angiopoietin-like 4 stimulates STAT3-mediated iNOS expression and enhances angiogenesis to accelerate wound healing in diabetic mice.* Mol Ther, 2014. **22**(9): p. 1593-604.
189. Julier, Z., et al., *Promoting tissue regeneration by modulating the immune system.* Acta Biomater, 2017. **53**: p. 13-28.
190. Boothby, I.C., J.N. Cohen, and M.D. Rosenblum, *Regulatory T cells in skin injury: At the crossroads of tolerance and tissue repair.* Sci Immunol, 2020. **5**(47).

191. Landen, N.X., D. Li, and M. Stahle, *Transition from inflammation to proliferation: a critical step during wound healing.* Cell Mol Life Sci, 2016. **73**(20): p. 3861-85.
192. McAndrews, K.M., et al., *Dermal alphaSMA(+) myofibroblasts orchestrate skin wound repair via beta1 integrin and independent of type I collagen production.* EMBO J, 2022. **41**(7): p. e109470.
193. Qian, L.W., et al., *Exacerbated and prolonged inflammation impairs wound healing and increases scarring.* Wound Repair Regen, 2016. **24**(1): p. 26-34.
194. Wang, Z. and C. Shi, *Cellular senescence is a promising target for chronic wounds: a comprehensive review.* Burns Trauma, 2020. **8**: p. tkaa021.
195. Kita, A., et al., *Altered regulation of mesenchymal cell senescence in adipose tissue promotes pathological changes associated with diabetic wound healing.* Commun Biol, 2022. **5**(1): p. 310.
196. Tomasek, J.J., et al., *Myofibroblasts and mechano-regulation of connective tissue remodelling.* Nat Rev Mol Cell Biol, 2002. **3**(5): p. 349-63.
197. Goh, Y.Y., et al., *Angiopoietin-like 4 interacts with integrins beta1 and beta5 to modulate keratinocyte migration.* Am J Pathol, 2010. **177**(6): p. 2791-803.
198. Krizhanovsky, V., et al., *Senescence of activated stellate cells limits liver fibrosis.* Cell, 2008. **134**(4): p. 657-67.
199. Gill, S.E. and W.C. Parks, *Metalloproteinases and their inhibitors: regulators of wound healing.* Int J Biochem Cell Biol, 2008. **40**(6-7): p. 1334-47.
200. Caley, M.P., V.L. Martins, and E.A. O'Toole, *Metalloproteinases and Wound Healing.* Adv Wound Care (New Rochelle), 2015. **4**(4): p. 225-234.
201. Martins, V.L., M. Caley, and E.A. O'Toole, *Matrix metalloproteinases and epidermal wound repair.* Cell Tissue Res, 2013. **351**(2): p. 255-68.
202. Fassl, A., Y. Geng, and P. Sicinski, *CDK4 and CDK6 kinases: From basic science to cancer therapy.* Science, 2022. **375**(6577): p. eabc1495.
203. Beausejour, C.M., et al., *Reversal of human cellular senescence: roles of the p53 and p16 pathways.* EMBO J, 2003. **22**(16): p. 4212-22.
204. Sage, J., et al., *Acute mutation of retinoblastoma gene function is sufficient for cell cycle re-entry.* Nature, 2003. **424**(6945): p. 223-8.
205. Wang, B., et al., *Pharmacological CDK4/6 inhibition reveals a p53-dependent senescent state with restricted toxicity.* EMBO J, 2022. **41**(6): p. e108946.
206. Kim, W.Y. and N.E. Sharpless, *The regulation of INK4/ARF in cancer and aging.* Cell, 2006. **127**(2): p. 265-75.
207. Wang, B., J. Kohli, and M. Demaria, *Senescent Cells in Cancer Therapy: Friends or Foes?* Trends Cancer, 2020. **6**(10): p. 838-857.
208. Kim, E.C. and J.R. Kim, *Senotherapeutics: emerging strategy for healthy aging and age-related disease.* BMB Rep, 2019. **52**(1): p. 47-55.
209. Robbins, P.D., et al., *Senolytic Drugs: Reducing Senescent Cell Viability to Extend Health Span.* Annu Rev Pharmacol Toxicol, 2021. **61**: p. 779-803.